
Masters Theses

Student Theses and Dissertations

Spring 2015

Determining rockfall volumes in three sites along Habs mountain road in southwestern Saudi Arabia, using LiDAR technology

Abdullah Ayed Al-Otaibi

Follow this and additional works at: https://scholarsmine.mst.edu/masters_theses



Part of the [Geological Engineering Commons](#), [Geotechnical Engineering Commons](#), and the [Remote Sensing Commons](#)

Department:

Recommended Citation

Al-Otaibi, Abdullah Ayed, "Determining rockfall volumes in three sites along Habs mountain road in southwestern Saudi Arabia, using LiDAR technology" (2015). *Masters Theses*. 7384.
https://scholarsmine.mst.edu/masters_theses/7384

This thesis is brought to you by Scholars' Mine, a service of the Missouri S&T Library and Learning Resources. This work is protected by U. S. Copyright Law. Unauthorized use including reproduction for redistribution requires the permission of the copyright holder. For more information, please contact scholarsmine@mst.edu.

DETERMINING ROCKFALL VOLUMES IN THREE SITES ALONG HABS
MOUNTAIN ROAD IN SOUTHWESTERN SAUDI ARABIA,
USING LIDAR TECHNOLOGY

by

ABDULLAH AYED AL-OTAIBI

A THESIS

Presented to the Faculty of the Graduate School of the
MISSOURI UNIVERSITY OF SCIENCE AND TECHNOLOGY

In Partial Fulfillment of the Requirements for the Degree
MASTER OF SCIENCE IN GEOLOGICAL ENGINEERING

2015

Approved by

Norbert H. Maerz, Advisor

Neil Lennart Anderson

J. David Rogers

©2015
Abdullah Ayed Al-Otaibi
All Rights Reserved

ABSTRACT

The rugged elevated topography is a characteristic feature of the western and southwestern regions of Saudi Arabia. Few arterial roads connect the scattered villages of these regions to major cities, such as Habs Road in Jazan region. Rock fall poses a serious hazard to people, property and animals along the rock cuts of this road. Although no traditional Rockfall studies have previously been applied to this road, accessibility and rock formation shape and structure variability influenced the choice of using Terrestrial Light Detection And Ranging (LiDAR) technology to calculate the volume of rockfall at selected sites along this road.

Software has been developed at the Geological Engineering Program of Missouri University of Science and Technology to calculate the volume of rockfall from a sequence of scans conducted at the selected sites (A1, A2 and A3), at the exact locations, during different time periods, extended for over two months. The pre and post processing of the point cloud data gathered using ScanStation II, measured the real and virtual gain and real and virtual loss of rockfall material due to rainfall, weathering factors, animal and human disturbance, degree of slope-face, and the effect of minor or major earthquakes occur in the region.

The results of the study showed that the site (A1) is more hazardous compared to the site (A2) and site (A3) is the most stable compared to the site (A1) and (A2). The compact rock formation of site A3, the disintegrated rocks of site A2 and the relative loose rocks of upper site A1 (possible valley deposits), were suggested by the study of the determining factors of road safety. The study also found that using terrestrial LiDAR technology and new software reduced time, effort and increased accessibility, despite the limited number of scans conducted.

ACKNOWLEDGMENTS

At the beginning and in the end, my ultimate thanks is for Allah for giving me the strength and power to do this work.

I would like to express my deep appreciation to the Saudi Geological Survey for supporting my study for the master's degree in Geological Engineering at Missouri University of Science and Technology, Rolla, USA. Dr. Zohair Nawab, the President of the Saudi Geological Survey, had a great role in making this possible, my sincere thanks to him and I extend my thanks to Dr. Abdullah Attas, the vice president of the Geological Survey for his encouragement for me to pursue my study.

I am lucky to be the student of Dr. Norbert H. Maerz, he enriched my knowledge in geological engineering and has been more than advisor; my thanks to Prof. Neil Anderson and Dr. David Rogers for being on my advisory committee.

I would like to thank Mr. Saleh Sefry, the director of the applied geology at (SGS) and Mr. Hassan Al-Harbi, the head of geological hazard department, for their support and assistance during the time of the project. In addition, I would like thank Mr. Turki Sehli and Mohamed Al-Moald for helping me in the fieldwork, and Mohammed Al-Ameri and Saeed Alzahrani for helping me in the desk study.

In addition, without the blessings of my mother, I would not have achieved success. My brother Honaisan, Brigadier-General, never stopped encouraging me to complete my study. I will never forget the patience and sacrifices of my wife, being far from relatives and homey environment, yet continued supporting me and be happy for my success. The support of my sisters and brother Fahad, is forever in my mind.

TABLE OF CONTENTS

	Page
ABSTRACT	iii
ACKNOWLEDGMENTS	iv
LIST OF ILLUSTRATIONS	vii
LIST OF TABLES	xi
1. INTRODUCTION.....	1
1.1. STUDY OBJECTIVES.....	2
1.2. LOCATION	2
1.3. RAINFALL.....	3
1.4. TOPOGRAPHY.....	4
1.5. TECTONIC SETTINGS.....	5
1.6. GEOLOGY	7
2. RESEARCH BACKGROUND.....	8
2.1. TYPES AND CAUSES OF ROCK FAILURE.....	8
2.1.1. Planar Failures.....	8
2.1.2. Wedge Failures.....	10
2.1.3. Toppling Failures	11
2.1.4. Circular Failures.....	12
2.1.5. Raveling Failures.....	13
2.2. ROCKFALL AND LIDAR	14
2.3. TERRESTRIAL LIDAR APPLICATION REVIEW	14

3. METHODOLOGY.....	17
3.1. SITES SELECTION	17
3.2. LOCATIONS DESCRIPTIONS	18
3.3. INSTRUMENTS AND DATA COLLECTION	20
3.4. LIDAR DATA (POINT CLOUD)	22
3.5. EXPORTING DATA.....	23
3.6. WORKING FILE STRUCTURE.....	23
3.7. DATA PROCESSING.....	24
4. RESULTS	28
4.1. SITE (A1)	28
4.2. SITE (A2)	34
4.3. SITE (A3).....	37
5. DISCUSSION.....	40
6. CONCLUSION.....	45
7. RECOMMENDATION	46
APPENDIX	48
BIBLIOGRAPHY	124
VITA.....	127

LIST OF ILLUSTRATIONS

	Page
Figure 1.1. The location of study area relative to the Kingdom of Saudi Arabia	2
Figure 1.2. The annual average rainfall of the study area, obtained at Fayfa and Ayban Mountain stations.....	3
Figure 1.3. The topographic setting of study area	4
Figure 1.4. The tectonic forces actively acting on the Arabian plate and seismically influencing the study area in the Southwest.....	5
Figure 1.5. Location of Earthquake in Southwestern Saudi Arabia.....	6
Figure 1.6. The major geologic formations and rock types of Habs Road study sites	7
Figure 2.1. Sketch diagram showing Planar Failure type of rock slope (After Norrish and Wyllie, 1996).....	9
Figure 2.2. Sketch diagram showing Wedge Failure type of rock slope (After Norrish and Wyllie, 1996).....	10
Figure 2.3. Sketch diagram showing Toppling Failure type of rock slope (After Norrish and Wyllie, 1996)	11
Figure 2.4. Sketch diagram showing circular Failure type of slope (After Norrish and Wyllie, 1996).....	12
Figure 2.5. Two types of raveling that are caused by weathering of rocks and removal of soft material (Maerz, 2012)	13
Figure 3.1. Location of three sites on Habs Mountain Road, selected for study.....	17
Figure 3.2. Location of Site A1	18
Figure 3.3. Location of selected Site A2	19
Figure 3.4. Location of selected Site A3	19
Figure 3.5. The picture shows the equipment used in collecting data.....	20
Figure 3.6. Fixed locations assigned for LiDAR ScanStation II for repeat scanning.....	21

Figure 3.7. Intensity image created from site A2 using ScanStation 2	22
Figure 3.8. RGB image created from site A2 using ScanStation 2.....	23
Figure 3.9 pts file format (x,y,z, intensity, R, B, G)	23
Figure 3.10. Flow Chart of Data Processing.....	24
Figure 3.11. Split Screen Registration Process	25
Figure 3.12. The figure shows vegetation before removal (right) and after removal (left)	26
Figure 4.1. Difference between Scan 1 (6/28/2012) and Scan 2 (6/29/2012) of site A.....	28
Figure 4.2. Histogram equalized color image of difference surface for 628-629, red is reported gained material, green is no change & blue is reported lost material ...	28
Figure 4.3. Control point 3-D residuals	29
Figure 4.4. Difference between Scan 1 (6/28/2012) and Scan 3 (6/30/2012) of site A1, shows a more realistic amount of lost material due to high precision of co-registration (RMSE = 2.6 mm).....	29
Figure 4.5. Histogram equalized color image of difference surface for 628-630, the large vertical red stripe is an anomaly caused by a passing vehicle	30
Figure 4.6. Control point 3-D residuals	30
Figure 4.7. Difference between Scan 1 (6/28/2012) and Scan 4 (7/02/2012) of site A1, show increased loose material (white)	31
Figure 4.8. Difference between Scan 1 (6/28/2012) and Scan 5 (8/23/2012) of site A1, show considerable increase of loose materials (white).....	31
Figure 4.9. Histogram equalized color image of difference surface for 628-823.....	32
Figure 4.10. Control point 3-D residuals	32
Figure 4.11. Difference between Scan 1 (6/28/2012) and Scan 6 (9/12/2012) of site A1, show considerable decrease of loose materials (white) from previous scan (4)..	33
Figure 4.12. Histogram equalized color image of difference surface for 628-912.....	33
Figure 4.13. Control point 3-D residuals	34

Figure 4.14. Difference between Scan 1 (6/28/2012) and Scan 2 (6/29/2012) of site A2, shows traces of loose material (white)	34
Figure 4.15. Difference between Scan 1 (6/28/2012) and Scan 3 (6/30/2012) of site A2, shows increase in lost material amount (white)	35
Figure 4.16. Difference between Scan 1 (6/28/2012) and Scan 4 (7/02/2012) of site A2, shows slight gained material (red), and increase in lost material (white); more pronounced compared to scan number 2	35
Figure 4.17. Difference between Scan 1 (6/28/2012) and Scan 5 (8/23/2012) of site A2, shows slight increase in gained material (red) and slight increase of lost material (white) compared to scan number 3.....	36
Figure 4.18. Difference between Scan 1 (6/28/2012) and Scan 6 (9/12/2012) of site A2, shows slight decrease in gained material (red) and slight decrease of rock fall (white) relative to scan number (3 & 4)	36
Figure 4.19. Difference between Scan 1 (6/28/2012) and Scan 2 (6/29/2012) of site A3, shows no change in slope face of outcrop	37
Figure 4.20. Difference between Scan 1 (6/28/2012) and Scan 3 (6/30/2012) of site A3, show no change in slope face of outcrop.....	37
Figure 4.21. Difference between Scan 1 (6/28/2012) and Scan 4 (7/02/2012) of site A3, shows traces of lost material (white)	38
Figure 4.22. Difference between Scan 1 (6/28/2012) and Scan 5 (8/23/2012) of site A3, shows traces of lost material (white)	38
Figure 4.23. Difference between Scan 1 (6/28/2012) and Scan 6 (9/12/2012) of site A3, shows insignificant amount of gain (red) and slight change of lost material (white)	39
Figure 5.1. Suggested paleo-channel location of Site A1.....	41
Figure 5.2. Site A1 shows the amount of lost/gained material during scan dates, measured in liters.....	41
Figure 5.3. The picture shows Site A2, where sharp edge, disintegrated blocks of Basalt dominating the location	42
Figure 5.4. The figure shows the amount of lost/gained material for Site A2 during scan dates, measured in cubic liters.....	43

Figure 5.5. Location of site A3, representing massive meta-sedimentary rock formation44

Figure 5.6. The figure shows the amount of lost/gained material during scan dates,
measured in liters in site A3.....44

LIST OF TABLES

	Page
Table 3.1. The data collected for the three study sites.....	22

1. INTRODUCTION

The frequency and volume of rockfall is one of the major indicators of the degree of hazard on roads in elevated and rugged topography. Measuring rockfall volumes using traditional methods of direct measurements encounter many risks, difficulties, and limitations. The development of technologies introduced new advances in the way rockfall volumes are measured, of which 3D LiDAR scanners are gaining wide acceptance for obtaining high accuracy measurement, reaching inaccessible locations and providing great safety measures and repeatability.

3D laser scanners emit laser light and receive back its reflection from objects, to accurately create point clouds. Repeating this process at different instances for the same object is used to calculate volume difference. This thesis used Terrestrial Light Detection and Ranging (LiDAR) technology to quantify rockfall volume by monitoring the study area during a period of two months. Erroneous data such as cars passing by, dust particles, or vegetation that comes between the scanner and rock slope during scanning is, removed by using automated methods.

The Habs road is an artery road linking many of the small villages to the main N-S access highway. Since being built, very little follow up, and maintenance on the road status was conducted, and no traditional or non-traditional estimation of rockfall volume count was attempted. Assessment of hazard levels is necessary to keep the road safe and operating. This study provides base-line information on the Habs Road by employing terrestrial LiDAR techniques to obtain rockfall volume counts, overcoming the difficulties of traditional methods in and assess the road hazard status.

1.1. STUDY OBJECTIVES

The objective of this study is to show the merits of utilizing LiDAR technology to accurately determine rockfall volume count and the level of hazard of road cuts along Habs Road in Jazan, Saudi Arabia.

1.2. LOCATION

Habs Mountain Road is located in Bani Malek county in the Jazan region, southwestern Saudi Arabia, at $170^{\circ}22'43.4''\text{N}$ and $430^{\circ}11'39.2''\text{E}$ (Figure 1.1).

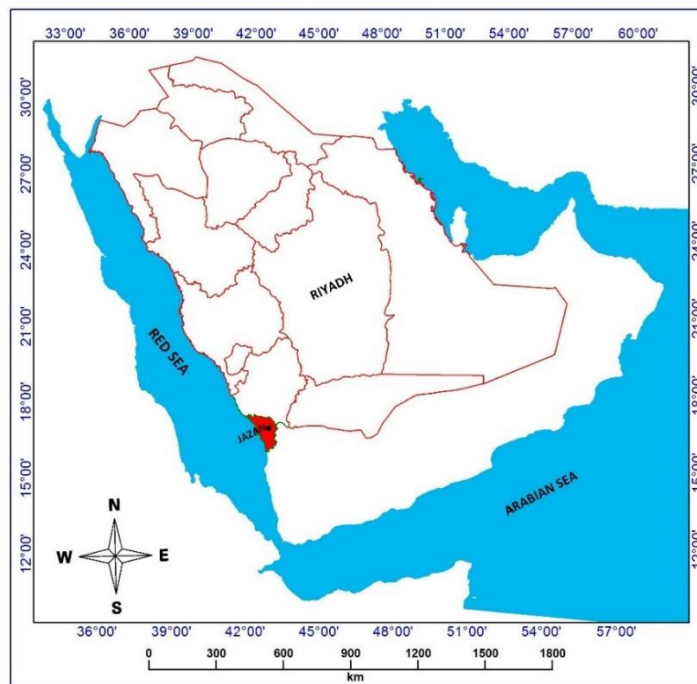


Figure 1.1. The location of study area relative to the Kingdom of Saudi Arabia

The road is the only access that connects the scattered villages with the highway of Alaidabi, which joins with the main highway linking the north of Saudi Arabia to its southern

extremes. The total length of the road is about 14 kilometers, over which it follows a very sinuous route over different types of rock formations.

1.3. RAINFALL

Annual average rainfall of the study area, obtained for the period 1960 to 2013, and represented by the two stations of Fayfa Mountain (SA110) and Ayban Mountain (SA140), show two maxima peaks of increasing rainfall (Figure 1.2).

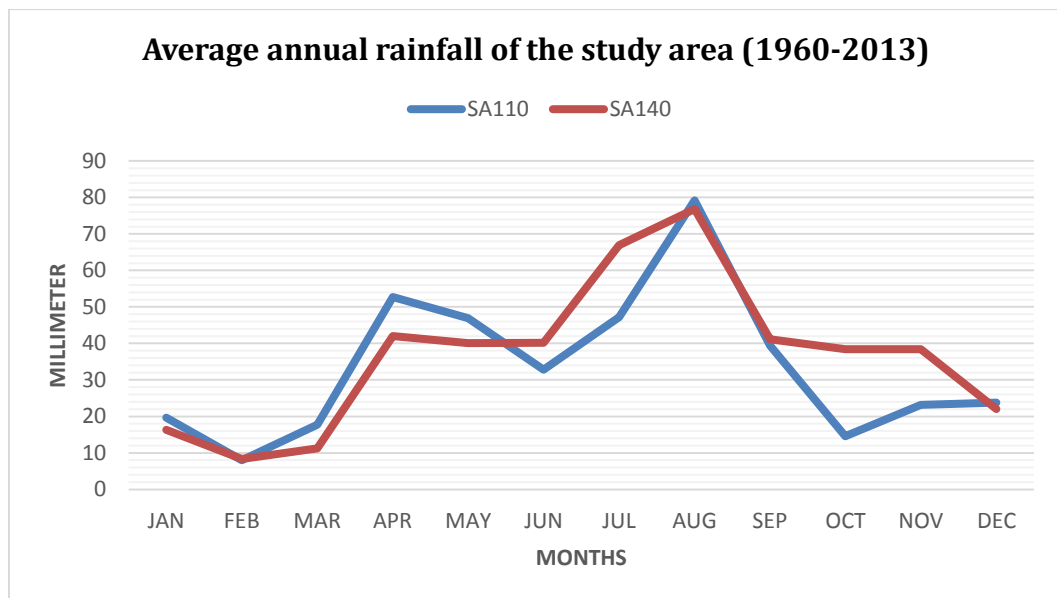


Figure 1.2. The annual average rainfall of the study area, obtained at Fayfa and Ayban Mountain stations

The first lower maxima peak reach an average of ~ 54 mm of precipitation, per month during April, and the higher maxima, in August shows a maximum amount of precipitation in the study area of about ~ 80 mm. The steady increase of rainfall during these months infiltrates

practices and other urban uses. The average slope angles of road cuts varies between 60 to 85 degrees, making this region one of the most inaccessible locations in Saudi Arabia in the past.

1.5. TECTONIC SETTINGS

The study area is affected with the total tectonic regimes of Saudi Arabia, where the Arabian plate falls under the influence of the collisional regime at its eastern boarder with Iran, and subduct under Zagros mountain ranges, the extensional regime of the Red Sea and East African Rift in its western boundaries and the contact of the Arabian plate with the Eurasian plate at its northeastern boundaries. These tectonic plates' activities were suggested as the main drivers for the earthquakes in Gulf of Aden, the Red Sea and the Dead Sea fault and at Zagros and Torus mountain ranges. (Figure 1.4).

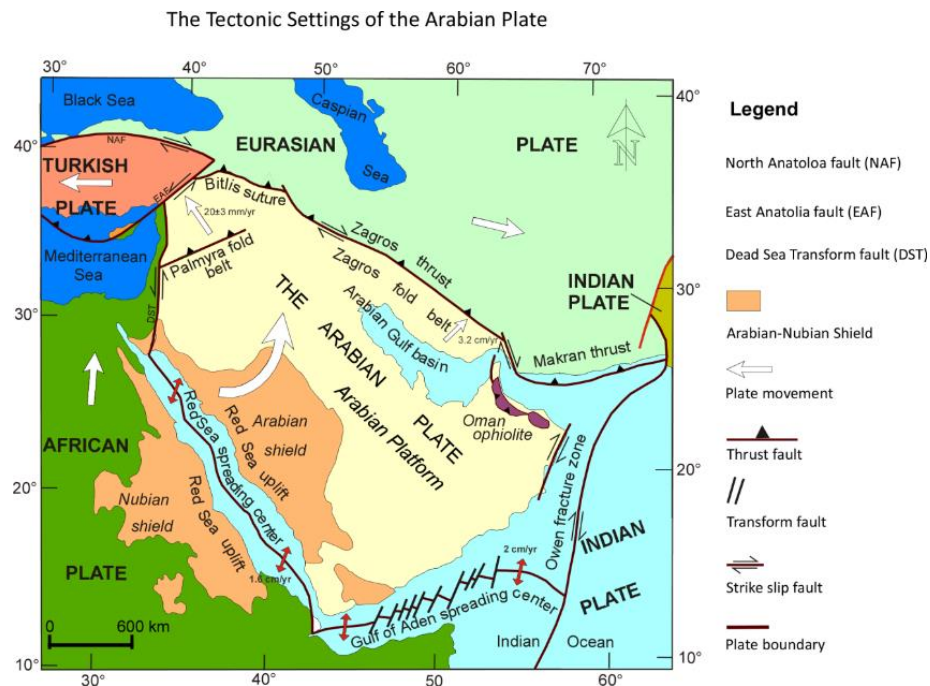


Figure 1.4. The tectonic forces actively acting on the Arabian plate and seismically influencing the study area in the Southwest

The southwest of Saudi Arabia, and the study area, in particular, are more affected by the extensional regime of the Red Sea and by the existing and pre-existing faults in the region (Figure 1.5), and the progress of a mantle plume from southeast to northeast, and the propagation of arms of the RRR triple junction rifting arms from Gulf of Aden, the Red Sea and the East African Rift, accompanied by the flow of basaltic lava, locally known as “harat”, along the eastern coast of the Red Sea.

Tectonic history records of the study area revealed that there are three major earthquakes occurred in the region (6.3, 6.0 and 5.5 Richter value), while recent historical records showed that about 400 earthquake have occurred between 1900 and 2011, of values between 3.0 to 6.6 on Richter scale (Figure 1.5)

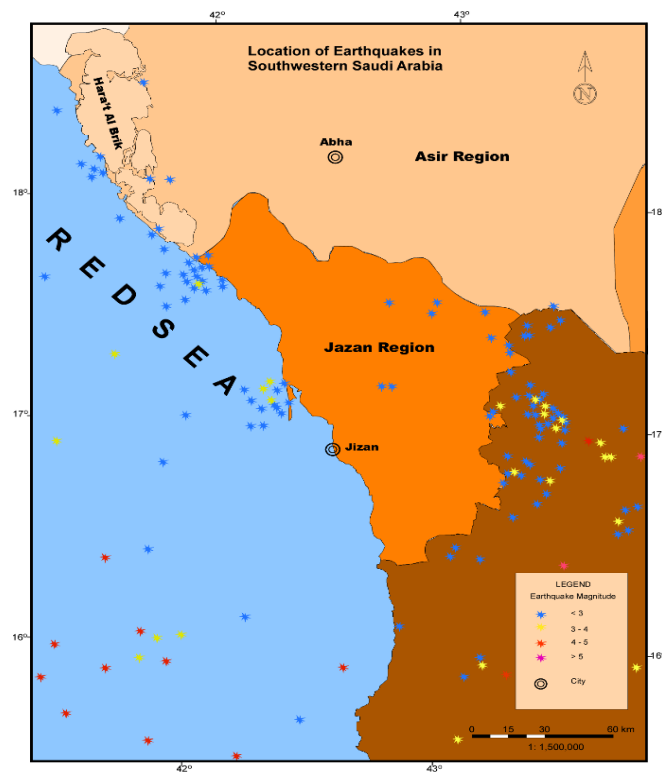


Figure 1.5. Location of Earthquake in Southwestern Saudi Arabia

1.6. GEOLOGY

The geology of the study area comprises three types of rocks: (i) the Sabia formation which are meta-volcanic rocks and schist of medium to high metamorphism. (This formation covers two third of Bani Malik County, which include Habs Mountain Road, and is composed of Quartz, Conglomerate and these formation formed ~700 Ma ago), (ii), the moderately weathered Granite, and (iii) the metasedimentary rocks, which form hazardous block in matrix (debris flows) when wetted by rains (Figure 1.6)

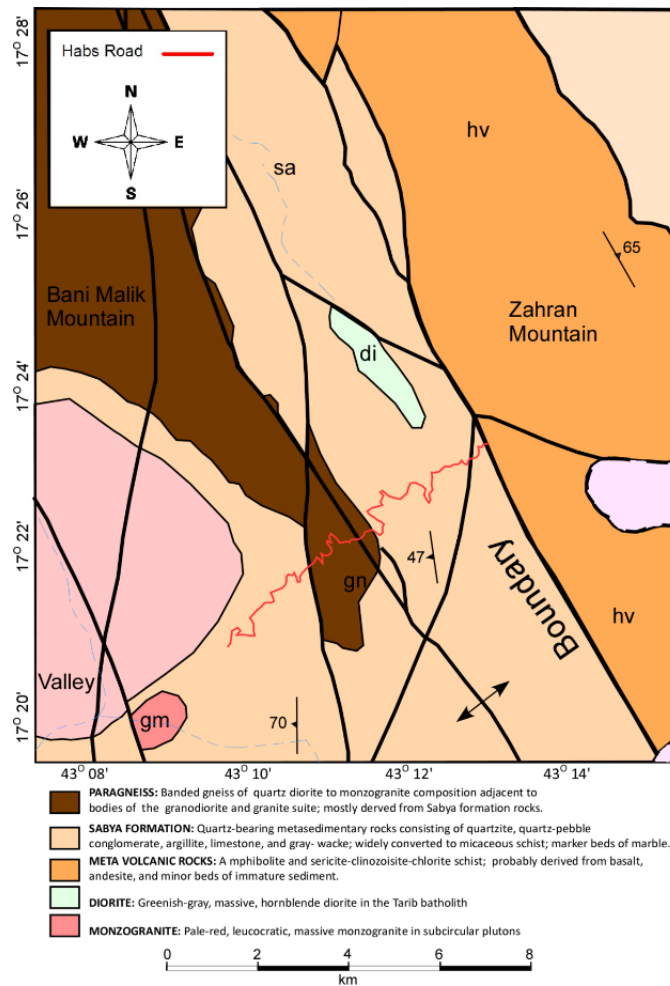


Figure 1.6. The major geologic formations and rock types of Habs Road study sites

2. RESEARCH BACKGROUND

2.1. TYPES AND CAUSES OF ROCK FAILURE

Rocks fail as a result of internal and external factors. The internal failure factors relate primarily to rock properties such as the type of rock, the nature of the discontinuities, and the ground water level, whereas the external factors depend on the conditions that ultimately change the forces acting on the rock such as rainfall, snowmelt, seepage, channeled water runoff, weathering, erosion, freeze-thaw and heating-cooling cycles, tree root, wind, disturbance by animals, and earthquakes (Pantelidis 2009). Hoek (2007) mentioned the anthropogenic factor, which includes construction practices, blasting, vibration from equipment and trains, and the stress relief due to excavation. The effectiveness of failure increases with the presence of internal factors coupled with the external factors. Most slope failures were classified in one of four categories depending on the geometrical and mechanical nature of the discontinuity, and the conditions of the rock masses. These include the circular, planar, wedge and toppling failures. Raveling is treated as a special slope failure category that is primarily controlled by environmental factors.

2.1.1. Planar Failures. Planar failures occur along prevalent and/or continuous joints dipping towards the slope, with the strike being near parallel to the slope face. There are two conditions govern the instability:

- (i) When critical joints dips less than the slope, and
- (ii) When the shear strength in the joint is not enough to assure stability.

Planar failures depend on the continuity of the joint and their sizes vary from few cubic meters to large-scale landslides.

The KM Mountain landslide in Washington State represents one of the examples where the sliding was controlled by bedding orientation (Lowell 1990).

Researcher found that four structural conditions requires the planar failure to occur, based on conditions (i) and (ii), and are shown in (Figure 2.1).

- 1- The dip direction of the planar discontinuity must be within 20 degrees of the dip direction of the slope face.
- 2- The dip of the planar discontinuity must be less than the dip of the slope face daylight in the slope.

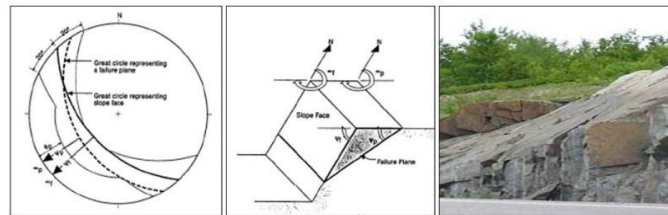


Figure 2.1. Sketch diagram showing Planar Failure type of rock slope (After Norrish and Wyllie, 1996). Note the photograph on the right is after Maerz, 2000

- 3- The dip of the planar discontinuity must be greater than the angle of friction of the failure plane.
- 4- The lateral extent of the potential failing masses must be isolated by lateral release surfaces, which allow blocks to slide freely.

This is the requirement that leads to the likelihood of planar failure occurrence. If structural analysis indicates that the orientation of the slope is unstable, that is, kinematically unstable, then stability evaluated using a limit equilibrium procedure.

2.1.2. Wedge Failures. Wedge failures result when a rock mass slide along two joints from different families whose intersection dips toward the slope. Wedge failure depends largely on the geometry, and residual shear strength. Further, this wedge failure depends on the joint attributes and conditions. This type of failure is more frequent than planar failure. The formation and occurrence of wedge failures are dependent primarily on lithology and the structure of rock mass. Piteau (1972) found that for wedge failures to occur, three conditions are required:

- 1- The trend of the line of intersection must be close to the dip direction of the slope face
- 2- The plunge of the line of intersection must be less than the dip angle of the slope face (daylights on slope),
- 3- The plunge of the line of intersection must be greater than the angle of friction of the failure plane.

Figure 2.2 shows the three stages explained by Piteau.

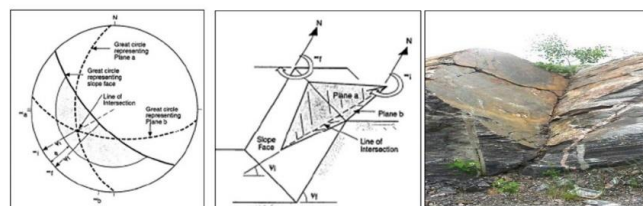


Figure 2.2. Sketch diagram showing Wedge Failure type of rock slope (After Norrish and Wyllie, 1996). Note the photograph on the right (after Maerz, N., 2000)

On the stereographic projection, the point of intersection of the two great circles representing the intersecting planes must plot within the shaded area, which is called the daylight zone, and lies on the convex side of the cut slope. If the structural analysis of wedge stability using stereographic methods indicates the possibility of a wedge failure, kinetic analysis performed.

2.1.3. Toppling Failures. Toppling failures occurred along a prevalent and/ or continuous family of joints, which dip against the slope, and with a strike near parallel to the slope face (Figure 2.3).

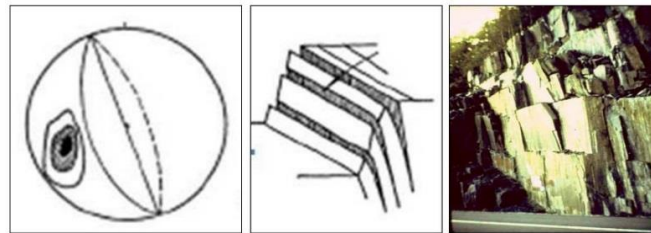


Figure 2.3. Sketch diagram showing Toppling Failure type of rock slope (After Norrish and Wyllie, 1996). Note the photograph on the right is after Maerz, 2000

There are two types of toppling instability. Minor toppling occurs near the surface of the slope, and deep toppling which can produce large deformations. The necessary conditions for toppling failure can be summarized into (1): The strike of the layers must be approximately parallel to the slope face, differences in these orientations of 20 degrees or less are required based on references in the literature, (2): The dip of the layers must be into the slope face, and (3): The discontinuity condition must satisfy the following equation: $(t/h < \tan \psi)$. Simple block and wedge pullout failures are easy to analyze with limit equilibrium analyses and numerical

modeling (Hoek and Bray, 1981; Piteau, 1979a; Piteau, 1979c; Piteau, 1979d; Piteau, 1979e). Piteau and Martin (1982) mentioned that the most common method was the simple limiting equilibrium technique to evaluate the sensitivity of possible failure conditions to slope geometry and rock mass parameters. Kinematic analysis based on the orientation of the combination of discontinuities, the slope face, the upper slope surface, and any other slope surface of interest together with friction that is examined to determine if certain modes of failure can possibly occur. This analysis is normally conducted with the aid of a stereographic representation of the planes and /or lines of intersection (Markland 1972). There are some advantages and disadvantages for this type of analysis.

2.1.4. Circular Failures. Circular failures occur along circular slip paths (Figure 2.4) which are commonly associated with highly weathered and decomposed, highly fractured, or weak rock masses. In general, structural discontinuities such as joints and bedding planes do not form distinctive patterns that lead to a circular failure path and develop into kinematical failure possibility. For the Raida escarpment rock cuts, it is unlikely that circular failures would be a major concern in the rock cut areas.

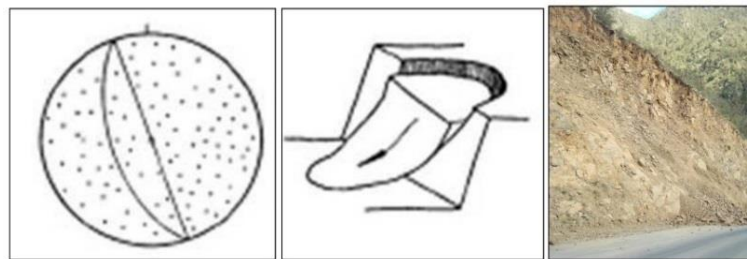


Figure 2.4. Sketch diagram showing circular Failure type of slope (After Norrish and Wyllie, 1996). Note the photograph on the right is taken from Raidah escarpment road. (Youssef, A. M., et al., 2012.)

2.1.5. Raveling Failures. Raveling failure is different from other failure modes, it occurs in both hard and soft rocks, as well. Baawner (1993), Goodman and Kieffer (2000), found that raveling occurs in weakly cemented Conglomerates and Breccia , and in highly fractured strong rocks and brittle sandstones interbedded with soft shale and mudstone (Selby, 1993) also in that; it is caused by weathering of rock, which is a time dependent process (Figure 2.5).



Figure 2.5. Two types of raveling that are caused by weathering of rocks and removal of soft material (Maerz, 2012)

This is the most frequently occurring rockfall type, and often releases smaller and fewer blocks. Serious large-scale disasters occur when undercutting causes failure of entire slope (Maerz, 2012). Unlike other failure modes, raveling is more difficult to control and accurately assess and analyze. Detailed assessment in Northern Ontario showed that all types of raveling compose 65% of failures, while other types of failure composes 35%, only (Maerz, 2012).

2.2. ROCKFALL AND LIDAR

Rockfall represents one of the major man-made hazards in southwestern Saudi Arabia. The types of rockfall introduced at the beginning of this section, including raveling occurred in different regions in Saudi Arabia, and are associated with various types of rock formations. Wedge failure, planar, toppling and circular types were reported in southern Saudi Arabia, while raveling type of rockfall, dominate the central region which is characterized by sedimentary rock formation. Various qualitative assessment methods and mitigation efforts applied in resolving complicated rockfall problems, especially along road-cuts, but raveling forms a continuous challenge to engineers and researchers, when quantitative measures, remediation and mitigation assessment are needed. LiDAR technology introduced more recently as a tool that capable of putting an end to this challenging situation. Other than this advantage, LiDAR largely reduced the high cost of conducting fieldwork, by reducing the number of personnel and logistics, and minimizing the time for achieving tasks, accessibility, and results in the collection of large amount of useful data.

2.3. TERRESTRIAL LIDAR APPLICATION REVIEW

LiDAR is a scanning device that is designed to send out laser pulses and receive back the reflected pulse from the object. The travel time of the out-going and incoming signals is used to obtain the physical distance to the objects using the equation:

$$Distance = \frac{(Speed\ of\ Light * Time\ of\ Flight)}{2}$$

(Andrew, R., et al., 2012). 3D Terrestrial LiDAR has been used in a variety of applications, such as assessing the different stages of construction of buildings, dams, bridges, ships, planes,

oil refineries, tunnels, and open pit and underground mines. Another application area of terrestrial LiDAR is, the study and monitoring of natural phenomenon, such as mass wasting, geomorphology and drainage systems, geology, tree and vegetation cover, and agriculture (Mongus, D. et al. 2014; Clark, C. et al. 2014; Majid, Z. et al. 2008; Lato, M. et al. 2014; Mizoguchi, T. et al. 2013; DeMann, A. 2010; Rooper, J. 2013; Brodu, N. et al. 2012; Beland, M. et al. 2014). Lato, M., et al, 2008 introduced guiding lines for optimizing automated structural discontinuity analysis based on LiDAR point cloud data. They concentrated primary on data collection location, scan orientation and data interpretation procedures. The method was further investigated by Voge, M., et al, 2013, where they tested some mathematical algorithms developed by Lato and Voge (2012), to automate discontinuity mapping on detected planes, and were able to obtain colored maps of discontinuity orientation categorized in sets of families. This automation removed human bias and increased the speed of obtaining results 10x faster than the manual methods. LiDAR was used in conjunction with remote sensing in rockfall hazard spatial modeling, and determining the characteristics of the 3D physical process of rockfall, and the distribution of frequency and energy of falling rocks (Lan, H., et al, 2010). Tracing of discontinuity is crucial in rockfall and mass wasting processes, since it was evident that catastrophic rockfall events were traced back to un-noticed discontinuities. Umili, G., et al., (2013) implemented a procedure to automatically identify traces of discontinuities from digital surface models, using curvature values of the digital surface.

The developments in using remote technology to study distant, difficult to access study locations, encouraged the use of optical instruments and LiDAR, together to solve some of the challenging problems concerning the co-existence of traces and facets. Otoo, J., et al., (2011), introduced a new software that was able to determine 3-D discontinuity orientations.

Terrestrial and air-borne LiDAR scanning were used also in monitoring steep, elevated study areas, and large scale sites of active slopes in Rügen, Germany by Kuhn, D., et al., (2014), and were utilized the technique to quantify change detection and volume balance from repeated scans. This volume quantification was time and effort consuming in the past, since rockfall volumes were obtained from direct measurements or by calculating volumes for single block at a time from digitally acquired data. Maerz, N., et al., (2012) in his recent research was able to measure and quantify the change in volume on sites exhibit raveling rockfall type, one of the most challenging types of rockfall and difficult to quantify. Raveling failure is unlike other rockfall types, it is dependent on the weathering conditions. Robust software was developed at Missouri University S&T, was utilized in rockfall volume determination, and was further applied in research by Kassebaum, T., 2013 to obtain a Master's degree. Rockfall volume data obtained in this study was correlated with rockfall triggering events, such as freeze and thaw cycles, precipitation levels, and seismic (blasting) data.

3. METHODOLOGY

3.1. SITES SELECTION

For this research, three sites were selected for the reasons listed below:

The Habs mountain road is important in connecting the many villages with the main road (Elidabi) and the highway (Figure 3.1).

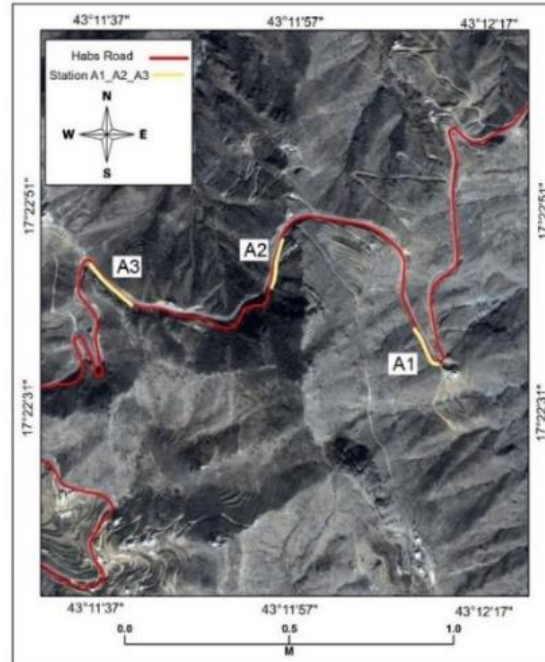


Figure 3.1. Location of three sites on Habs Mountain Road, selected for study (After: Google Earth)

The study area is characterized by different types of road cuts, including one cut in massive rock, another cut in a loose assemblage rock and a road cut through a debris flow deposit.

For comparison? Moreover, using LiDAR will allow comparison of rock fall volume for the three different sites.

The high degree of rockfall risks associated with this road on people and properties.

3.2. LOCATIONS DESCRIPTIONS

The field data for this study was collected at three sites located in southeastern Jazan, Saudi Arabia.

Site A1, located at $17^{\circ} 22' 37.85''\text{N}$ and $43^{\circ} 12' 11.42''\text{E}$, and has width of 23 m, and height of 24 m (Figure 3.2).

This site is characterize by two sections, lower of which is stable near vertical hard rock, approximately 2.5 m in height, and an upper lower angle section representing a block in-matrix (channel), extending to the top of the outcrop.



Figure 3.2. Location of Site A1

Site A2 is located at $17^{\circ} 22' 47.2''$ N $43^{\circ} 11' 56.1''$ E. The outcrop selected, has a width of 19.15 m and a height of 19.5 m (Figure 3.3). It is characterized by disintegrated blocks of rocks at its upper part and regolith covering the lower part.



Figure 3.3. Location of selected Site A2

Site A3 is located at $17^{\circ} 22' 42.9''$ N and $43^{\circ} 11' 40.05''$ E, and has a width of 20.6 meters and a height of 23.5 meters (Figure 3.4). This site is characterized by jointed rocks.



Figure 3.4. Location of selected Site A3

3.3. INSTRUMENTS AND DATA COLLECTION

The equipment utilized included a ScanStation II[®], tripod, tribrach, laptop computer with the Cyclone[®] program, generator, power supply for LiDAR and computer, and Ethernet connection cable (Figure 3.5).



Figure 3.5. The picture shows the equipment used in collecting data

The start and end of each site was mark by spray paint and the distance was measured using a measuring tape. The height was obtained using a clinometer.

The scan resolution for each site was selected based on the site size (width and height) of the cut and the processing limitations of the software used. The location of the LiDAR was set using fixed metal stakes for sites A2 and A3 and by using red spray paint for site A1, to assure repeated precise data collection (Figure 3.6)



Figure 3.6. Fixed locations assigned for LiDAR ScanStation II for repeat scanning

The tripod and ScanStation were levelled using the tribrach bubble, although the complete leveling importance decreases with the increasing size of scanned object. On the other hand, the registration process developed for this project, does not need leveling of the scanner.

Following the determination of the LiDAR setting, the distance between the LiDAR position and the target outcrop was determined by clicking on “Probe” in the ScanStation II software. The probe function displays the distance from the LiDAR to the center of the scanning domain window. This distance is required later during processing. The data parameters for the three study sites shown in Table 3.1, below:

Table 3.1. The data collected for the three study sites. The scan resolution was manually chosen dependent on the estimated time for scanning.

Outcrop Name	Scan Resolution(mm)	Probe Distance(mm)	Height(m)	Length(m)	Point of Number
A1	8	14384	24	23	2,641,944
A2	6	15341	19.5	19.15	9,500,000
A3	10	12477	23.4	20.6	5,011,652

The final step in the data collection was the scanning of objects at different dates, collected from the same scanner position, saved as raw data.

3.4. LIDAR DATA (POINT CLOUD)

The data obtained by LiDAR scanners in its simplest form, are measurements of the (XYZ) distance's, and the light intensity (I), reflected from a scanned object (Figure 3.7)



Figure 3.7. Intensity image created from site A2 using ScanStation 2

These measurements are collected for millions of points, which ultimately forms a cloud-like data set that can be presented in an RGB color format using the photography integrated in LiDAR scanners (Figure 3.8).



Figure 3.8. RGB image created from site A2 using ScanStation 2

3.5. EXPORTING DATA

Although, point cloud data can be exported to different file formats, Missouri S&T developed software uses the (.pts) format for further processing of the point cloud data. each point in the point cloud is represented by a single line in the pts file (Figure 3.9)

```
-6.866426 8.429932 -2.176701 -808 153 152 113
-6.902613 8.474385 -2.179079 -771 154 154 111
-6.941738 8.522446 -2.182240 -755 136 137 93
-7.093397 8.708940 -2.220519 -562 137 137 94
-7.102941 8.720685 -2.213958 -462 127 128 86
-7.107734 8.726596 -2.205848 -540 123 121 86
-7.118383 8.739698 -2.199489 -731 119 118 83
```

Figure 3.9: pts file format (x,y,z, intensity, R,B,G)

3.6. WORKING FILE STRUCTURE

The S&T LiDAR software converts the raw point cloud data to a depth image format projected on a spherical surface. This depth image is 4300 cells wide and 3400 cells in height.

Each cell represents a single point in the LiDAR point cloud, and contains the distance, intensity and RGB color values of that point. The working file format is stored in binary for processing efficiency.

3.7. DATA PROCESSING

The data obtained from LiDAR scans were converted into (.pts) file format. A C++ program developed by (Boyko, K 2012) at Missouri University of Science and Technology was used to process the data and determine the volume of rockfall. Processing of data conducted through a series of steps, explained in a flow chart (Figure 3.10).

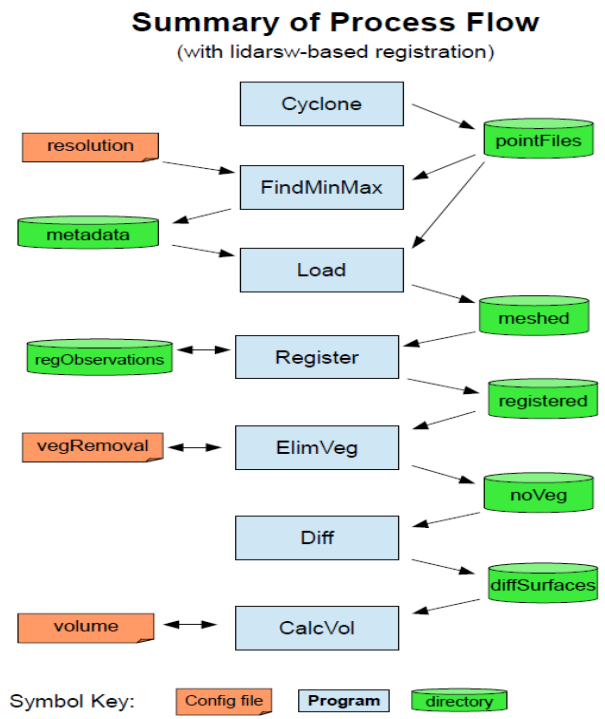


Figure 3.10. Flow Chart of Data Processing

The ultimate goal of the processing is to clean the data, geo-reference subsequent scans, and compute the volume of rockfall. The steps included:

(1) Cyclone

The Leica cyclone software is used to control the LiDAR scanner during data acquisition and to export the data.

(2) FindMinMax

FindMinMax determine the xyz values for the range of the point cloud in both the vertical and horizontal direction were first determined for each cloud scan for the pre-loaded (.pts) raw data, with the first scan considered as the reference frame for subsequent scans.

(3) Load

The load step creates grid/mesh of the raw point data, with a resolution consistent with the resolution use for scanning. This step also fills in empty cells in the grid by interpolation.

(4) Register

Register is a crucial step, in data processing, in which subsequent LiDAR scans were co-registered to the highest precision (Figure 3.11). The user selects four conjugate control points in each scan. These are used to compute a 7-parameter 3D conformal transformation to translate all scanned data to the coordinate system of base date.

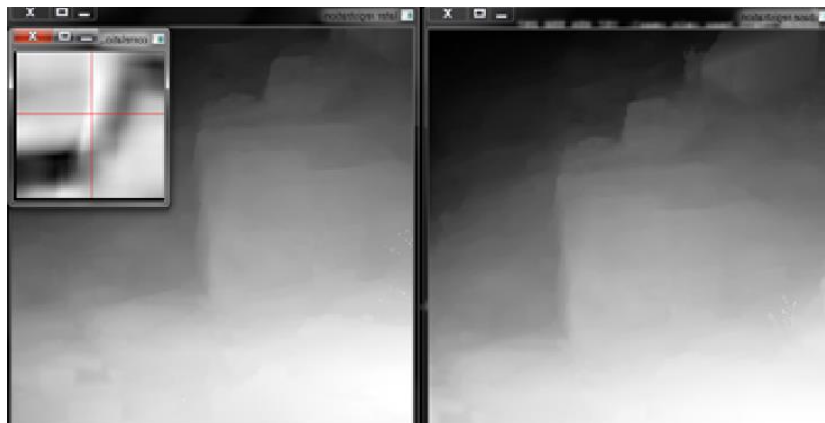


Figure 3.11. Split Screen Registration Process. The smaller box shows how well the two points correlated with one another

(5) ElimVeg

ElimVeg detects and eliminates the spikes in data caused by vegetation using specialized filters developed at Missouri S&T. The virtual articulating conical probe algorithm can identify and eliminate thin vegetation, while preserving the sharp edges of rocks (Figure 3.12).



Figure 3.12. The figure shows vegetation before removal (right) and after removal (left)

(6) Diff

Diff creates a difference surface, by subtracting one registered scan from another. This difference surface is created by performing cell-by-cell subtraction. In theory, this will result in negative and positive values that represent the fallen blocks, in one hand and the positive value on the other hand representing the accumulated debris.

(7) CalcVol

CalcVol is the final step for calculating the volume of fallen rocks, but prior to volume calculation a number of possible errors need to be assessed, which include artifacts, the incomplete removal of vegetation, location and scan date discrepancy and scanner accuracy and configuration.

It is very important to notice that, the positioning of the LiDAR scanner in the same location, and the high precision of image – to –image co-registration, will produce highly accurate volume calculation results (see Appendix A for detailed steps).

4. RESULTS

Scanning of three study sites was conducted between 28 June and 12 October 2013.

The scans were processed and the results shown in Figure 4.1 to Figure 4.23

4.1. SITE (A1)

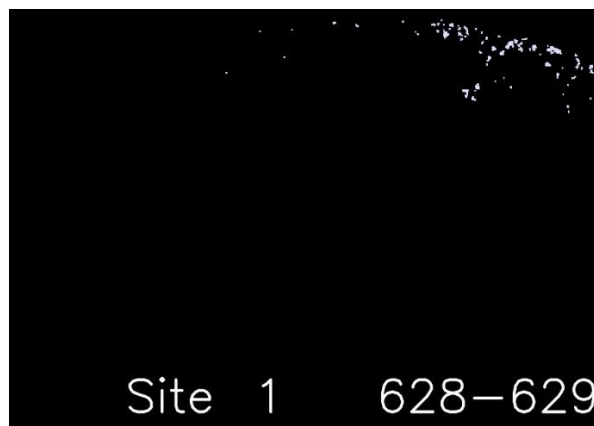


Figure 4.1. Difference between Scan 1 (6/28/2012) and Scan 2 (6/29/2012) of site A. The white color captured in this image is due to high value of check root mean square error (RMSE) of co-registration (7.8 mm)

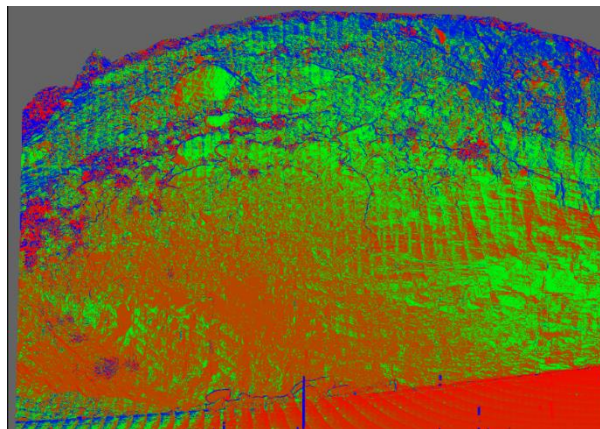


Figure 4.2. Histogram equalized color image of difference surface for 628-629, red is reported gained material, green is no change & blue is reported lost material

Note the color gradient from the lower left to the upper right. This indicate slight tilt in the registration of the 629 surface. Examining the 3D residuals from 629 to 628 registration the overall RMSE = 7.8 mm and the individual control point residual were as follows:

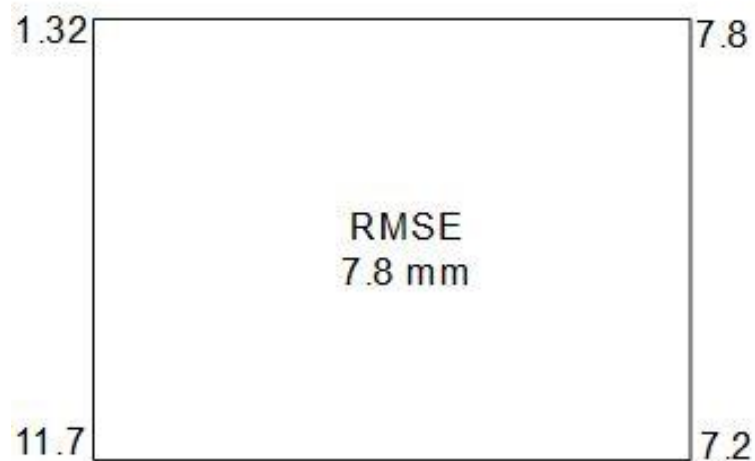


Figure 4.3. Control point 3-D residuals



Figure 4.4. Difference between Scan 1 (6/28/2012) and Scan 3 (6/30/2012) of site A1, shows a more realistic amount of lost material due to high precision of co-registration (RMSE = 2.6 mm)

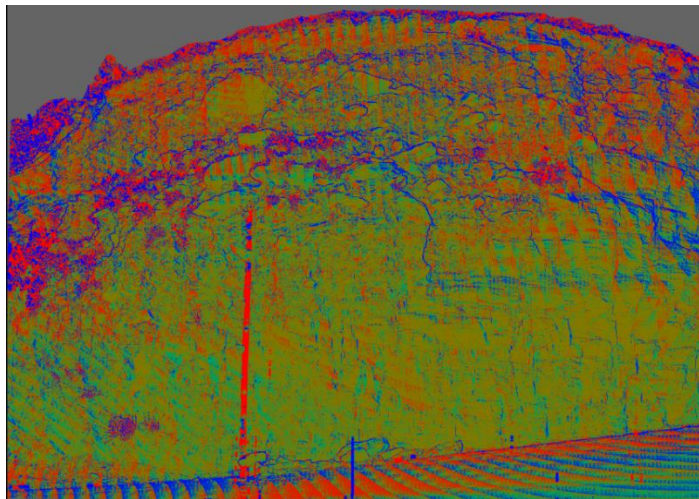


Figure 4.5. Histogram equalized color image of difference surface for 628-630, the large vertical red stripe is an anomaly caused by a passing vehicle. This anomaly will be masked out prior to volume computation

Note the lack of a color gradient across the image. This indicates that this registration is better than the registration of the first scanning. This can be verified by examining the overall 3D residuals, which was 2.6 mm and magnitude of the individual control point residual were as follows:

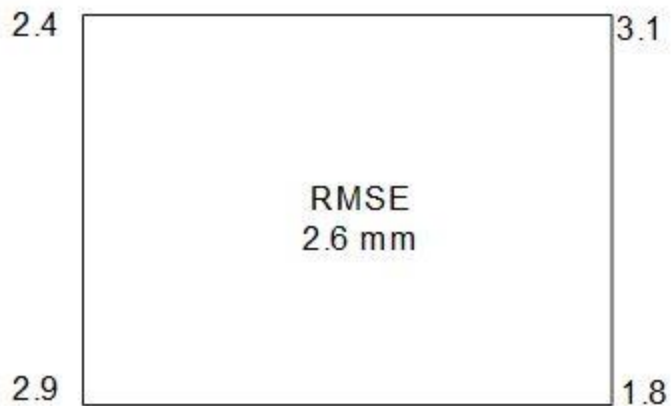


Figure 4.6. Control point 3-D residuals

3D residuals are indicative of the overall “fit” between two sets of observations. The registration process uses 7- parameter conformal transformation capable of applying three transformations, three rotations, and a universal scale factor. The 3-D RMSE residual indicates how well the 3-D “shape” from the base-date observations fit the “shape” of the later-date observations.

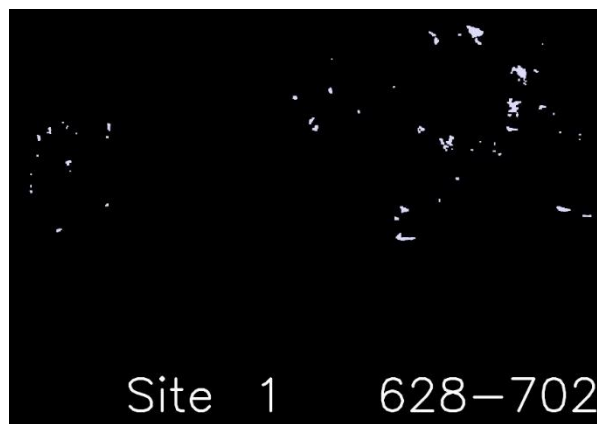


Figure 4.7. Difference between Scan 1 (6/28/2012) and Scan 4 (7/02/2012) of site A1, show increased loose material (white)

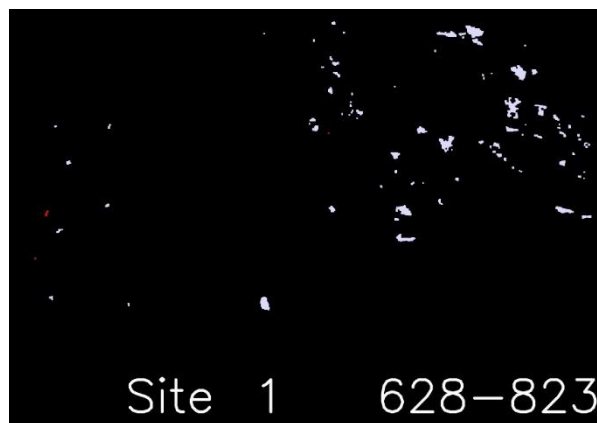


Figure 4.8. Difference between Scan 1 (6/28/2012) and Scan 5 (8/23/2012) of site A1, show considerable increase of loose materials (white)

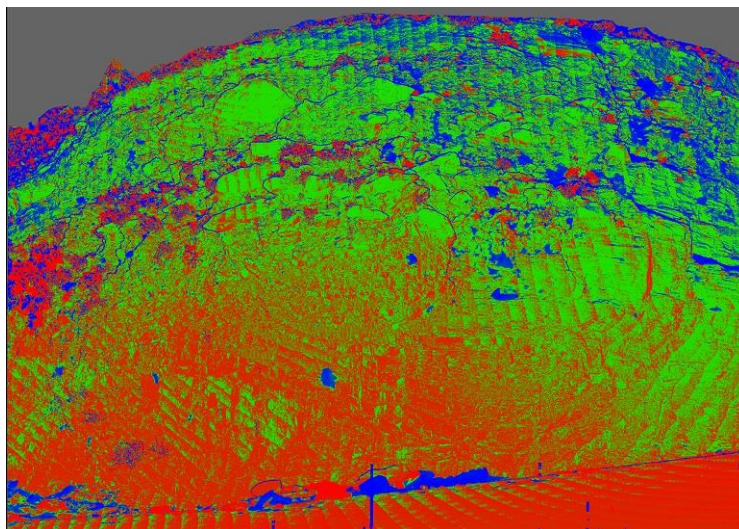


Figure 4.9. Histogram equalized color image of difference surface for 628-823

Note the gradient color from top to bottom tilt caused by high residual control point on the lower edge and the individual control point residual were as follows:

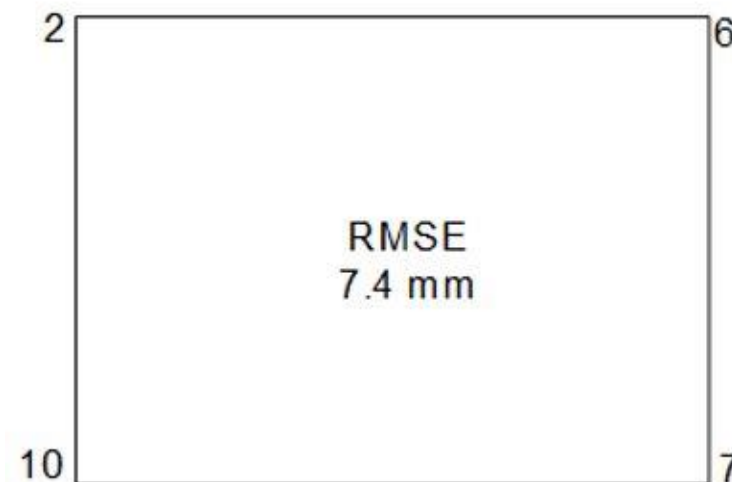


Figure 4.10. Control point 3-D residuals

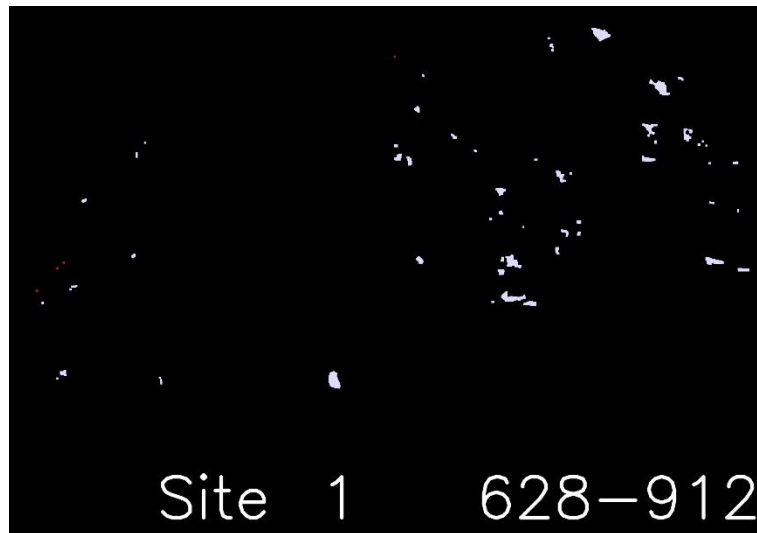


Figure 4.11. Difference between Scan 1 (6/28/2012) and Scan 6 (9/12/2012) of site A1, show considerable decrease of loose materials (white) from previous scan (4)

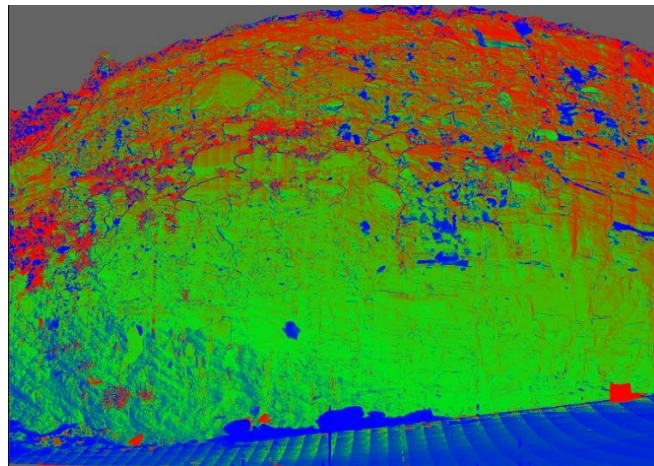


Figure 4.12. Histogram equalized color image of difference surface for 628-912

Note the gradient color from bottom to top (opposite of the previous scan, as in (Figure 4.12) tilt caused by high residual control point on the lower edge and the individual control point residual were as follows:

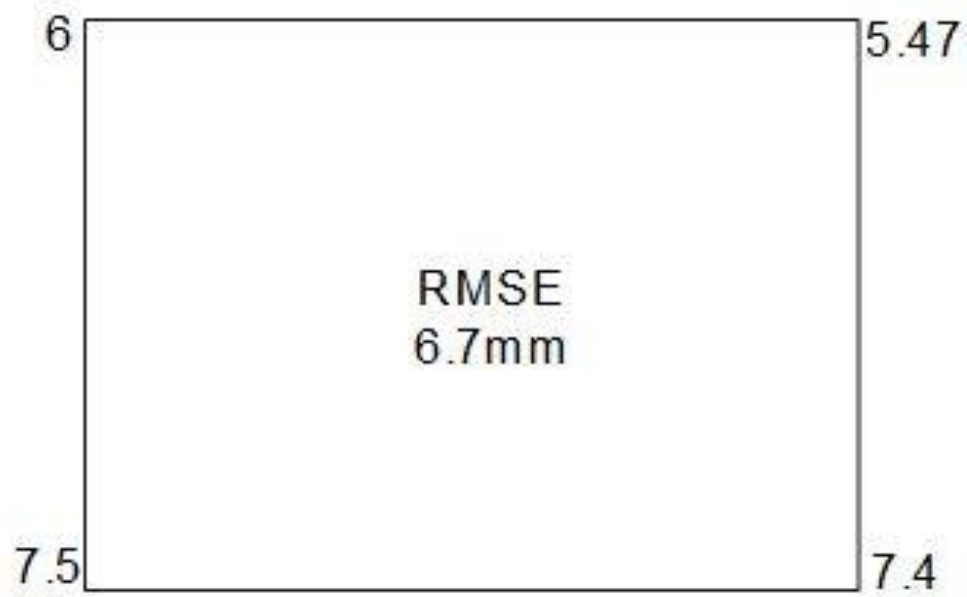


Figure 4.13. Control point 3-D residuals

4.2. SITE (A2)

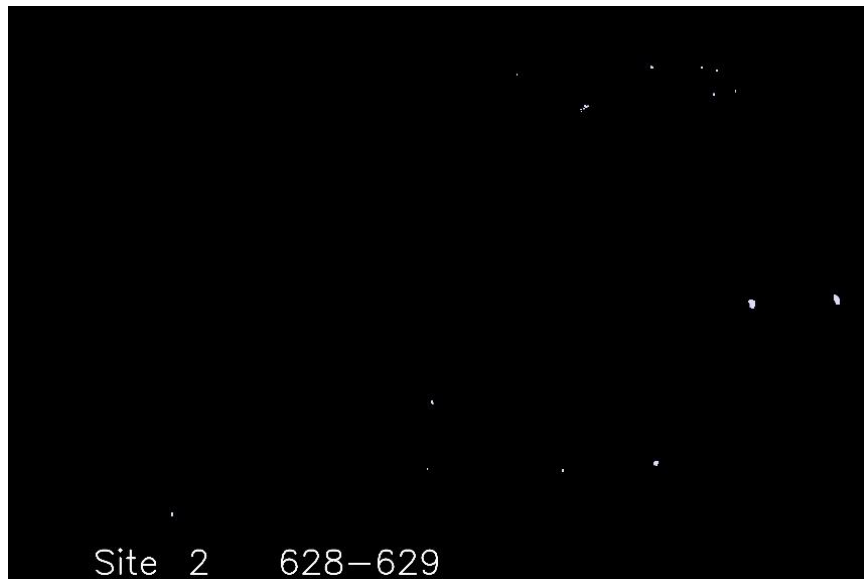


Figure 4.14. Difference between Scan 1 (6/28/2012) and Scan 2 (6/29/2012) of site A2, shows traces of loose material (white)



Figure 4.15. Difference between Scan 1 (6/28/2012) and Scan 3 (6/30/2012) of site A2, shows increase in lost material amount (white)

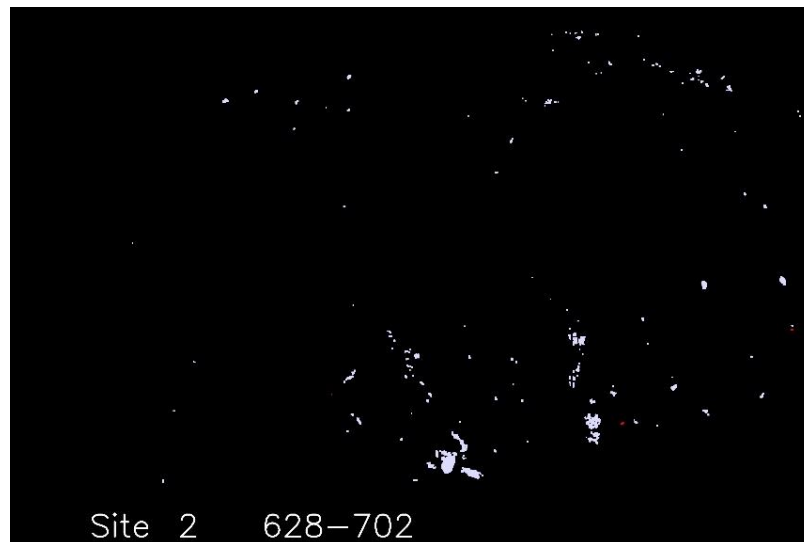


Figure 4.16. Difference between Scan 1 (6/28/2012) and Scan 4 (7/02/2012) of site A2, shows slight gained material (red), and increase in lost material (white); more pronounced compared to scan number 2

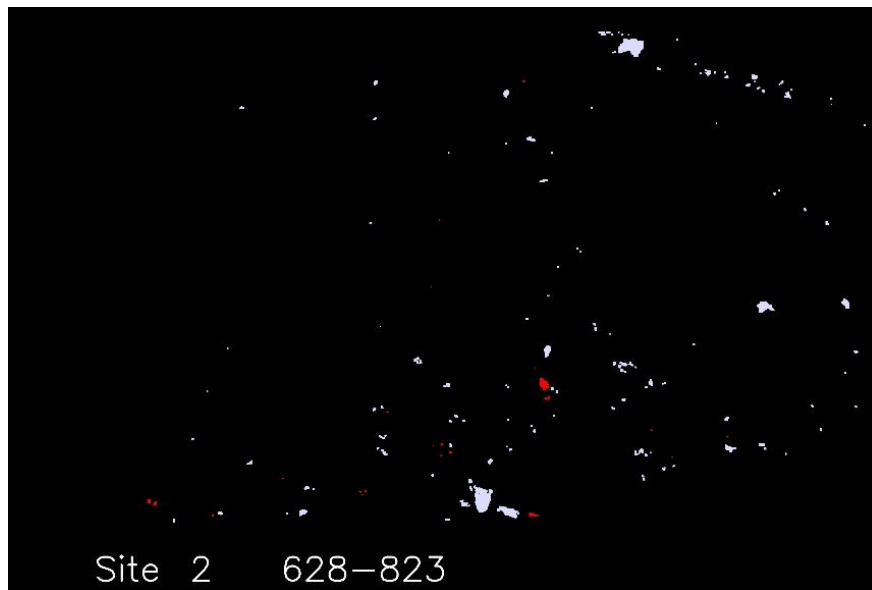


Figure 4.17. Difference between Scan 1 (6/28/2012) and Scan 5 (8/23/2012) of site A2, shows slight increase in gained material (red) and slight increase of lost material (white) compared to scan number 3

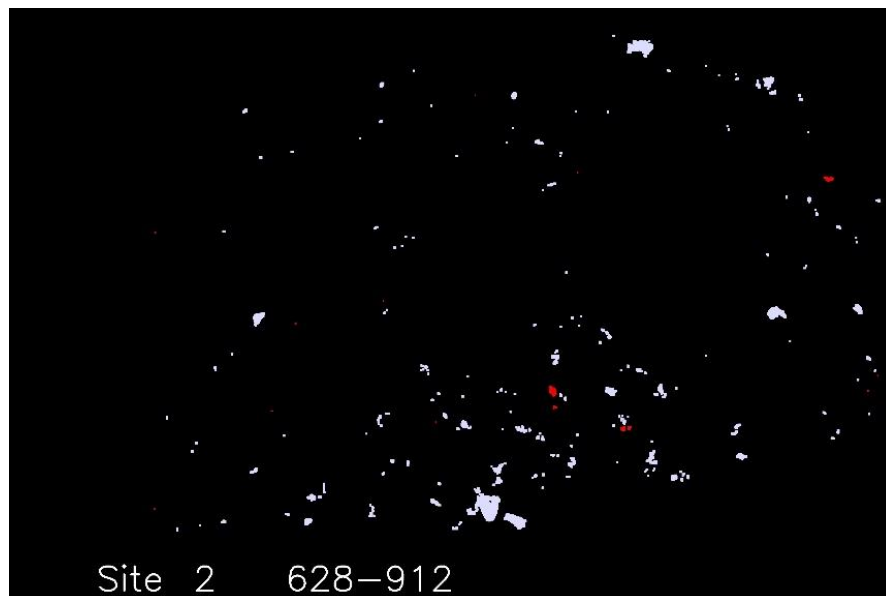


Figure 4.18. Difference between Scan 1 (6/28/2012) and Scan 6 (9/12/2012) of site A2, shows slight decrease in gained material (red) and slight decrease of rock fall (white) relative to scan number (3 & 4)

4.3. SITE (A3)

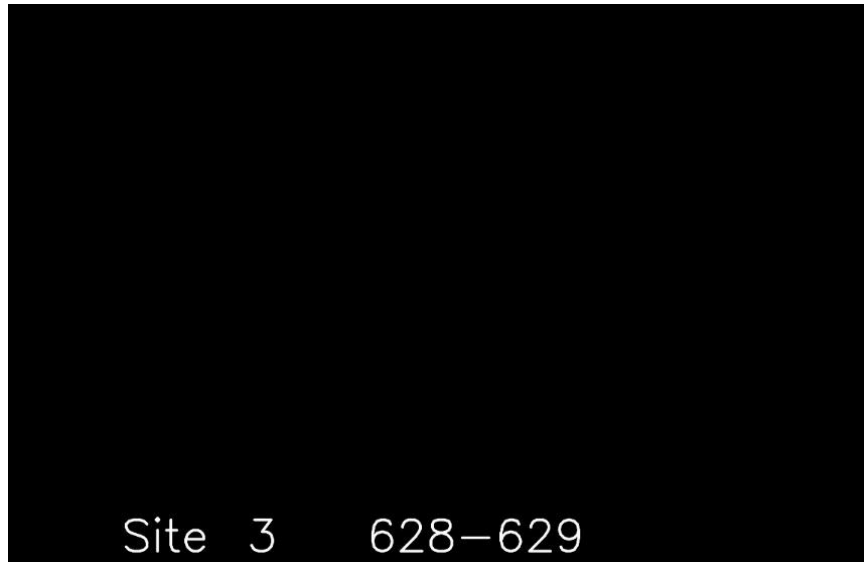


Figure 4.19. Difference between Scan 1 (6/28/2012) and Scan 2 (6/29/2012) of site A3, shows no change in slope face of outcrop



Figure 4.20. Difference between Scan 1 (6/28/2012) and Scan 3 (6/30/2012) of site A3, show no change in slope face of outcrop

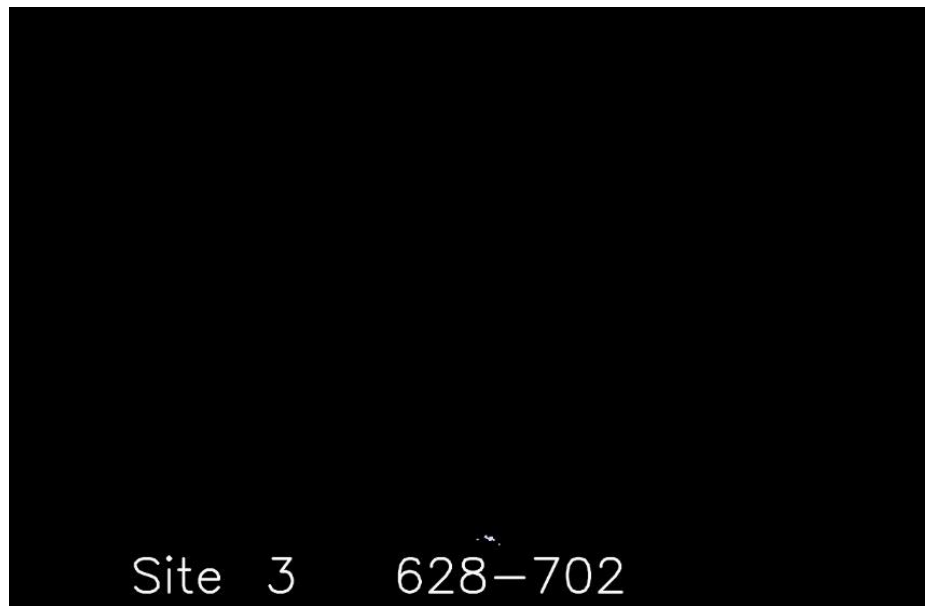


Figure 4.21. Difference between Scan 1 (6/28/2012) and Scan 4 (7/02/2012) of site A3, shows traces of lost material (white)

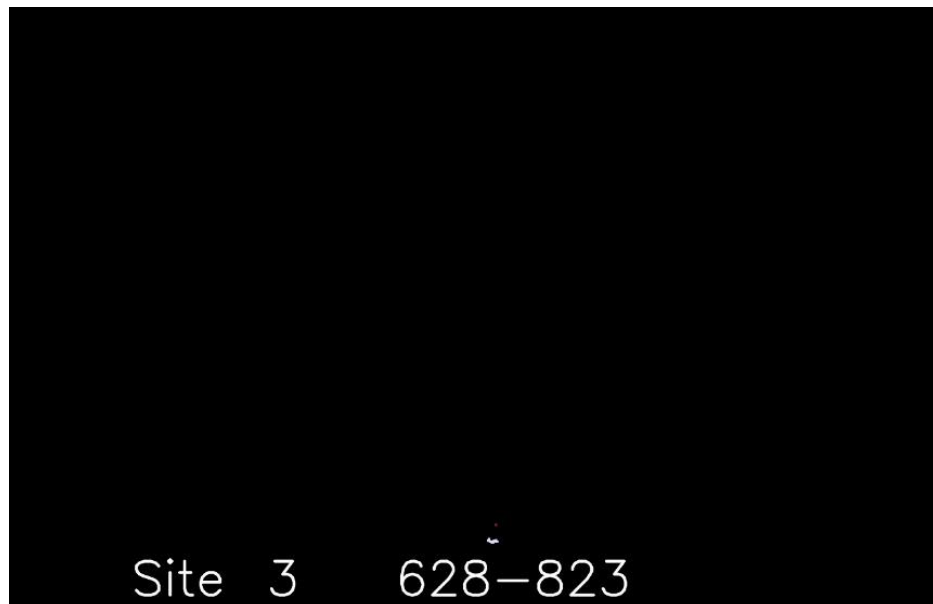


Figure 4.22. Difference between Scan 1 (6/28/2012) and Scan 5 (8/23/2012) of site A3, shows traces of lost material (white)

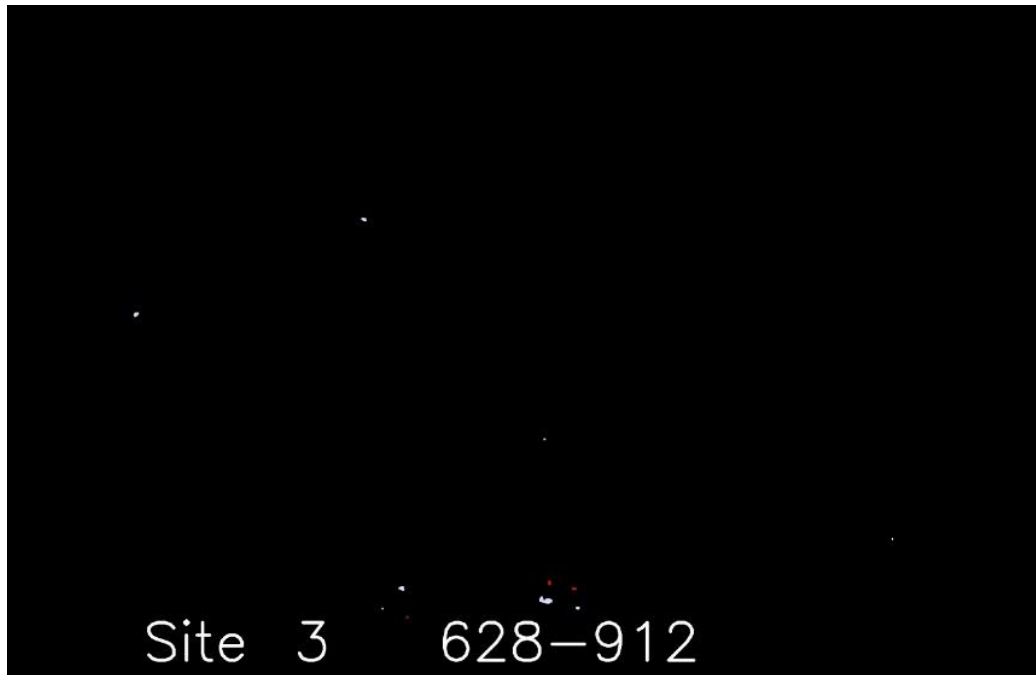


Figure 4.23. Difference between Scan 1 (6/28/2012) and Scan 6 (9/12/2012) of site A3, shows insignificant amount of gain (red) and slight change of lost material (white)

5. DISCUSSION

Results obtained by this study for site A1 and A2, as displayed in Figure 4.1 to Figure 4.18, indicate different degree of hazard due to rock fall on Habs road.

Figure 4.1 of site A1 represents the reference scan, and it shows traces of lost material in the upper right corner of the scan. Due to coarse co-registration of images, indicated by the high value of RMSE (7.8 mm), the lost material (white) is not real value for the scan conducted between 6/28/2013 and 6/29/2013. The scan conducted in the following day for site A1 (6/30/2013), showed removal of material only recorded in 6/29/2013. The primary reasons for this removal attributed to the high precision of co-registration. Other factors that contribute to gain and/or loose of material, include climatic factors, were rain fall carries soft material through joints and fractures to subsurface forming slippery surfaces, and differential heating by sun leads also to rock cracking . Animal on the other hand affect loose and gain by moving loose material into voids, while wind can also have the same affect by sweeping transportable earth material into voids or remove the material binding rocks together . These factors affect the scan results by re-working the material, and could lead to filling the depressions or further excavate voids. On the other hand, the material transported down slopes to the ground surface, in relatively steep slope faces. The study area falls within a region, which experiences frequent earthquakes that often felt by the population, and recorded by earthquake recorders. During my research in 2012, there has been no earthquake activities.

These earthquakes would likely affect the stability of slope faces materials and may cause falling loose material.

Of the main factors that explains the increase in lost material in Site A1, is the block-in-matrix nature of this site, in which large blocks dominate its upper section, whereas its lower part is relatively stable.

This research suggests that the upper part of Site A1 was probably a paleo channel, where large trimmed blocks occupy the base of the upper part, and the smaller, softer materials occupy the upper part (Figure 5.1). The results of site A1 are shown in (Figure 5.2).



Figure 5.1. Suggested paleo-channel location of Site A1

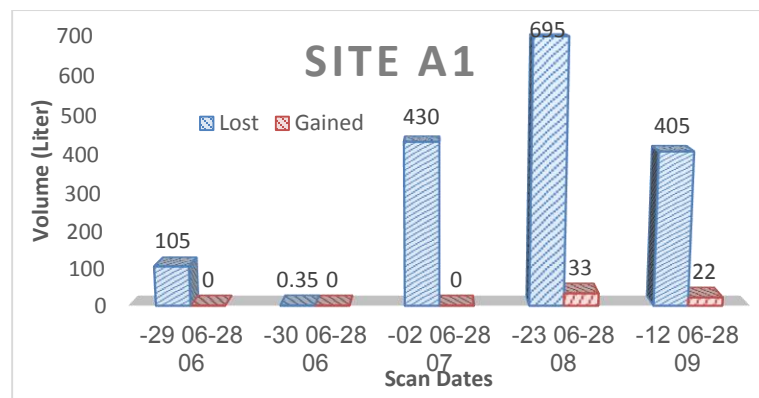


Figure 5.2. Site A1 shows the amount of lost/gained material during scan dates, measured in liters

Figure 4.1 showed false increase in the reported volume material lost (105 liter) that dropped to the real volume count of 0.35 liter in the following day scan. Increase in reported volume continued to a maximum value in the 4th scan to reach 695 liter for this site. The last scan (6), showed decrease in reported volume, compared to previous scans (Figure 4.11), which could be attributed to the reasons stated previously.

Site A2 consist of a relatively medium to small blocks that primarily represent disintegrated meta-sedimentary rocks. The sharp edges of these blocks indicate its high-grade metamorphism and its less susceptibility to weathering processes (Figure 5.3).



Figure 5.3. The picture shows Site A2, where sharp edge, disintegrated blocks of Basalt dominating the location

Similar to site A1, site A2 displayed linear, steady increase of lost material from 150 liter to maximum of 588 liter (Figure 5.4). Fluctuation for gained material (0, 11, 2, 45 & 43), could be attributed to fill of voids by unconsolidated material.

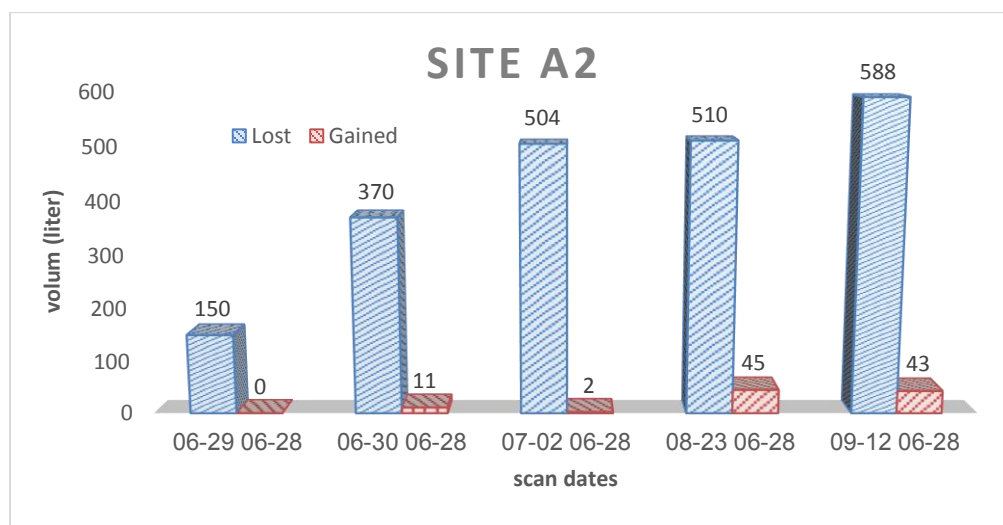


Figure 5.4. The figure shows the amount of lost/gained material for Site A2 during scan dates, measured in cubic liters

Site A3 This site is different from both site A1 and A2 in that it is composed of massive Meta-sedimentary rocks (Figure 5.5), and scans conducted on this site showed no lost volume change in material in second and third scan (Figure 4.20 and Figure 4.21). a slight increase of lost material was recorded in the 4th and 5th day of the scan, while noticeable increase of lost material (10 Liter) recorded in the last scan (Figure 5.6). No change in gained material was observed in this site in the scans conducted in the 1st, 2nd, 3rd and 4th scan, with the exception of the 5th and 6th scan days, where slight increase in gained material was recorded. The massive nature of this road cut was the major cause of stability of this section of the road, despite the possibility of the occurrence of major and disastrous rock failures in occasions of effective earthquakes or due to extension of fractures to great depths and presence of lubricated slip surfaces.



Figure 5.5. Location of site A3, representing massive meta-sedimentary rock formation

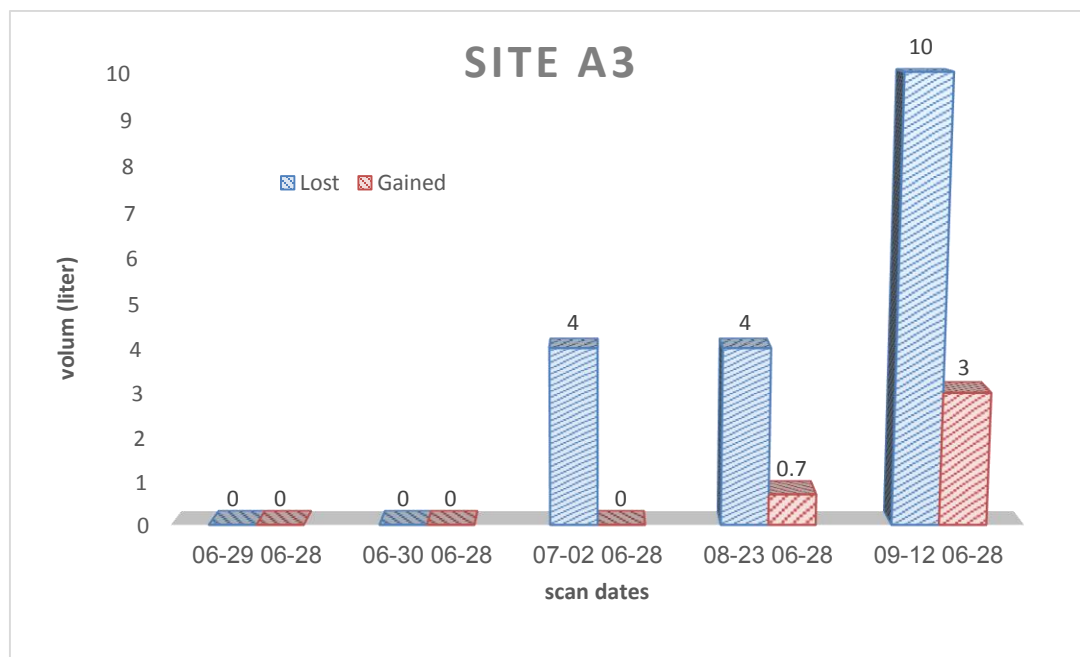


Figure 5.6. The figure shows the amount of lost/gained material during scan dates, measured in liters in site A3

6. CONCLUSION

No previous measurements of rockfall volume counts were conducted in this study area. So could that be used for reference and comparison with the findings obtained by this research. Traditional rockfall volume count, as mentioned in literature, have a number of limitations such as inaccessibility and safety, and as well, prone to human errors, since studies require measuring irregular shapes of rocks. On the other hand, there are difficulties covering relatively large areas, as this require considerable number of working force, capital, and logistics.

The use of LiDAR in this research helped in resolving the major issues, deemed difficult using traditional methods. The study highlighted a number of points:

(1) In steep sloping road cuts, voids left by falling blocks could possibly be refilled by loose material falling down from higher above, otherwise, falling rocks reach state of stability when they rest on the ground surface

(2) The program developed at Missouri University of Science and Technology successfully utilized in obtaining precise measure for lost and gained material.

(3) Modifications on the program by considering slope steepness and the other factors (animal trampling, human activity, rainfall wash and wind) added to the refinement of the results and increased accuracy.

7. RECOMMENDATION

This study recommends:

A- Engineering solutions

1- Data collection need to be extended for a year to cover different climatic conditions, and number of scans need to be increased to allow for better interpretation and testing of the significance of LiDAR as a tool for rockfall volume count

2- Site A1 requires:

- Constructing deep and wide ditches, with the base of the ditch be covered by a layer of gravel to absorb the energy of falling rock.
- Installation of double twisted wire mesh blankets for the upper part of the road-cut.
- Installations of Warning signs

3-Site A2 requires:

- Installation of perpendicular flexible rock fall fence at the lower end of road cut, to collect the frequently falling rock blocks from the slope.
- Frequent cleaning of fence

4-Site A3 requires:

- Scaling of loose materials.

B- Recommendations applicable to data acquisition and processing

- The study recommends increasing image resolution by changing scanner resolution setup from 6, 8 and 10 mm (used in this study) to 3,4 or 5 mm
- For perfect co-registration, use of spherical fixed targets are superior over unstable flat surfaces or points (applied in this study), in producing extremely accurate image-to-image co-registration.
- The study recommends changing the maximum value of (RMSE) to ~ 0.5 instead of to 1.5, such that, ScanStation II pixel resolution of 4.0 mm, produce co-registration discrepancy of 2.0 mm instead of 6.0 mm.

- This study recommends increasing the number of control points to minimum of 9 points, distributed on the corners, the middles sides of rectangle, and a point at the center of the scanned area.

APPENDIX

**LIDAR APPLICATIONS TEAM
MISSOURI UNIVERSITY OF SCIENCE AND TECHNOLOGY
ROLLA, MISSOURI
NOVEMBER 2014**

Kenneth J. Boyko

Content

- Focus of Missouri S&T Lidar Software
- Overview of S&T Lidar software
 - Linux development environment
 - Windows port of software
 - Software License
 - Differences between research and consumer-oriented software
- Characteristics of Lidar data
 - Random point cloud
 - Mirror swing inertia error
 - Lidar Export data format
- Directory structure
- Internal data structure
- Mapping Options
- Processing Limitations
- Overall flow – programs, inputs, outputs
 - Lidarsw-based registration process
 - Cyclone-based registration process
 - Console operation
 - Dir command
 - Running an application
 - Stopping an active process

- Major Software Modules
- Site Selection
- Acquiring a Scan
- Exporting Data from Cyclone
- Detailed Instructions for each Software Module
 - ckrmse
 - regpts
 - findMinMax
 - load
 - register
 - elimVeg
 - diff
 - calcvol
 - view2Surf

Focus of Missouri S&T Lidar Software

The focus of the Missouri S&T Lidar software is change detection. Applications which require static measurement of large complex objects could probably be fulfilled using Cyclone alone. However, if quantitative measurements of change (volume determination) are required, the specialized functions developed within the suite of the Missouri S&T software may be of value.

Overview of S&T Lidar software

The basic approach used in change detection is to acquire a high-resolution Lidar scan at two different dates, subtract them from one another to create a 'difference' surface, and analyze that difference surface for the changes which occurred over time. While simple in concept, there are several processing steps required to accomplish this task.

First of all, when Lidar data is acquired, it represents the object being scanned with millions of (x,y,z) triplets based on a local coordinate system that physically depends on how the Lidar unit was set up. In other words, every time the Lidar unit is set up for a scan, it will be in a slightly different position and orientation relative to the object being scanned, and a slightly different coordinate system will be used for object representation. Therefore, before the two Lidar datasets can be subtracted from each other, they must be brought to the same coordinate system. This process is called registration, and is accomplished by one of two methods within the Missouri S&T Lidar software.

Secondly, the raw point-cloud data exported from Cyclone, at least in the xxx.pts format, is highly unstructured. It can be viewed as a random bucket of (x,y,z) triplets in no particular order. It would be meaningless to attempt to subtract one unordered bucket of points from another – some degree of structure must be created before the data can be manipulated by higher-order functions such as surface subtraction. The **findMinMax** and **load** programs are responsible for providing the required structure to the Lidar data to support further processing.

Finally, there are many data artifacts that must be dealt with if accurate change volume is desired. For example, vegetation within the scene may introduce false changes due the fact that it is changing in position (blowing in the wind) both during the scanning operation, and between scanning dates. It may itself be growing in volume, which would introduce significant error if not dealt with. Other artifacts are caused by vehicles, insects, falling leaves, birds, or other things passing between the Lidar and the object being scanned during a scanning operation. These situations cause large spikes in the Lidar surface which must be removed prior to volume determination.

While some of these artifacts may be easily removed manually within Cyclone using the basic fencing functions provided, the more complex artifacts are difficult to remove. For example, small tufts of vegetation embedded within rock coves would be very difficult or require too much time to remove manually. Further, the inconsistency of manual removal would introduce additional error in the surfaces. The Missouri S&T Lidar software provides some automated approaches to deal with many of these practical processing issues.

Linux development environment

The Missouri S&T Lidar software is being developed primarily within the Linux operating system, due to the several advantages that Linux offers for research-oriented software. No other commercial libraries are used in the suite – only freely available libraries such as OpenCV and OpenGL are used.

The software is written in C++, using the GNU GCC compiler. Everything in the entire software suite is platform-independent, meaning that while the development is primarily conducted within Linux, there is nothing preventing the porting of the software to other operating systems, such as Windows.

Some of the more computation-intensive software is in the process of being converted from the original single-thread, single-CPU implementation to a parallel environment involving several CPU's and GPU's. These parallel ports are research in nature and in some cases, has resulted in improvements in performance over two orders of magnitude. Due to the specialized hardware (Nvidia GPU cards) and software (CUDA development environment), the parallel versions of selected software modules will most likely remain in a research environment. The primary operational environment for most of the Lidar applications will continue to be within the Windows environment – simply because this is the most common environment within the Lidar Applications Team.

Windows port of software

A windows port of this research code was created during the spring of 2013 using the latest version of the software. This port represents a snapshot of the May 2013 version. The port was created using Visual Studio Express 2010 and currently runs on both Windows 7 and Windows 8 operating systems.

Being research-oriented code, the port was mainly focused on providing similar functionality to the Windows environment as currently exists within the Linux version. Since most of the Linux software operates in terminal windows, the Windows version currently operates similarly – as a console application. The next Windows port will most likely be wrapped in a Graphical User Interface (GUI), thus, making it appear more like mainstream Windows applications.

Software License

The software is being released (executables only) to the Saudi Geological Survey (SGS) for research and/or academic use only. The software is not licensed for any commercial applications. The software executables may be copied to any SGS government computer system as long as the terms of the license release are honored.

The software has undergone basic technical testing of the algorithms, but has not been certified for applications involving assessment of risk to human health, life, or property.

The Missouri University of Science and Technology assumes no liability for use of this software outside it's intended research-oriented purpose.

Differences between research and consumer-oriented software

It is important to stress that the Missouri S&T Lidar software, at this stage, is still primarily research-oriented code. The following table highlights some differences between research-oriented software and consumer-oriented software:

Characteristic	Research-oriented software	Consumer-oriented software
Focus	Algorithm development	Ease of use, simplifying complex functions to make them accessible to the public at large
Operating environment	Terminal-based	Graphical User Interface (typical Windows environment with drop-down menus, dialogs, wizards, etc)
Target user	Programmers, developers	Users with varied backgrounds, may be non-technical
Error trapping	Minimal and cryptic	Extensive hand-holding and anticipation of common user errors
Progress messages	Extensive and tied to internal implementation	Minimal and usually in form of graphical 'progress' bars
Setup	Run-time parameters and manually-built configuration files	Wizards, dialog boxes, menus, option preferences
User-base	Small	Large
Flexibility / Adaptability	High – constantly being modified to handle newly discovered requirements	Low – capabilities static within a release
Frequency of versions	New At times, hourly – highly dynamic	Infrequent - yearly
Stability	Bleeding edge versions can be unstable, longer term builds more stable	Very stable
Degree of testing before release	Variable – long term versions are tested for technical cases	Extensive – formal testing against extreme conditions to handle just about any anticipated circumstance.
Expertise of User	High – usually the developer	Low - Software is made idiot-proof.

The Windows port was created to make this research-oriented software accessible to other research-oriented individuals and organizations. The Windows port does **not** represent any intent to move the state of this software towards a consumer orientation. That may occur in the future, but the current state of both the Linux and Windows implementations of this software is still primarily research-oriented.

Characteristics of Lidar data

The ScanStation-II Laser Lidar Scanner is a surveying instrument which creates highly accurate 'point cloud' data of an object. When in scanning mode, the Lidar sends out pulses of laser

light, and for each pulse, keeps track of the time it takes the pulse to leave the Lidar, reflect off some object, and return to the Lidar – this is known as time-of-flight. Knowing the speed of light in air, the Lidar calculates the distance from the Lidar to whatever the pulse hit. The Lidar also keeps track of the horizontal and vertical angles of the laser beam – this, together with the time-of-flight determined distance allows the Lidar to compute a precise (x,y,z) coordinate of where the pulse hit on that object.

The Lidar sends out approximately 15,000 pulses per second. While the pulses are being sent out, an oscillating mirror directs the pulse train up and down. In addition, while the vertical mirror is oscillating, the whole unit slowly revolves. This results in a relatively equally spaced pattern of points being established on the surface of the object being scanned. The point cloud density can be controlled by the user, and usually represents a point density of 5-20 mm spacing between the points in both the horizontal and vertical directions. The collection of points collected during a scanning operation is known as a point cloud.

In just a matter of a few minutes, the Lidar is capable of collecting millions of points describing the outside surface of an object. For each point, the data collected include its 3-D coordinate (x,y,z) in some local coordinate system, the intensity return (a number indicating how much energy was detected on the return path), and the color of the object hit as represented by three color values – a red, green, and blue (RGB) color representation.

The spatial coordinates (x,y,z) are in a local coordinate system defined by how the Lidar was set up. The Lidar is always at position (0,0,0). The positive Y axis is in the direction the Lidar is pointing at its 'home' position. The positive X axis is aligned to the right of the Lidar (normal right-hand coordinate system). The positive Z axis is 'up', relative to the actual orientation of the Lidar. If care is taken to level the Lidar unit, the positive Z axis points up. If the Lidar unit is not level, the Z axis may not represent a vertical direction. The user can select any units for the spatial coordinates, but normally, the units are defined to be in millimeters. The spatial coordinates are represented by floating point numbers usually to at least 3-4 decimal places. The accuracy of these points depends on their distance from the Lidar, but are usually within a few millimeters for distances under 30 meters.

The intensity return is an integer that ranges from approximately -2000 to +2000, and represents the relative brightness of the object at the point where the laser beam hit. In reality, it can be thought of as the albedo (reflectivity) of the object at the wavelength of the laser (green laser light). The intensity return is relative reflectivity value – highly specular (mirror) surfaces reflect the laser pulse off to some other direction, so no energy is ever returned to the Lidar unit. These points tend to have very dark intensity. Flat white, or retro-reflective materials, such as reflective tape, tend to have very high intensity return values, since much of the original pulse energy is returned.

The color information (RGB values) are derived from a separate lower-resolution color camera used to acquire preview images prior to scanning. While these images are useful for planning the actual scan, they are less useful for analytical use because of slight miss-registration between the RGB image and the actual object. Up to 1-2 cm of image shift has been observed

in the RGB image. Therefore, the RGB images should never be used for analytical purposes – they are mainly to be to the set-up for a scanning session.

The RGB values are unsigned positive integers with 8-bit domains (values vary from 0 to 255). Colors are represented by the relative value of these three numbers, for example, red would have RGB values of (255,0,0). RGB values for common colors are as follows:

Color	Red value	Green value	Blue value
Red	255	0	0
Green	0	255	0
Blue	0	0	255
Magenta	255	0	255
Cyan	0	255	255
Yellow	255	255	0
Black	0	0	0
Dark Gray	80	80	80
Light Gray	160	160	160
White	255	255	255

The points in a Lidar point cloud represent the 'first return' for each pulse of laser energy sent out. More sophisticated Lidar systems employed in aerial acquisition platforms typically record multiple returns per laser pulse. Having the whole 'return waveform' enables analysis of the texture and transparency of the object being scanned – for example, when forested areas are being scanned with a multi-return Lidar, some indication of the forest structure (height of canopy, density of undergrowth, forest floor) can be ascertained from the multiple returns. Since the ScanStation-II Lidar is a single-return device, each point represents the spatial and reflective properties of the first object hit by each pulse.

If some other object drifts in front of the laser beam during a scanning operation, there will be anomalous points within the point cloud data. These points, floating in space between the object being scanned and the Lidar unit are most often caused by small insects, falling leaves, or other objects that happen to drift into the field during an active scan.

Frequently when scanning rock cuts along a road, the Lidar unit is set up across the road to obtain a good view of the whole area under study. With this set-up, it is common for vehicles to pass in front of the Lidar during the scanning operation, especially if a very fine resolution is being used, and the scan takes several minutes to complete.

All of these types of data artifacts must be removed prior to quantitative analysis because they introduce large spikes in the data. Many of the simple artifacts, such as those caused by passing vehicles or flying insects can be easily removed using the 'polygon fence' and 'delete outside' functions available within Cyclone. However, more complex artifacts, such as those caused by wind-driven moving vegetation or insects flying within a rock cove cannot be easily removed with the basic edit tools available within Cyclone. To detect and remove these types of artifacts, the program **elimVeg** can be used.

Random spatial ordering in point cloud data

Since the points are collected in sequence, one might expect that the individual points in a point cloud file would be in some regular order – related to the sequence in which they were collected. With Leica ScanStation-II data in the xxx.pts format, this is not the case. While the points seem to follow large-scale ordering, on a micro-scale, the point order in the file is not related to the point's spatial position or sequence of acquisition. This makes it necessary to spatially order the points into a regular mesh. The spatial ordering of raw points into a complete mesh is the function of the programs **findMinMax** and **load**.

Mirror swing inertia error

On sharp horizontal edges, a small timing error relating to the position of the vertically oscillating mirror results in adjacent columns in the point cloud being slightly offset from each other – appearing similar to an interlace offset. This effect is minor, and results in points vertically out of position by as much as one or two cell units, where the cell unit is equivalent to the scanning resolution. This error cannot be accurately modeled – it is only mentioned as a reminder that the raw point cloud data has a few natural visible anomalies, this being one of them. The interlace error occurs on horizontal edges only, and does not affect vertical edges:



Lidar Export Data format

The Missouri S&T Lidar software uses Lidar data exported from Cyclone in the Leica PTS format. This is a simple ASCII text format where each point in the point cloud is represented

by a single line in the file. For each point, seven data elements are presented: the (x,y,z) coordinates of the point, the intensity return, and the (R,G,B) color of the point.

The xxx.PTS files can be rather large – a point cloud dataset consisting of 4 million points is typically 250MB in size. While these files can be viewed in a simple text editor such as NotePad, because of their size, the NotePad application either runs very slow, or hangs up. If the user wishes to cancel a hung-up application, the Windows Task Manager can be used to halt and end the NotePad application.

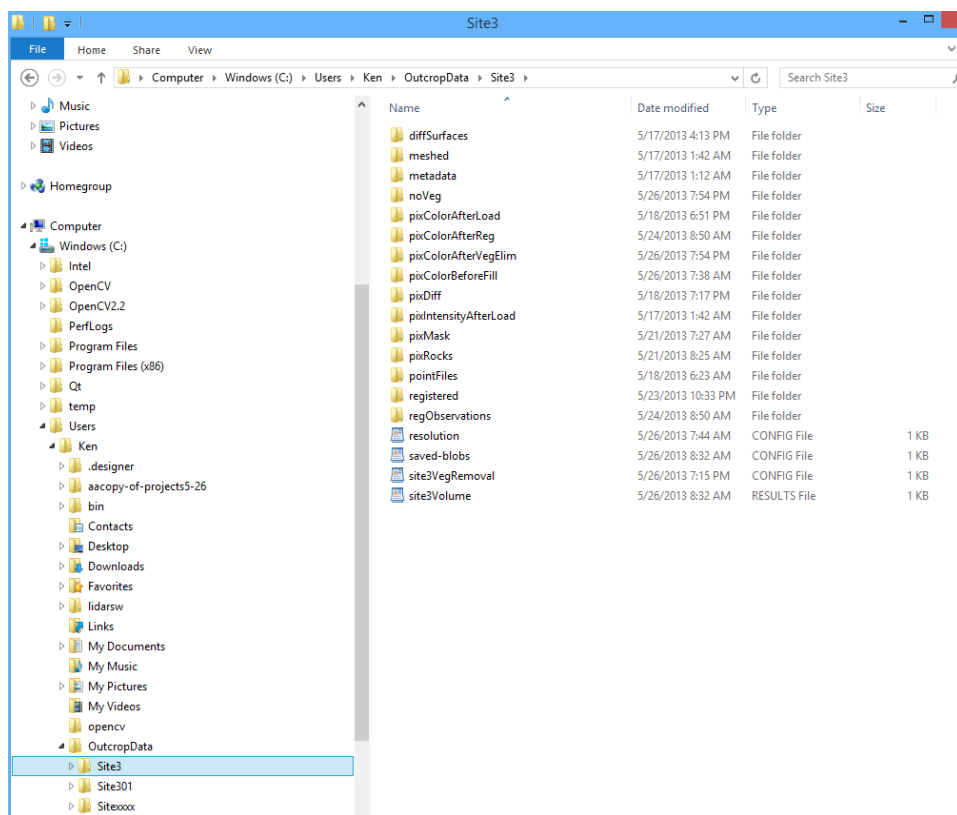
Directory structure

The directory structure for Lidar data processing is as follows:

```
C:
  Users
    Username    (this will vary – depending on the name of the user)
      OutcropData
        Site1
        Site2
        Site3
        .
        .
        .
        Site202
        Site203
        (etc)
```

OutcropData is the highest level directory for all Lidar data. Each 'Site' represents a geographic location under study. Sites are named using a number; sites cannot have names like 'Site1-a' or 'site red rocks'.

Sample Directory Structure:



Each site has a fixed number of directories for representing the Lidar data at different phases of processing. For example, when the xxx.PTS files are first exported from Cyclone, they are copied into the 'pointFiles' directory. After the findMinMax and load programs are run, the meshed Lidar data is written to the 'meshed' directory. The 'registered' directory contains Lidar data that has been run through the registration process. After vegetation is eliminated, the resultant Lidar data is written to the noVeg directory. The various 'pix.....' directories are used to store pictures generated at various points in the processing.

In addition to the directories established for each site, there are two configuration files – resolution and sitexVegRemoval. These are set-up files which control the behavior of the **load** and **elimVeg** programs.

The resolution configuration file contains user-set options to define how the Lidar data is to be loaded. Important data elements such as mesh resolution and mapping options are defined in this file.

The sitexVegRemoval configuration file contains user-set parameters that define how the vegetation elimination program is to operate. This file is automatically generated after the first time **elimVeg** is run on any dated dataset in a site, and contains a saved copy of all the slider settings established by the user during the interactive **elimVeg** session. When **elimVeg** is subsequently run on all the other dated datasets in the site, this file is used to apply the same saved slider settings to those datasets.

The 'Sitexxxx' directory can be used as an empty template to copy and rename if additional sites are desired. For example, if the user wishes to create a new site numbered 243, the following steps can be taken:

1. Copy Sitexxxx directory
2. Paste to OutcropData directory
3. Rename 'Copy of Sitexxxx' to 'Site243'

Now Site243 is established with a fresh set of empty directories. Make sure that the file resolution.config is updated to reflect the processing parameters desired for this new site.

Each site represents a single geographic area under study. The spatial domain (scanning boundaries) and scanning resolution will always be the same for all scans conducted on a site. Any number of dated scans can be inserted into a site. For example, if site 267 was scanned each week for one year, the pointFiles directory for site 267 would contain 52 xxx.PTS files (exported from Cyclone). Each PTS file would have a name which encodes the date and site in the following format:

yyyy-mm-dd-s.pts

For example, the scan from April 23, 2013 would be named: 2013-04-23-267.pts

Internal data structure – the xxx.bin files

Within each of the directories holding Lidar data such as such as meshed, registered, noVeg, files with a 'bin' extension are used to represent the Lidar data. These files cannot be opened or viewed with any program – they are compact binary representations of the Lidar data used only by the Missouri S&T Lidar software.

Some computers miss-interpret the '.bin' extension and might lead the user to believe these files are video files which can be viewed in a video viewer. Of course, this is not the case, and any attempt to open these files risks damaging them if an application attempts to write to them. Therefore, the '.bin' files should be left alone – they are only to be used internally by the Missouri S&T Lidar software.

Mapping Options

There are two options to define how the coordinate system of the pts file are mapped to the internal cell-based data structure – spherical mapping and ground plane mapping. The internal cell-based data structure can be thought of as a grid or raster structure (similar to an image format) having 4300 columns and 3400 rows. Each cell within this structure stores information about an idealized 'point' within the Lidar point cloud.

With the spherical mapping option, a grid is laid out on an imaginary spherical surface with the Lidar unit at the center of the sphere, and the sphere radius being equal to the probe distance used during the scan. The grid is laid out with the wide dimension (4300 cells wide) aligned with the horizontal direction (X-axis of the pts coordinate system), and the shorter dimension (3400 cells high) aligned with the vertical direction (Z-axis of the pts coordinate system). Since the grid is projected on a spherical surface, each cell is defined using angular units. This representation model most closely reflects how the Lidar data was actually collected, and is the option most often used.

With the ground plane mapping option, the grid is laid out using a normal Cartesian coordinate system with the width (4300 cells wide) aligned with the Y-axis of the pts coordinate system (+Y facing right) and the height (3400 cells high) aligned with the X-axis of the pts coordinate system (+X facing down). Since the grid is planar, each cell is defined using linear units.

For projects involving change-detection and volume calculation for slopes ranging from 40 degrees to vertical faces, the spherical mapping option should be used. For projects involving relatively flat areas (subsidence studies), the ground plane mapping option should be used.

Processing limitations

The internal cell structure used for all the programs utilizes statically allocated fixed-size arrays for the performance advantages they offer. The arrays were sized to handle a wide variety of research requirements, but do have limitations.

The horizontal extent is limited to 4300 cells, while the vertical extent is limited to 3400 cells. The maximum areal coverage for projects depends on the mesh resolution used and these limits. For example, if a mesh resolution of 10mm is used, the software would be capable of handling an area 43 meters in width and 34 meters in height. (4300 cells * 10mm/cell = 43000mm = 43 meters)

The mesh resolution (in millimeters) multiplied by the number of cells (horizontal and vertical) defines the largest area that can be processed. Alternatively, the actual project width and height divided by the applicable cell limits (4300 horizontal and 3400 vertical) would determine the smallest mesh resolution that could be used for that site. For example, if a site had a width of 85 meters and a height of 75 meters, the smallest computed horizontal mesh resolution would be $85000\text{mm} / 4300 \text{ cells} = 19.76 \text{ mm per cell}$. The smallest computed vertical mesh resolution would be $75000 \text{ mm} / 3400 \text{ cells} = 22.05 \text{ mm per cell}$. Therefore, since the cell shape is always maintained to be 'square' internally, the smallest mesh resolution that could be used for this project would be 22.05 mm per cell (the **larger** of the computed horizontal and vertical mesh resolutions)

It is important to note that the mesh resolution specified in the resolution.config file is quite independent of the scanning resolution used during data acquisition. Normally, the mesh resolution is set to the same resolution used for scanning, but this is not strictly necessary.

If the scanning resolution is finer (smaller) than the mesh resolution, there will be, on average, several lidar 'hits' per cell – and the software will assign the 'depth' of the cell using either the closest, farthest, or average of all hits for that cell (this option is also set in the resolution.config file). If the scanning resolution is coarser (larger) than the mesh resolution, some cells will receive no hits. During the load program, the software will detect cells having no lidar 'hits' and will determine a depth and color for that cell using a weighted average of the surrounding cells that did have hits.

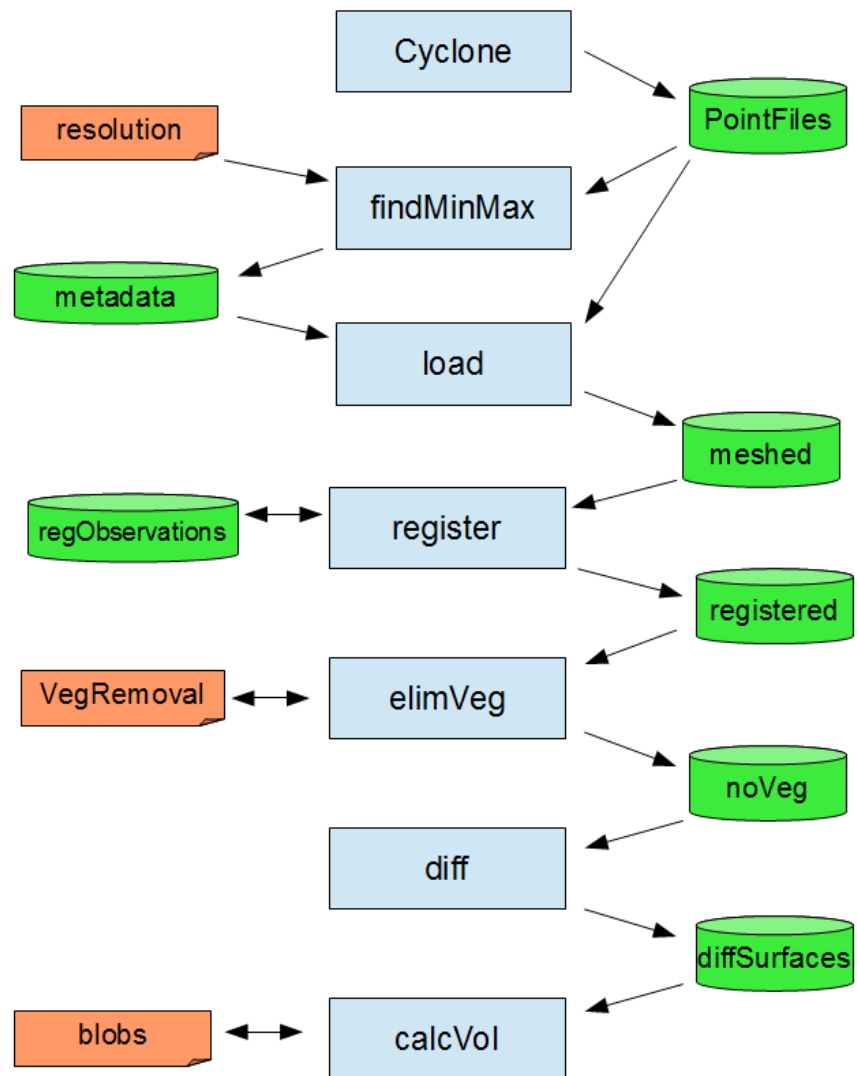
When the scanning resolution is finer than the mesh resolution, the main result is wasted scan time, since the preserved object detail can never be finer than the mesh resolution. When the scanning resolution is coarser than the mesh resolution, empty cells will be filled in, but the dataset will contain a large amount of artificially created data for these filled cells. If it is important to preserve the maximum amount of original object detail, and minimize scanning time, it is best to use a mesh resolution that matches the scan resolution used.

Overall flow – programs, inputs, outputs

There are two overall production flows – one if registration is accomplished using the Missouri S&T Lidar software (lidarsw), the other if registration is accomplished using Cyclone. For most situations, the registration method using lidarsw will be faster, easier, and just as accurate. The Cyclone-based method is more manual, more tedious and time-consuming, but may have slight accuracy advantages in certain circumstances. The Cyclone-based approach is only used in cases where the control points are scanned separately at a higher resolution than that used for the rest of the object under study.

Summary of Process Flow

(with lidarsw-based registration)



Symbol Key:

Config file

program

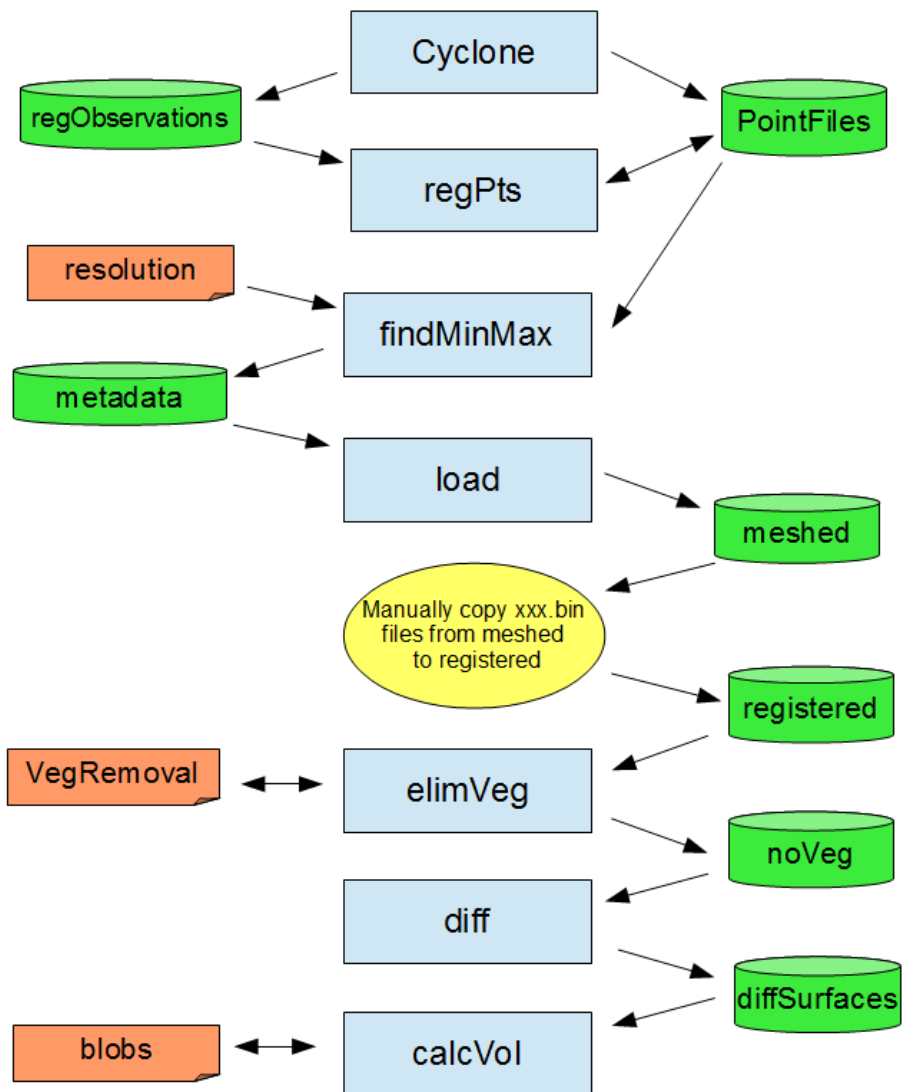
directory

Lidarsw-based Registration Process

1. Crop Lidar data in Cyclone for consistent left-right and top-bottom borders
2. Export Lidar data using pts format and file naming convention (yyyy-mm-dd-s.pts)
3. Establish a new (empty) site in the OutcropData directory
4. Copy exported pts files to pointFiles directory within the new site just created
5. Review resolution.config to ensure the right parameters are set
6. Run **findMinMax** for every dated Lidar dataset in the site
7. Run **load** for every dated Lidar dataset in the site
8. Examine the pixColorAfterLoad directory to ensure all files were processed correctly
9. Manually copy the base-date (earliest date) Lidar binary file from the 'meshed' to the 'registered' directory
10. For each of the dated Lidar datasets past the base-date, run **register** to transform the coordinates to those of the base date.
11. Run **elimVeg** on the base-date dataset. The first time **elimVeg** is run for a site, the program will initiate an interactive session to allow the user to experiment with various filter settings. After this interactive session is completed, all slider values will be saved to the file sitexVegRemoval.config – where it will be used when running **elimVeg** on all subsequent dated Lidar datasets.
12. Run **elimVeg** on the remaining dated Lidar datasets beyond the base-date. All of these runs will be conducted in a batch-mode using the vegRemoval.config file to define the operating parameters.
13. Run **diff** on all the non-base Lidar datasets
14. Examine the pixDiff directory to ensure the difference surfaces were built correctly
15. Run **calcvol** on all the non-base Lidar datasets
16. Examine the volume results in the volume report sent to the site directory

Summary of Process Flow

(with cyclone-based registration)



Symbol Key:

Config file

program

directory

manual action

Cyclone-based Registration Process

1. Crop Lidar data in Cyclone for consistent left-right and top-bottom borders
2. Establish a new (empty) site in the OutcropData directory
3. Manually read out control points in Cyclone and record the (x,y,z) coordinates for all four control points from both before and after lidar datasets.
4. Using NotePad, record the four control points in the following format: before (x,y,z), after (x,y,z), inserting a space between each number. Make sure to include all signs and decimal values. Save this file to the properly named file in the regObservations directory.
5. Run **ckrmse** to verify that 3-D rmse is under 1.5 times the mesh resolution
6. Export the base-date Lidar data to the site pointFiles directory and use the normal .pts extension
7. Export the all the non-base-date Lidar data to the site pointFiles directory, but instead of using the .pts extension, use the .after extension
8. Run **regpts** on all the non-base-date Lidar datasets. This will create pts files that have the same coordinate system as the base-date.
9. Review resolution.config to ensure the right parameters are set
10. Run **findMinMax** for every dated Lidar dataset in the site
11. Run **load** for every dated Lidar dataset in the site
12. Examine the pixColorAfterLoad directory to ensure all files were processed correctly
13. Manually copy all the Lidar binary files from the 'meshed' to the 'registered' directory

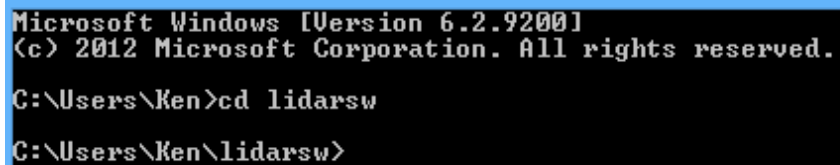
From this point on, the processing is identical to the lidarsw method of registration described above. Pick up at step 11 (**elimVeg**) of that process.

Console operation

For this release of the Missouri S&T Lidar Software, all programs are run in a terminal console. In Windows 7, the console can be invoked by: Start > All Programs > Accessories > Command Prompt. Alternatively, the terminal console can be sent to the desktop for easier retrieval. The terminal console window should be maximized at this point to make it easier to read all the program messages.

At this point, the terminal will be indicating the name of the current user (C:\Users\Ken>). In order to run the software, the directory needs to be changed to 'lidarsw' - this can be accomplished using the windows 'change directory' command as follows:

```
cd lidarsw <enter>
```



```
Microsoft Windows [Version 6.2.9200]
(c) 2012 Microsoft Corporation. All rights reserved.

C:\Users\Ken>cd lidarsw
C:\Users\Ken\lidarsw>
```

Now the user will be in the software directory, ready to run any of the programs.

Dir command

Once the user is in the lidarsw directory, the 'directory' command can be used to remind the user of the actual names of the programs.

```

Microsoft Windows [Version 6.2.9200]
(c) 2012 Microsoft Corporation. All rights reserved.

C:\Users\Ken>cd lidarsw

C:\Users\Ken\lidarsw>dir
Volume in drive C is Windows
Volume Serial Number is 8462-ECEE

Directory of C:\Users\Ken\lidarsw

05/26/2013  11:37 AM    <DIR>        -
05/26/2013  11:37 AM    <DIR>        ..
01/27/2013  06:18 PM                179,920  baboon.jpg
05/26/2013  08:31 AM                50,176  calcvol.exe
05/16/2013  10:17 PM                28,672  ckmse.exe
05/24/2013  09:19 AM                34,304  diff.exe
05/23/2013  10:30 PM                62,976  elimUeg.exe
05/23/2013  01:21 PM                 12     externalDriveName.txt
05/18/2013  06:48 PM                41,472  findMinMax.exe
05/16/2013  07:17 PM                 9,216  first.exe
05/22/2013  08:09 AM                 12     laptop-externalDriveName.txt
05/26/2013  07:31 AM                52,224  load.exe
05/23/2013  08:06 AM                 10     oneTouch-externalDriveName.txt
04/30/2013  01:55 PM                 219    osp1.txt
05/24/2013  08:46 AM                67,584  register.exe
05/26/2013  11:37 AM                50,176  regpts.exe
05/22/2013  08:47 AM               21,526,553  seg200xyz-ver2.txt
05/21/2013  07:43 AM                 278    site3Volume.results
05/23/2013  07:28 AM               152,596  test1.zip
05/25/2013  06:01 PM                34,816  view2surf.exe
05/23/2013  07:53 AM                38,912  writexyz.exe
          19 File(s)                22,330,128 bytes
          2 Dir(s)                40,228,155,392 bytes free

C:\Users\Ken\lidarsw>

```

Running an application

Programs have the extension '.exe' at the end of their name. To run any program listed after the DIR command is run, enter the program name (just the first part – the '.exe' is not necessary), followed by the run-time parameters defined for that program. A single space should be inserted between the program name and each run-time parameter. If the number or format of the run-time parameters is unknown, the user can either look that information up in this software manual, or simply type in the name of the program with no run-time parameters. The required run-time parameters will be displayed.

For example, the run-time parameters for the program view2surf can be determined by typing in the name of that program:

```

C:\Users\Ken\lidarsw>view2surf
initialize cell structures
external drive name: C:/Users/Ken
done initializing

initialize cell structures
external drive name: C:/Users/Ken
done initializing

initialize cell structures
external drive name: C:/Users/Ken
done initializing

*** error *** incorrect run-time arguments  correct form is:  view2surf s dir1 date1 dir2 date2 <enter>
s: site number
dir1: directory of first surface
date1: date of first surface
dir2: directory of second surface
date2: date of second surface

example to examine outcome of vegetation elimination: view2surf 1 meshed 2013-05-15 noUeg 2013-05-15 <enter>
example to examine outcome of registration: view2surf 1 registered 2013-05-15 registered 2013-05-16 <enter>

```

When a program finishes its processing with no errors, the message: **'orderly end of program'** is displayed to the console. The user should always look for this message on the console output. If the program stops without this message being displayed, it may be an indication that the program encountered an internal fault, which would require some follow-up investigation to determine the cause.

Stopping an active process

To stop an active process, left click anywhere within the terminal console (if other interactive windows are being displayed), hold down the 'ctrl' key, and hit the 'c' key. This will stop any program being run in the console terminal.

When a program is halted in this fashion, the program may be restarted by hitting the 'up' arrow key, which displays the last command line from the command line buffer. Hitting <enter> at this point will re-run the program. This feature uses the command line history buffer feature of Windows.

When a program is manually stopped using this process, the normal 'orderly end of program' message will not be displayed.

Major Software Modules

The current release of the Missouri S&T Lidar Software suite consists of nine programs:

ckrmse
regpts
findMinMax
load
register
elimVeg
diff
calcvol
view2surf

The full documentation for each program (what it does, how it operates, user instructions, examples, screenshots, etc) is covered in the next section of this software manual.

Site Selection

- Site should cover area with evidence of recent rockfall activity
- Site should be relatively void of vegetation – software can handle only thin-stemmed and small-leaved vegetation
- Measure or estimate the width and height of the site and considering the size of rocks to measure, the scanning and processing time required, and the processing limitation of the software, compute the resolution that should be used for scanning and mesh generation. Use this same scanning resolution for all scans of this site.
- Find stable, sharp rock corners to use as control points in the four corners of the site area.
- Mark control points with paint if possible to make subsequent recovery easier. If points cannot be reached, take a photo of the site and mark both the boundaries of the site and the control points on the photo to ensure that the same site domain is scanned for each date.
- Mark the center of the area with paint if possible to assist with the Lidar set-up
- Mark position of tripod

Acquiring a Scan



Set up tripod in pre-marked location

- Push legs firmly into ground and bring height of the top of tripod to the previously recorded height for this site.

- Attach tribrach to tripod. Face the the optical plummet (eyepiece projection) towards the previously marked center of the site area.
- Level the tribrach.
- Place ScanStation2 unit on top of tribrach.
- ScanStation2 power supply hookups should be faced away from the rock slope of interest, as this puts zero degrees directly center of the rock slope.
- Secure ScanStation2 to the tripod by engaging the tribrach lidar lock
- Remove lens covers and unlatch Lidar so rotation is possible.
- Start generator and then plug in ScanStation2 power supply.
- Start up laptop and connect Ethernet cable from laptop to ScanStation2. Secure Ethernet cable to something stable at both ends to relieve strain at end-connectors.
- Open Cyclone on the laptop.
- To begin a new project a new database should be made. On the top toolbar, go to “Configure”>”Databases...” and add a new database. Enter the database name (twice), hit “OK”, then close dialog box. This step is only needed for the first time when starting a project, multiple scans can be done in a single database, and reused anytime.
- Now connect to the scanner. Go to “Scanners”>”ScanStation2” and double click. Find the database which was made in step 7, and create a new project folder. Highlight new project folder and select ok. On the top toolbar, go to “Scanners”>”Connect to scanner”.
- Wait for the green light to come on on the Lidar unit.
- When the “dual axis” message appears, hit “OK”
- Once the status bar in the bottom left of the Modelspace viewer says “Connected and Ready” it is time to gather the image.
- Make a rough estimate with the field of view, knowing the center of the rock outcrop of interest (the direction the optical plummet is pointing to if set up correctly) is zero degrees.
- The field of view can be changed by either inputting numbers into the field of view window on the right hand side, or by using the fence mode located in the top toolbar (looks like a rectangle).
- Once the field of view is set up, click “Image”, located at the bottom right of the modelspace viewer.
- Depending on the brightness, the internal camera exposure may need more or less light. This can be adjusted by going to “Image” located on the top toolbar and selecting “Adjust Exposure...”. From here the exposure length can be increased or decreased.
- Next the field of view can be adjusted to the image, so that only the area of interested is located within the box. This can be adjusted using the fence mode.
- Now probe the distance from the scanner to the center of the area of interested, by selecting “Probe” on the right side, in the “Resolution” window. Once the scanner status (located bottom left) says “Probe Completed”, change the “Sample Spacing” to the desired point distance. This measurement is the average distance between points

for that probe distance. Finally hit “Scan” and wait for the scanner to finish (Scanner status at bottom left will say “Scan Completed”).

- If another scan is desired from the same location immediately afterwards, the user can press “New ScanWorld” located on the right hand side in the “Project Setup” window.
- Once scanning is completed for the day, Cyclone should be shut down, and the data can be exported back in the office.

Exporting Data from Cyclone

- Open Cyclone on the laptop, and find the database of interested in the SERVERS folder.
- Open the modelspace which data is located in and trim the point-cloud data to just the site area. If rgb data is desired (image color imported onto the point cloud), go to “View”>”View Object As...” and then select “Point Cloud” in the dropdown box, then select “Color Map...”. This should open another window, where the first dropdown box (Mode) should be changed to “Colors from Scanner”. Click on “Apply” and then “Ok” and close the property window.
- Trim the site to consistent left, right, top and bottom boundaries by using the fence and delete outside functions.
- To select all the data, go to “Selection” on the top toolbar, and “Select All”.
- To export, go to “File”>”Export...” and select the folder the data should go to. Also change the type of file which the data will be exported to: “Text – PTS Format (*.pts)”. Then click “Save”. Two clicks of 'save' will be required. On the second save click, a new window should open. Make sure “Selected” is check marked and then click “Export”.
- Wait until the export function is completed before starting any new operation.

**DETAILED INSTRUCTIONS
FOR EACH
SOFTWARE MODULE**

ckrmse – check root-mean-square error

Purpose

This program examines a manually built registration control-point file and computes the root-mean-square error. It also reports the individual control point residuals which is useful for analyzing which control points may need to be replaced with better readings.

How to run program and Run-time Parameters

```
ckrmse site control-point-file-name <enter>
```

site: site number

control-point-file-name : full path name of control point file in Site directory.

Example: ckrmse 3 july4.txt <enter>

Input Directory for Lidar Data: none – this program does not operate on Lidar data

Other input sources: Control point file in site directory

Output Directory for Lidar Data: none – this program does not operate on Lidar data

Other output destinations: All output is sent to the console.

Control Point file setup

The control point file is manually built using Notepad. It must be saved as a text file – no special formatting characters can be in the file. Do not use Word or any other higher-end word processor – they embed special control characters.

The file has four lines, each line represents a control point. The order of points doesn't matter, but it is best to pick a point order and use that for all processing – this makes analysis of errors easier. It is suggested that the points be collected in the following clock-wise order: 1 = upper left, 2 = upper right, 3 = lower right, 4 = lower left.

This file is built using xyz values obtained from Cyclone. When running Cyclone, it is best to make a diagram of the before and after rectangles on a piece of paper, and record the xyz values for both the before and after scans on each corner of the diagram. Then, after values for all control points are recorded, type them into Notepad in the proper format.

For each control point, the 'before' x,y,z coordinate values are listed, followed by the 'after' coordinate values (six numbers total, with a space between each number) . Be careful to include all decimal values, and signs.

Format:

before-x before-y before-z after-x after-y after-z (all for control point 1)
 before-x before-y before-z after-x after-y after-z (all for control point 2)
 before-x before-y before-z after-x after-y after-z (all for control point 3)
 before-x before-y before-z after-x after-y after-z (all for control point 4)

Example of control point file:

```
-2190.59 9311.63 949.83 -2493.02 9233.49 950.82
807.66 10099.25 1026.48 471.26 10133.49 1025.73
1070.08 6652.58 -1293.24 856.98 6684.68 -1292.51
-1831.54 6609.97 -680.88 -2024.04 6526.58 -684.20
```

The first three numbers are the x,y,z of control point 1 on the 'before' scan. The next three numbers are the x,y,z values of that same control point on the 'after' scan. The next three lines follow the same format for the remaining control points.

This control point format is exactly the same as the 'sitex-yyyy-mm-dd-reg-obs.config' file (in directory regObservations) generated when the program register is run.

Explanation of Console Output

```
C:\Users\Men\lidarsu>ckrmse osp1.txt
checking to see if config file is open: osp1.txt
registration config file does exist - run registration in batch mode on dataset using observations in config file
prior observations i: 1 -1377.16 17992.8 -2524.35 -3157.85 16295.6 -2036.15
prior observations i: 2 8830.08 17437.4 -2670.64 7045.84 16677.8 -1820.17
prior observations i: 3 -1792.48 10285.3 -2404.05 -2880.92 8584.22 -2009.48
prior observations i: 4 -2039.06 5142.82 -2347.14 -2644.56 3442.61 -2000.45

control point 1 before distance: 18221.1 after distance: 16723.2 difference: -1497.98
control point 2 before distance: 17727.2 after distance: 18196.3 difference: -1530.93
control point 3 before distance: 19713.5 after distance: 9275.85 difference: -1430.46
control point 4 before distance: 6009.61 after distance: 4779.86 difference: -1229.75

*** 3-D transformation results from previous registration ***
3-D rmse: 6.06599 mm number of points: 4

*** verifying 3-d transformation ***

cp: 1 lx.ly.lz: -1377.16 17992.8 -2524.35 tx.tly.tlz: -3162.72 16295.5 -2030.33 hx.hy.hz: -3157.85 16295.6 -2036.15 residuals: -4.8676 -0.0707428 -2.17797
cp: 2 lx.ly.lz: 8830.08 17437.4 -2670.64 tx.tly.tlz: 7046.84 16676.9 -1820.13 hx.hy.hz: 7045.84 16677.8 -1820.17 residuals: 0.996092 -0.903536 0.0430626
cp: 3 lx.ly.lz: -1792.48 10285.3 -2404.05 tx.tly.tlz: -2873.03 8584.69 -2004.18 hx.hy.hz: -2880.92 8584.22 -2009.48 residuals: 7.88660 0.465996 5.30163
cp: 4 lx.ly.lz: -2039.06 5142.82 -2347.14 tx.tly.tlz: -2648.58 3443.12 -2003.62 hx.hy.hz: -2644.56 3442.61 -2000.45 residuals: -4.01517 0.508282 -3.16672

*** end of verifying 3-d transformation ***

*** orderly end of program ***
```

In the above example, ckrmse was run on file osp1.txt. The overall 3-D rmse was 6.06mm. The residuals for the individual control points are shown last.

Operational Strategy

The RMSE should be no higher than 1.5 times the mesh or scan resolution. For example, if a site were scanned and meshed at 4 mm resolution, the 3-D RMSE should not be greater than 6 mm ($4 * 1.5 = 6$).

If the RMSE is above this limit, the control point residuals should be examined. Usually, if a read-out error occurred on just one point, that point will have a higher residual error, and should be re-read. If the residual errors are high on all the points, all the points should be re-read.

regpts – register point file

Purpose

This program is used to transform the points in an 'after' pointcloud file to the coordinate system used in the 'before' scan. This program is only required if using the 'Cycone-based' registration process. If the normal (lidarsw-based) registration process is used, regpts is not run.

How to run program and Run-time Parameters

regpts site before-date after-date control-point-option <enter>

site: site number

before-date: base (before) date for site in yyy-mm-dd format

after-date: later (after) date for site in yyy-mm-dd format

control-point-option (y or n): paints white dots over control points in image (usually set to 'n')

example:

regpts 1 2013-05-15 2013-05-16 n <enter>

Input Directory for Lidar Data: pointFiles

Other input sources

Control-point file located in Sitexx/regObservations directory and renamed to:
'sitexxlaterdate-reg-obs.config'

example: site3-2013-05-16-reg-obs.config

Both the before and after lidar point files should be located in pointFiles directory.

The before file should be named beforedate-site.pts (example: 2013-05-15-3-1.pts)

The after file should be named afterdate-site.after (example: 2013-05-16-1.after)

Output Directory for Lidar Data: pointFiles

After running regpts, the file laterdate-site.pts will be created (example: 2013.05.16.1.pts) . This file is basically the after point file transformed to the coordinate system of the before point file.

Other output destinations

Progress and status information is output to the console during execution.

Configuration file setup

For control-point file setup, see **ckrmse** documentation.

Explanation of Console Output

```
C:\Users\Ken\lidarsu>regpts 3 2013-05-15 2013-05-16 n
in regpts
external drive name: C:/Users/Ken
opening: C:/Users/Ken/OutcropData/Site3/resolution.config

mapOption: s
checking to see if config file is open: C:/Users/Ken/OutcropData/Site3/regObservations/site3-2013-05-16-reg-obs.config
registration config file does exist - run registration in batch mode on dataset using observations in config file

control point option: n
prior observations i: 1 -1812.65 6601.51 -666.675 -1801.87 6587.11 -661.725
in addControlPoint n: 1 -1801.87 6587.11 -661.725 -1812.65 6601.51 -666.675
prior observations i: 2 -1757.52 9362.14 669.336 -1761.2 9356.89 664.406
in addControlPoint n: 2 -1761.2 9356.89 664.406 -1757.52 9362.14 669.336
prior observations i: 3 931.956 8719.14 167.214 928.465 8726.29 167.339
in addControlPoint n: 3 928.465 8726.29 167.339 931.956 8719.14 167.214
prior observations i: 4 524.493 7344.55 -774.317 531.696 7344.79 -770.916
in addControlPoint n: 4 531.696 7344.79 -770.916 524.493 7344.55 -774.317
control point: 1 before dist: 6861.1 after dist: 6878.23 difference: -17.1374
control point: 2 before dist: 9544.35 after dist: 9549.17 difference: -4.81322
control point: 3 before dist: 8777.14 after dist: 8770.4 difference: 6.74066
control point: 4 before dist: 7404.25 after dist: 7402.86 difference: 1.38892
*** 3-D transformation results from previous registration ***

3-D rmse: 2.03707 mm    number of points: 4

*** verifying 3-d transformation ***

cp: 1 resids: -0.206795 -1.97413 -0.433329
cp: 2 resids: 2.19991 1.29645 0.0943508
cp: 3 resids: -2.08088 0.204753 0.974296
cp: 4 resids: 0.0877575 0.469923 -0.635318

*** end of verifying 3-d transformation ***

base date will now be examined to pick up min max xyz's and average z
```

The first part of the output echos run-time parameters and the coordinates in the control point file. It then computes the RMSE (2.03 mm in this case), and reports the residuals for the

```
base date will now be examined to pick up min max xyz's and average z

base PIS file to be examined for min max: C:/Users/Ken/OutcropData/Site3/pointFiles/2013-05-15-3.pts
base pts file to be examined opened OK
skipping this line (count for next scan in this pts file) : 712455
skipping this line (count for next scan in this pts file) : 167678
skipping this line (count for next scan in this pts file) : 139839
in regpts: base pass. numpts: 1080000
skipping this line (count for next scan in this pts file) : 185594
skipping this line (count for next scan in this pts file) : 88298

base file numpts: 1213856
base hxa range: 1.35802 1.86484 base vra range: -0.221656 0.13767
examination of base PIS file complete
later PIS file will now be 3-D transformed to coordinate system of base PIS file

later PIS file to be transformed: C:/Users/Ken/OutcropData/Site3/pointFiles/2013-05-16-3.after output transformed PIS file: C:/Users/Ken/OutcropData/Site3/pointFiles/2013-05-16-3.pts
later pts file to be translated opened OK
output translated pts file opened OK
skipping this line (count for next scan in this pts file) : 732306 output points so far: 0 numoutside: 0 sum: 0
skipping this line (count for next scan in this pts file) : 189048 output points so far: 643396 numoutside: 88910 sum: 732306
skipping this line (count for next scan in this pts file) : 185882 output points so far: 752444 numoutside: 88910 sum: 841354
skipping this line (count for next scan in this pts file) : 185598 output points so far: 858326 numoutside: 88910 sum: 947236
skipping this line (count for next scan in this pts file) : 82288 output points so far: 964916 numoutside: 88910 sum: 1053826

translated numpts: inside: 993888 numoutside: 143826 sum: 1136114
transformation of PIS file complete
deleting dynamic classes
orderly end of program
C:\Users\Ken\lidarsu>
```


individual control points. Next, the base date lidar data will be examined to determine the ranges of x,y,and z coordinates.

After the ranges have been determined, the xxxxx.after file (which is the 'after' point file) is transformed to the coordinate system of the base date lidar data. The result is written to the pointFiles directory.

The end result is a xxx.pts file that has the same minimums and coordinate system of the base date pts file. When both the base date and later date pts files are processed through **findMinMax** and **load**, they will be positioned in the same relative location in the binary files – thus, they will be able to be subtracted from one another to produce a “difference” surface.

Operational Strategy

This program is only used for the Cyclone-based registration process.

1. Manually collect control points (4 from before and 4 from after) and format them as described in the **ckrmse** documentation.
2. Copy the control point file to the regObservations directory for that site, and rename the file to the proper name, encoding the later date and site within the file name.
3. Export the 'before' and 'after' point cloud data from cyclone to the pointFiles directory for that site.
4. 'Before' point cloud should be named the usual xxx.pts, while the 'after' point cloud should be named xxx.after
5. Run **regpts** and examine the console output to ensure the program operated successfully. The rmse error should be the same as that reported during running of **ckrmse**. **Ckrmse** should always be run prior to **regpts** to identify and control point errors.

findMinMax – Find the minimum and maximum coordinate ranges

Purpose

This program examines a xxx.pts file and determines the minimum and maximum ranges of the x,y, and z coordinates. The program also determines the minimum and maximum ranges of horizontal and vertical coordinates if a spherical mapping option is chosen. This information, together with the user-selected mesh resolution, is used to construct meta-data which is used by the **load** program to properly position and orient the Lidar data within the binary data structure used for all the Missouri S&T Lidar software.

How to run program and Run-time Parameters

findMinMax site date <return>

site: site number

date: date of scan in yyyy-mm-dd format

example: findMinMax 1 2013-05-15 <enter>

Input Directory for Lidar Data: pointFiles

Other input sources

The file resolution.config in the site directory defines several options which control how findMinMax operates. See configuration file setup below.

Output Directory for Lidar Data: None

Other output destination

Metadata for the Lidar is stored in a binary file called yyyy-mm-dd-s.meta in the metadata directory.

Configuration file setup

The file resolution.config defines how all dated scans in the site will be processed. Use of a single file to define the set-up of all dated scans in a site ensures that all data is collected to the standard (same resolution, same mapping option, etc.)

This file is usually built in NotePad, and contains 8 data elements, each separated by a space. Frequently, this file is built by opening an example resolution.config from another site, modifying certain fields if necessary, and saving it to the site needing a resolution.config file.

The eight data elements are :

Mesh resolution

Unit multiplier

Image Option

Mapping option

Number of point files

Multi-hit option

Probe distance

z-offset

Mesh resolution the cell size in mm at the probe distance. The mesh resolution is usually set to the same scanning resolution set in Cyclone and represents the average point spacing within the point cloud at the probe distance. The mesh resolution is, in reality, independent of the resolution used during scanning. If the mesh resolution is smaller than the scan resolution, some fraction of the cells will never get a point 'hit'. The load program will detect these 'holes' and fill them using values from adjacent cells. If the mesh resolution is larger than the scan resolution, cells will, on average, be hit by more than one point. In this case, the value assigned to the cell will depend on the multi-hit option selected.

The Unit Multiplier is used if the pts file happens to use units other than millimeters. If millimeters are used during scanning, then the Unit Multiplier will be 1.0. If the scanning process was set up to use meters, the Unit Multiplier should be set to 1000.0 (this will internally convert the coordinates of the points from meters to millimeters). Users are encouraged to always use millimeters in the scanning set-up to avoid confusion.

The image option exists to handle older Leica Lidars which did not have the capability to collect RGB information for every point. For scans collected by the ScanStation-II, this element should always be set to 'c' (color).

The mapping option describes how the point-cloud coordinate system is mapped to the internal data structure used within the Missouri S&T Lidar software. This option is usually set to 's' (spherical mapping). Full discussion of the mapping option can be found earlier in this document.

The number of point files option is normally set to '1'. This option exists for the case where multiple pts files are to be loaded into a single internal data structure. Since Cyclone allows multiple scans to be collected within a project, there is no reason to have multiple point files for most work. This option was created to support some earlier unique research projects where it was necessary to have multiple pts files for the same scene.

In most cases, the multi-hit option is set to 'a'. For the case of multiple hits per cell, the values assigned to the cell will be determined by averaging the values from all the points which 'hit' that cell. The multi-hit option 'c' uses only the closest point (nearest to the Lidar unit) to assign values to the cell. Similarly, the 'f' option uses only the farthest point (most distant from the Lidar unit) to assign values to the cell.

The Probe Distance is the distance from the Lidar unit to the middle of the study area, in millimeters. This distance is displayed during the probe operation which is run just prior to scanning an area, and should be recorded. If this value is not recorded, it can be recovered invoking the Cyclone scene viewer and picking a point near the center of the study area. The Y coordinate of the selected point can be used as the probe distance.

The z-offset is used when FARO data is acquired with the altimeter not disabled. Normally, the altimeter should be disabled – this will result in the lidar unit having a z-coordinate of 0.0. If the data is acquired with the altimeter enabled, the lidar instrument will have a z-coordinate equal to the elevation of the instrument above mean sea level. If a scan is accidentally acquired

with the altimeter enabled, the z-coordinates can be brought back to zero by applying the z-offset, which will be the altimeter setting of the FARO at the time of data acquisition in mm.

For example, if the FARO altimeter read 459.345 m at the time of data acquisition (with the altimeter was enabled), all z coordinates in the xxx.pts file will have z-coordinates relative to this instrument height. To bring these values down to zero, an offset of 459345.0 should be used.

In the following example of a resolution.config file, the meaningful information is all contained in the first line. The subsequent lines serve to document the various fields:

4.0 1.0 c s 1 a 8300 0.0

```
C:\Users\Ken\Lidarsu>
C:\Users\Ken\Lidarsu>findMinMax 3 2013-05-15
external drive name: C:/Users/Ken
opening: C:/Users/Ken/OutcropData/Site3/resolution.config
determining min max for raw lidar points site: 3 date: 2013-05-15
cellRes: 4
unitMult: 1
imgOption: c
mapOption: s
numPointFiles: 1
multiHitOption: a
external drive name: C:/Users/Ken

before loading - determining min-max for file: C:/Users/Ken/OutcropData/Site3/pointFiles/2013-05-15-3.pts
cell res: 4
unitMult: 1
imgOption: c
mapOption: s
numPointFiles: 1
skipping this line (count for next scan in this pts file) : 712455
skipping this line (count for next scan in this pts file) : 167678
skipping this line (count for next scan in this pts file) : 139839
in findMinMax numpts: 1000000
skipping this line (count for next scan in this pts file) : 105594
skipping this line (count for next scan in this pts file) : 88290

numpts: 1213856
xmin: -3338.99 xmax: 2695.1 ymin: 2064.51 ymax: 12607.3 zmin: -1519.23 zmax: 1757.23
distmin: 2000.44 distmax: 12884.6
average distance to surface: 8463.83 mm
heamin: 1.35805 heamax: 1.86484 hearange: 0.506789 degrees: 29.0369
veamin: -0.221656 vemax: 0.13767 veorange: 0.359227 degrees: 20.5879
apparent resolution based on adjusted cell spacing and average distance: 3.27724 mm
vertical rock face mesh will be based on user provided cell resolution of 4 mm occurring on an average surface distance of 8463.83 mm
*****
for given resolution of 4 mm (raSpacing: 0.000481920), horurrange predicted to be: 1052 verurrange predicted to be: 746
*****
initial brightness values (before histogram equalization) bmin: -1708 bmax: 557 borange: 2265
writing metadata binary file: C:/Users/Ken/OutcropData/Site3/metadata/2013-05-15-3.meta
heamin: 1.35805 heamax: -0.221656
minlup: 0 minlup: 0
maxlup: 1051 maxlup: 745
distmin: 2000.44
distmax: 12884.6
avgdist: 8300
bmin: -1708
bmax: 557
done writing binary file
orderly end of program
C:\Users\Ken\Lidarsu>
```

documentation of fields

4.0 resolution in mm for site

1.0 unitMult (multiply raw x,y,z's by this number to get to millimeters - use 1.0 if already in mm)

c imgOption c: color (rgb's present) b: no rgb info included in pts file

s mapOption g: ground plane s: spherical (vertical rock face)

1 numPointFiles (used to loop thru multiple pts file for the same scene)

a multiHitOption 'a': use average

'c': use closest (highest z for g mapOption)

'f': use farthest (lowest z for g mapOption)

8300 probe distance in mm

0.0 z-offset in mm (altimeter reading if altimeter was enabled during the scan)

Explanation of Console Output

Most of the console output involves echoing user input (from the resolution.config file) and providing progress messages as the pts file is being processed. Other information such as number of points processed, the ranges of x, y, and z coordinates, and the apparent resolution are useful for debugging purposes.

The main item to look for is the number of cells in the horizontal and vertical direction to ensure that processing limits will not be exceeded. These numbers are indicated by the maxHur (1051 in this case) and the maxVur (745 in this case) values. These values should be less than the processing limits of 4300 and 3400, respectively.

Operational Strategy

None – as long as the resolution.config file was properly built, no other interaction is required.

load – load a xxx.pts file into the binary data structure

Purpose

The **load** program loads a pts file into the internal binary data structure using the set-up information contained in the metadata file produced by **findMinMax**. The spatial sorting and binning process occurs here – as each point in the pts file is read, the **load** program determines the appropriate cell to load that point in, and loads the information about that point (position, intensity value, and color) into that cell.

After all points are processed, the program examines the resultant surface for holes or gaps. Holes are cells that were not 'hit' by any points in the point cloud. All holes are filled using values from surrounding adjacent cells on a weighted basis based on distance.

How to run program and Run-time Parameters

load s date <enter>

s: site number

date: scan date in yyyy-mm-dd format

For example, to load the scan collected on April 23, 2013 for site 37:

load 37 2013-04-23 <enter>

Input Directory for Lidar Data: pointFiles

Other input sources

Metadata created by **findMinMax**

Output Directory for Lidar Data: meshed

Other output destinations

pixColorBeforeFill contains images of the surface before the fill operation within load

pixIntensityAfterLoad contains images of the intensity surface after the fill operation

pixColorAfterLoad contains images of the RGB surface after the fill operation

Configuration file setup

See **findMinMax** documentation for details on how to set up the resolution.config file.

Explanation of Console Output

Most of the messages echo user input and give progress messages on how many points were processed, how many cells were used, the distribution of hits per cell, and other general information.

Operational Strategy

None – as long as the resolution.config file was properly built, no other interaction is required.

When the load program is finished, the user should check the directory 'pixColorAfterLoad' to examine pictures of the study site. If the pictures look good, chances are the load program performed it's function properly. If the pictures are all black, or exhibit some other peculiarity, the console output from **findMinMax** and/or **load** should be examined for clues as to what the error was.

register – Registers later-date Lidar data to the base-date data

Purpose

Before two Lidar surfaces can be subtracted from one another, they must be registered to each other. Typically, a site will have been scanned several times at different dates. The earliest scan is called the 'base date', as it provides the base against which all future change will be

measured. The other scans are called 'later dates', as they occur later in time. It is the common practice to register all of the 'later dates' to the 'base date'. This results in all the data being in the same coordinate system as the 'base date'.

The **register** program applies a 3-D 7-parameters conformal transformation to the later date Lidar data to bring it to the same coordinate system of the base date. This conformal transformation allows x,y, and z translation, x,y, and z rotations, and a universal scalar. It is conformal in the sense that 3-D shapes remain the same. The transformation cannot shear or skew the model space – nor will it allow differential scaling. No 'rubber sheeting' takes place.

The transformation parameters are determined by a least-squares method using four control points. Each control point represents some surface feature which is clearly visible on both the base and later surfaces. For each control point, the x,y,z on the before surface and the x,y,z on the later surface is collected. Thus, a total of 12 observations are collected and used to solve a set of equations with 7 unknowns. This over-determined solution makes it possible to calculate residuals which indicate 'goodness of fit' for the set of observations.

The program employs an automatic correlation function which attempts to find a 'matching' point in the later surface based on it's local topographic expression. The program keeps track of both the manual pointings and the correlated pointings, calculates the RMSE for both, and uses the solution that has the lowest RMSE if the user elects to accept the results of the registration.

How to run program and Run-time Parameters

register site base date later-date <enter>

site: site number

base-date: earliest date for that site

later-date: date of the scan being registered to the base date

For example, to register a scan taken on July 17, 2013 to the first scan taken for site 45 (base-date: February 19, 2013):

register 45 2013-02-19 2013-07-17 <enter>

Input Directory for Lidar Data: meshed

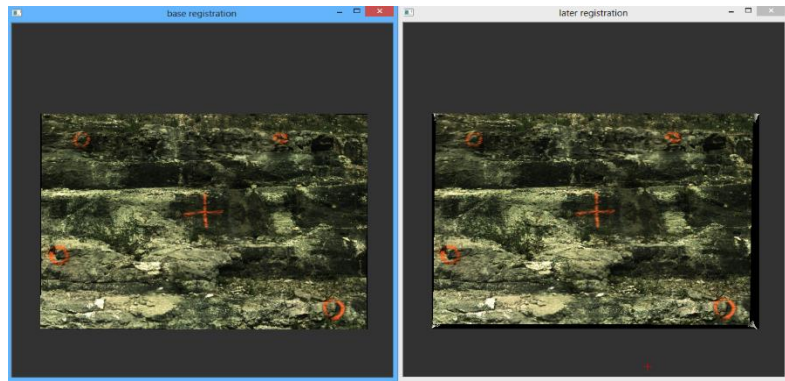
Other input sources: None, other than interactive mouse clicks during the registration session.

Output Directory for Lidar Data: registered

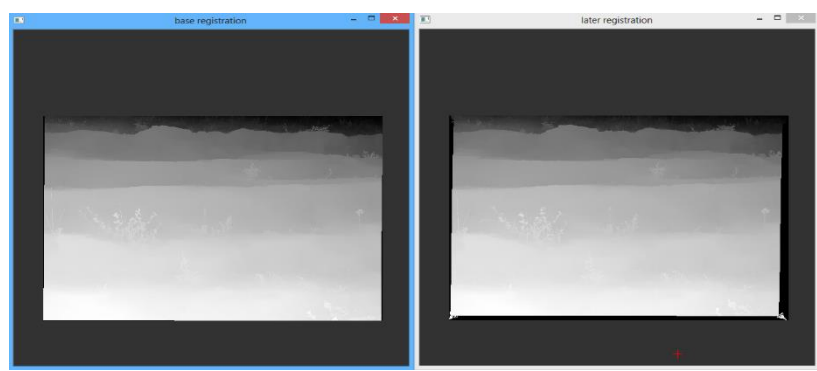
Other output destinations

The intensity image represents the reflected energy of the Lidar pulses. It is useful for general navigation, but should not be used for final control point selection because it does not reveal subtle topographic detail which is critical for control point identification.

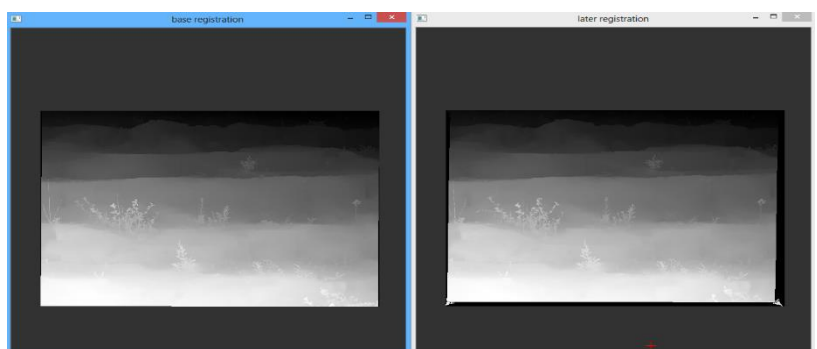
The following screen dumps illustrate the four display options (color, linear depth, histogram depth, and intensity):



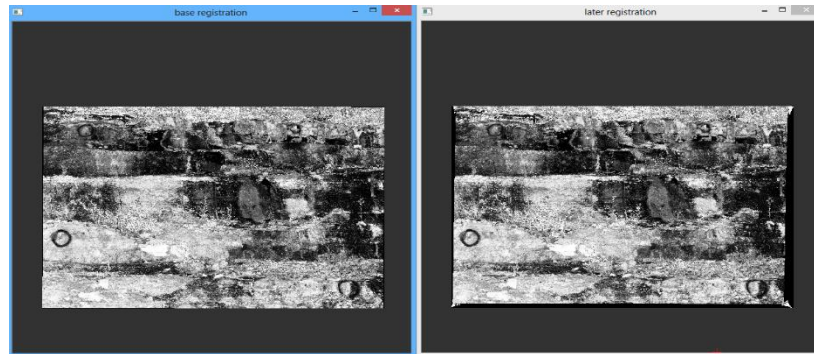
Color image display (from preview camera)



Linear Depth image display – gray shade determined by relative depth



Histogram-equalized image display – provides better contrast



Intensity image display

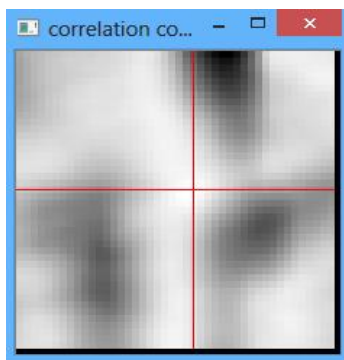
Collection of Control Points

Control points are stable identifiable features which have not moved (and are unlikely to move) during the duration of the study. Any feature can be used as a control point – as long as it is unique to the local area and clearly identifiable on both the 'before' and 'after' depth images.

The control points should be located close to the corners of the surface. This pattern minimizes the area of the surface that would lie outside the control points. Cantilevering beyond control results in less-accurate registration and volume determination. While it is not always possible to obtain a good control point in the corner area, every effort should be made to do so.

The best control points are stable rocks that have a pointy surface facing the Lidar unit. This type of object is easy to identify in the histogram-equalized depth image, and easy to match in the right image display. When selecting control points, the user should stay away from edges and large flat areas. Areas of high local topographic detail make the best control points.

To select a control point, left click the location on the left window display, then find the same point on the right window display, and left-click that point. A small correlation window will appear showing the results of the automatic feature-matching correlation. A good correlation is indicated when the center of the correlation image is small and bright compared to the surrounding area:



Accept the point by hitting <enter> after the correlation image is displayed.

After the fourth point is collected, the program calculates and displays the RMSE resulting from both the manual and correlated set of observations, and asks the user if the transformation is to be applied to the later surface:

```

*** control point added - number of control points: 4
manual later h,u: 988 175 correlated later h,u: 990 177
bx,by,bz: -1769.04 6553.89 -933.086 mx,my,mz: -1771.73 6563.88 -937.845 clx,clz: -1779.42 6567.19 -931.88

*** 3-D transformation results for manual pointings ***
3-D manual rmse: 2.01253 mm number of points: 4

*** verifying 3-d transformation - manual pointings ***
cp: 1 lx,ly,lz: -2128.5 9358.38 958.576 tlx,ty,tz: -2130.18 9353.12 963.354 bx,by,bz: -2131.92 9352.55 962.75 residuals: 1.73748 0.567108 0.663925
cp: 2 lx,ly,lz: 1132.87 10092.3 826.82 tlx,ty,tz: 1133.45 10102.1 817.911 bx,by,bz: 1133.83 10100.8 817.656 residuals: -0.382533 1.29229 0.255252
cp: 3 lx,ly,lz: 647.327 7404.24 -752.742 tlx,ty,tz: 652.424 7405.28 -757.53 bx,by,bz: 654.681 7406.09 -760.237 residuals: -2.2568 -0.809915 0.706502
cp: 4 lx,ly,lz: -1771.73 6563.88 -937.845 tlx,ty,tz: -1768.13 6552.84 -934.652 bx,by,bz: -1769.04 6553.89 -933.086 residuals: 0.901052 -1.04949 -1.56568

*** 3-D transformation results for correlated pointings ***
3-D correlated rmse: 3.11847 mm number of points: 4

*** verifying 3-d transformation - correlated pointings ***
cp: 1 lx,ly,lz: -2120.84 9359.87 963.461 tlx,ty,tz: -2130.21 9352.02 961.338 bx,by,bz: -2131.92 9352.55 962.75 residuals: 1.70633 0.464707 -1.41221
cp: 2 lx,ly,lz: 1132.87 10092.3 826.82 tlx,ty,tz: 1133.39 10102.7 820.523 bx,by,bz: 1133.83 10100.8 817.656 residuals: -0.433773 1.85054 2.06693
cp: 3 lx,ly,lz: 648.145 7404.35 -759.927 tlx,ty,tz: 652.041 7404.35 -763.049 bx,by,bz: 654.681 7406.09 -760.237 residuals: -2.63988 -1.7395 -2.01204
cp: 4 lx,ly,lz: -1779.42 6567.19 -931.88 tlx,ty,tz: -1767.67 6553.32 -931.729 bx,by,bz: -1769.04 6553.89 -933.086 residuals: 1.36732 -0.575745 1.35731

*** manual 3D rmse was better, so manual pointing set will be used
*** end of verifying 3-d transformation ***
apply 3D transform to later surface? (enter 'y' or 'n' )

```

As seen in the above example, the manual RMSE was 2.01 mm and the correlated RMSE was 3.11 mm. The register program will use the better of these two (the manual in this case) for the transformation if the user elects to proceed with the transformation.

The RMSE should be no greater than 1.5 times the cell mesh resolution. In the example above, the mesh resolution was 4mm. Therefore, the RMSE limit would be 6 mm ($4 \text{ mm} * 1.5 = 6 \text{ mm}$).

For this example, since the best reported RMSE achieved during this registration session was under that limit, the user would first make the console window active, then would enter 'y' and hit <enter>. The program would then proceed to create a transformed version of the later surface, and write it to the 'registered' directory.

If the reported RMSE was over this limit, the user should make the console window active, enter 'n', and hit <enter>. This will terminate the program so the user can try running **register** again.

elimVeg – Eliminate Vegetation from Lidar data

Purpose

Vegetation and other small moving objects which float in front of the Lidar unit during an active scanning operation introduce artifacts into the Lidar surface which must be removed if accurate quantitative measurements are to be made for volumetric change. These types of artifacts are characterized by spikes in the data having high spatial frequencies and small individual but large cumulative volumes.

Commonly used methods of vegetation detection and removal are based on simple edge detection. While these methods are effective for identifying and removing features exhibiting high spatial frequencies, they don't discriminate between the types of high-frequency data we want to eliminate, like vegetation, and other types of high-frequency data we want to preserve, like the sharp edges of rocks. The Missouri S&T Lidar software includes specialized filters which detect and eliminate thin vegetation while preserving the high-frequency edges of rocks.

How to run program and Run-time Parameters

elimVeg site date <enter>

site: site number

date: date in yyyy-mm-dd format

Input Directory for Lidar Data: registered

Other input sources

User-selected parameters are determined during the interactive session. These values are saved to a configuration file, which may be used for other dates to eliminate vegetation using the same parameters to reduce subjectivity and the variable outcome that would result if every date were processed with it's own set of vegetation removal parameters.

Output Directory for Lidar Data: noVeg

Other output destinations

Progress and status messages are output to the console.

Configuration file setup

The file 'sitexVegRemoval.config' (x:site number) contains the five user-selected parameters to define the vegetation removal process. These are usually determined when running **elimVeg** on the first (base-date) scan of a site. All other dated scans for that site will be run with the same parameters defining these vegetation removal tuning parameters.

Method used within the Vegetation Elimination Program

The vegetation detect and elimination method uses a two-step process. The first process (Roof filter) identifies potential vegetation using a relatively fast edge-based method. This method does a good job identifying all the vegetation, but because it is based only on edge criterion, it falsely includes all sharp rock edges as well. The second process (Probe filter) is run on all the cells identified as potential vegetation and is more discriminating – it can differentiate rock edges from vegetation. While the second process is smarter, it is also much slower. The optimum solution is to pre-identify potential vegetation using the first process, which only takes a few minutes. Even with liberal settings, only 15% of the Lidar surface is typically identified as potential vegetation. Because the second, slower process only needs to be run on 15% of the total cell count, it operates much faster. Even with this time-saving pre-process, the second process can take up to 45 minutes to execute, depending on the Lidar surface size, mesh resolution, and settings for the second process.

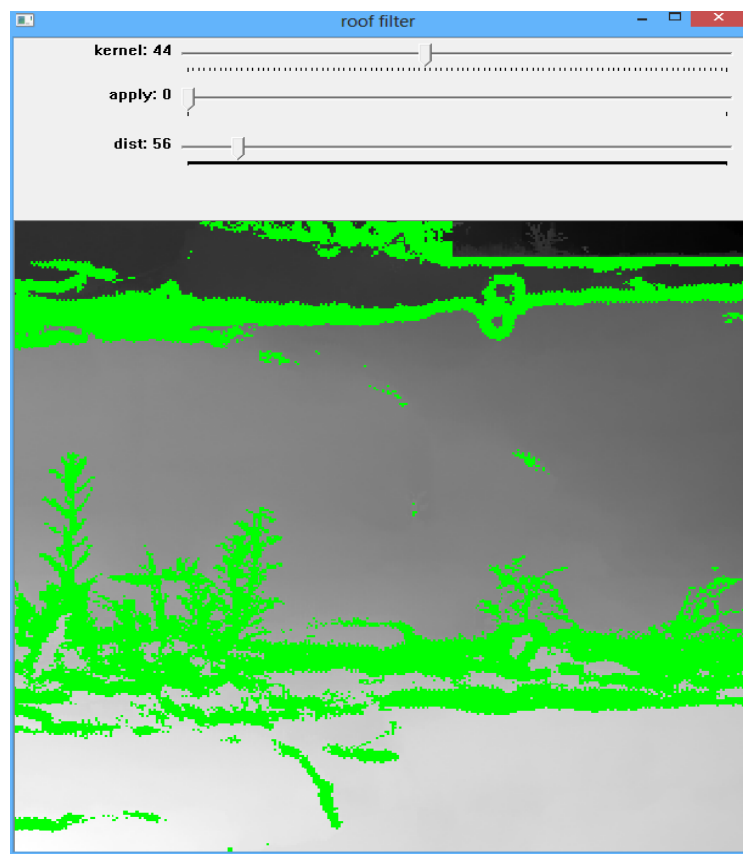
The 'sitexVegRemoval' configuration file contains all the settings saved from an interactive **elimVeg** session. The first process is controlled by two parameters: a kernel diameter, and a distance below roof threshold. The kernel diameter defines a sampling area to compute the average local depth. The distance below roof threshold is the difference in depth between a single cell, and its local average depth. The kernel is normally set to be equal to the diameter of the visible vegetation stems and leaves. The distance threshold is set to a value that highlights all the vegetation, and just some of the rock edges. The user should be liberal in assigning these first two values, as the only penalty for being too liberal is increased run time for the second process. The consequences of being too conservative in assigning the first two values is that some real vegetation might not get flagged as being potential vegetation. Since only cells identified as potential vegetation are examined by the second process, those cells representing real vegetation would not be examined, thus the vegetation over those areas would have no possibility of being detected or eliminated.

The second process is controlled by three parameters: virtual cone solid angle (in degrees), virtual cone length (in millimeters), and the limits of articulation (wobble, in degrees). In this second process, a virtual articulating conical probe scans the back-side of the rock face. Any cell that can be reached by the end-point of the virtual cone without the cone intersecting anything else is classified as rock. If a cell cannot be reached by the conical probe, the probe begins a wobbling motion – increasing in angle using a spiral pattern. This action allows the probe to reach into sharp corners of rock blocks. If the limits of articulation are reached and

the probe could not find an orientation that resulted in the probe point hitting the cell without any intersections, the cell is classified as vegetation and marked for removal.

Operational Strategy

For the first part (Roof filter) , the user should set the kernel diameter to the size of the thin stems or leaves, and adjust the distance slider until all the vegetation is high-lighted. The display should look something like this:



When the 'apply' slider is activated, the console will display the percentage of vegetation highlighted – this will normally be between 15-25%. In this example, the percent of highlighted vegetation is 20.6%:

```

veg is 0 percent of display area
veg is 0 percent of display area
veg is 0 percent of display area
veg is 0 percent of display area
veg is 20.6017 percent of display area

```

The user should roam around the image to confirm that all the vegetation is high-lighted. After this confirmation, hit the 'escape' key **twice** to advance to the second part of elimVeg, the Probe filter.

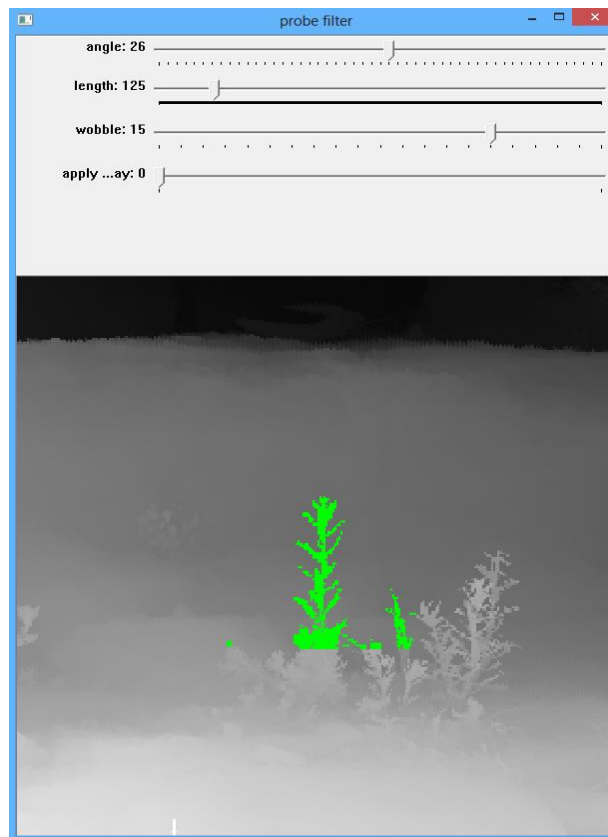
The second part of **elimVeg** is the Probe filter. When the probe filter window is displayed, zoom in to some typical vegetation and left-click. The display should look something like this:



The green line represents a horizontal plane cutting into the rock face. The red line represents the profile of the Lidar surface at that cutting plane (viewed from above). The down-ward spikes are caused by the vegetation. The bright yellow triangle is the virtual articulating conical probe behind the rock face, and the darker yellow lines represent the limits of articulation.

The sliders can be adjusted to set the solid angle of the probe, the length of the probe, and the limits of articulation (wobble). The wobble should always be at least as large as half of the solid angle. For example, if the solid angle is 26, the wobble should be set to at least 13. In the above example, the wobble is set to 15.

The parameters can be tested by panning within the image to position some test vegetation in the middle of the display window and hitting 'apply'. This will run the probe filter on the middle third of the display for review.



The user should pan around the surface and test the parameters on various types of vegetation. When it appears that the settings work for most of the cases, the 'escape' key is hit while in

the probe filter display. A message appears on the console asking if the user wishes to save the settings:

```
Are you satisfied with entire veg removal (roof and probe)?? enter 's' to save config or 'r' to reset and start over with roof
s
executing probe filter on entire file

applying conical probe searchBoxWidth: 16
*** batch probe h.v bounds: 0 1051 0 745
applying conical probe h: 0
progress: 0%
estimate of remaining time: -1.#IND minutes
applying conical probe h: 10
progress: 0.951475%
estimate of remaining time: 9.7854 seconds
applying conical probe h: 20
progress: 1.90295%
estimate of remaining time: 12.8875 seconds
applying conical probe h: 30
progress: 2.85442%
```

Enter 's', then <enter> This will save the settings and run the probe process on the whole dataset. Depending on the resolution, site size, and parameter settings, the elimVeg program will require anywhere from 2 minutes to 45 minutes to run.

All subsequent dated scans for the site will need to run through the elimVeg program, however, since the settings from the initial base-date are saved, the program will operate in a batch (non-interactive) mode for the remaining sites. Running all scans using the same vegetation parameter settings helps to ensure that objective criteria is applied to all scans equally. If it is desired to run a particular date with different settings, the 'sitexVegRemoval.config' file in the site can be temporarily renamed to something else – this will allow the **elimVeg** program to be run in an interactive mode for that particular date.

diff – Creates a difference surface

Purpose

The **diff** program subtracts one Lidar surface from another – producing a 'difference' surface. Prior to this operation, the Lidar datasets must be structured into a raster data structure (performed by **load**), registered to each other (performed by **register**), and have thin vegetation removed (performed by **elimVeg**).

The resultant 'difference' surface represents a cell-by-cell difference of the two surfaces. In theory, the difference surface would contain large negative areas where rocks have fallen, and large positive areas where falling debris had accumulated. In practice, the difference surface contains not only these expected features, but numerous other data artifacts caused by residual registration error, parallax anomalies caused by slight positional error in the Lidar unit setup from date to date, vegetation which did not get removed due to improperly assigned tuning parameters or limitations within the vegetation removal algorithm, and from accuracy limitation of the Lidar unit itself. Separating these artifacts from true change data is the job of the final program, **calcvol**.

The **diff** program examines every cell within the domain of the base surface. If that cell has data in both the base and later surface, the difference between the cells is computed as assigned to the corresponding cell in the difference surface. For the most part, the surface metadata from the later surface is used to populate the difference surface metadata.

How to run program and Run-time Parameters

diff site base-date later-date diff-date <enter>

site: site number

base-date: earliest date in the site in yyyy-mm-dd format

later-date: some later date that will be subtracted from the base date in yyyy-mm-dd format

diff-date: constructed from the base and later date by using the month a day as follows:

For a base-date of '2013-05-23' and a later-date of '2013-07-05', the diff-date would be '523-705'

For example, to create the difference surface for the scan taken April 24, 2013 on site 25 where the base-date for that site was January 15, 2013:

diff 25 2013-01-15 2013-04-24 115-424 <enter>

Input Directory for Lidar Data: noVeg

Other input sources

None

Output Directory for Lidar Data: diffSurfaces

Other output destinations

Status and progress output sent to the console.

Pictures of the result are sent to the pixDiff directory.

Configuration file setup

None.

Explanation of Console Output

After echoing the metadata of the two input Lidar files, the actual diff program subtracts the two surfaces from each other, and displays some statistics concerning the process:

```

in createDiffSurf - creating difference surface
diff site: 3
diff sdate: 515-516
creating diff surface h: 0
creating diff surface h: 1000
numCells: 784792 numBothExist: 742569 < 94.6198% >
mindiff: -1725.14 maxdiff: 1634.27
average difference: 0.642987
setting up pointers
writing binary file: C:/Users/Ken/OutcropData/Site3/diffSurfaces/515-516-3.bin
writing dist
writing bu
writing rual
writing goal
writing boal
writing status
done writing binary file

```

Here we see that 94.6% of the base-date cells existed in the later-date Lidar data.

Finally, some pictures are created and written to the pixDiff directory. Information on the pictures is sent to the console output.

calcvol – Calculates the volume of lost and gained material in a difference surface

Purpose

The **calcvol** program accomplishes two tasks – first, it eliminates the remaining artifacts from the raw difference surface (separating artificial features from true 'missing' or 'gained' material), and second, computes the volume of lost and gained material.

How to run program and Run-time Parameters

calcvol site diff-date base-date later-date <enter>

site: site number or name

diff-date: constructed from the base and later date by using the month a day as follows:

For a base-date of '2013-05-23' and a later-date of '2013-07-05', the diff-date would be '523-705'

base-date: first date in sequence

later-date: some later date in the sequence

For example, to run **calcVol** on a scan taken December 22, 2013 for site 18 where the base-date for that site was March 12, 2013:

calcvol 18 312-1222 2013-03-12 2013-12-22 <enter>

Input Directories for Lidar Data: diffSurfaces, noVeg

Other input sources

User input received during an interactive session – slider values, hot key commands, and cropping.

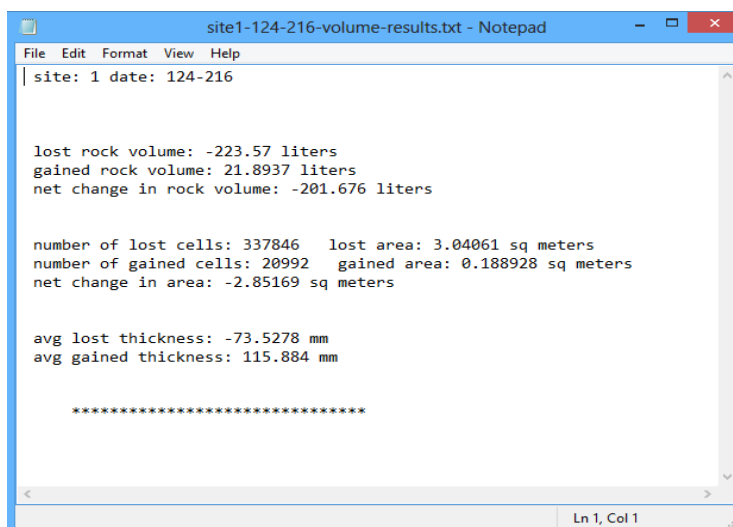
When run in a batch-mode, the file volume.config contains all the settings established during the interactive session. This ensures that all dates in a sequence are run with the same parameter-tuning settings. The file cropMask.bin is a binary file (non-viewable) which contains the cropping mask created during the interactive tuning session. This is used to ensure that all subsequent dates use the same domain for calculation of the change in volume.

Output Directory for Lidar Data: None

Other output produced by calcvol

Informational, diagnostic, and debugging messages are presented to the console when running the program in the interactive (first time filter-defining) mode.

A summary report of lost and gained material volume (given a name reflecting the diff-date) is written to the site directory:



```

site1-124-216-volume-results.txt - Notepad
File Edit Format View Help
| site: 1 date: 124-216

lost rock volume: -223.57 liters
gained rock volume: 21.8937 liters
net change in rock volume: -201.676 liters

number of lost cells: 337846   lost area: 3.04061 sq meters
number of gained cells: 20992   gained area: 0.188928 sq meters
net change in area: -2.85169 sq meters

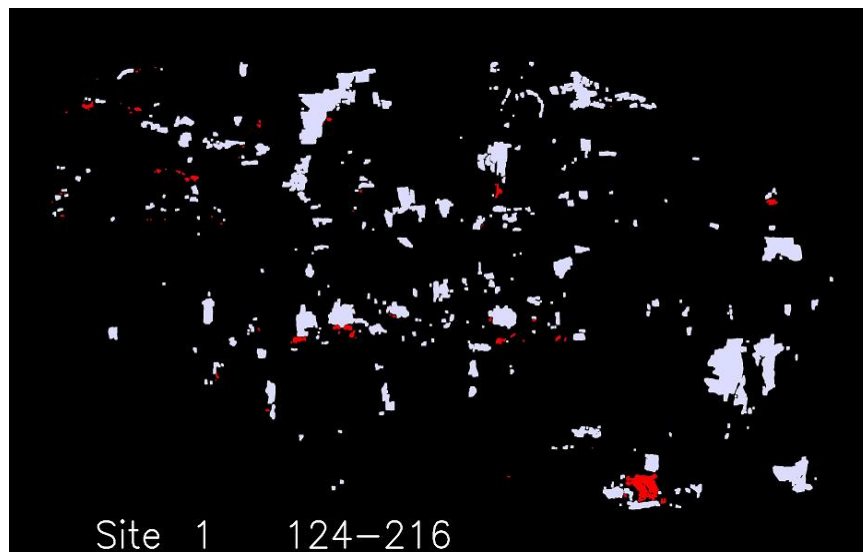
avg lost thickness: -73.5278 mm
avg gained thickness: 115.884 mm

*****

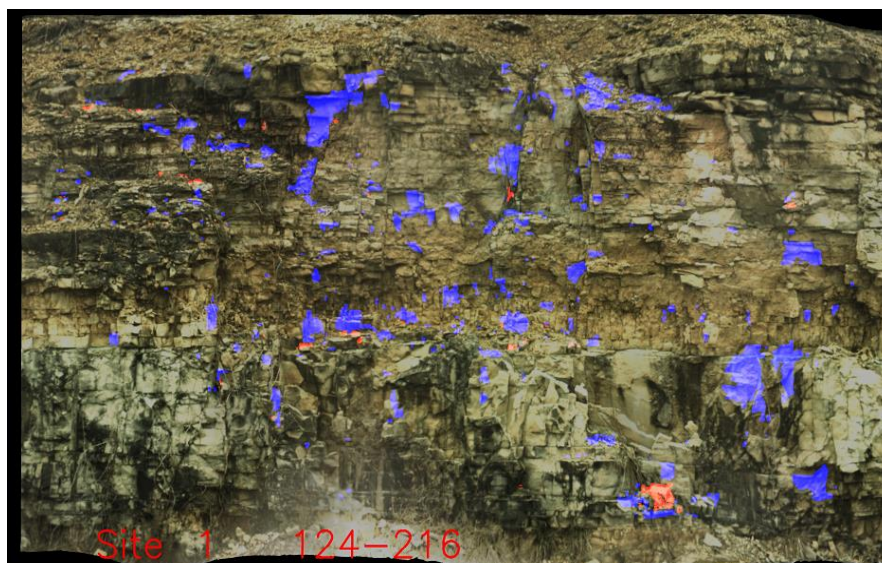
Ln 1, Col 1

```

Pictures of the lost and gained rocks are also created:



Binary image of lost (light blue) and gained (red) material is created in the pixMask directory.



An image of Lost (blue) and gained (red) material overlaid on RGB color surface image is created in the pixRocks directory.

Operational Strategy

The computed volumes of lost and/or gained material are highly dependent on the settings of several tuning parameters used to differentiate real rocks from residual artifacts. Therefore, for sites having multiple later dates, it is critical that the same set of tuning parameters be used for all later dates. The software facilitates this by saving all tuning parameter settings in the file `volume.config`.

When **calcVol** is executed, the program first checks for the existence of the file `volume.config`. If this file exists, it means at one point, the user had an interactive session with `calcvol` and set all the tuning parameters for that site. In this case, the `calcvol` program reads the `volume.config` file to capture all the tuning parameters, and proceeds to run in a batch mode, using those fixed tuning parameter settings.

If the file `volume.config` does not exist, it means that the tuning parameters were never established, so the program initiates an interactive session to allow the user to set the various tuning parameters.

During the interactive session, the user will invoke a number of functions to eliminate residual artifacts from the difference surface. The user will also create a domain mask which will be used as a common clipping boundary for all subsequent processing of all the later dates in a sequence.

It is recommended that the terminal window be maximized before invoking the **calcVol** program – this way, progress, status, and error messages generated on the terminal screen can be visible during execution of the program. This is most critical when **calcVol** is run for the first time during the interactive parameter setting session.

Interactive parameter-setting operation

Typically, the user will invoke the following functions in this order:

1. Set the lost noise slider (minimum thickness of lost material to be used)
2. Set the gained noise slider (minimum thickness of gained material to be used)
3. Build the cropping mask and save it
4. Run erode on the lost rocks some number of times
5. Run dilate on the lost rocks some number of times
6. Run erode on the gained rocks some number of times
7. Run dilate on the gained rocks some number of times
8. Run the inside rule to clean up small 'holes'
9. Run the function which computes the volume of lost and gained rock
10. Hitting the 'escape' key will save all tuning parameter settings, generate the diagnostic pictures, and terminate execution of the program

The Difference Surface

After the surfaces are all registered to each other, a difference surface is created by subtracting some later-date surface from the base-date surface. The distance value of each cell in a difference surface is simply the base-date distance minus the later-date distance for that cell. Therefore, lost material will be represented by a negative value, and gained material will be represented by a positive value.

Some sites, such as vertical rock cuts, have mostly lost material. As the material is lost, it drops all the way to the bottom of the cut without accumulating in any shelf or pocket. On the other hand, some sites have mostly gained material - for example, at the bottom of a slope failure. Finally, some sites have a mixture of both lost material and gained material, such as medium slopes with shelves to catch moving material. Previous versions of the software dealt only with lost material. This limitation limited the ability of the software to model more complex situations involving both lost and gained material.

Mr. Abdullah Alotaibi, a graduate researcher at Missouri S&T, came up with the idea that lost material and gained material should be tracked separately because they each have different characteristics. He proposed that each of these sets (lost material and gained material) should have their own set of noise-elimination functions, such as minimum depth sliders and geomorphic operators such as the erode and dilate functions. Having separate and independent tuning parameters for lost and gained material allows the analyst to more precisely model the true characteristics of the moving material and to better segregate real data from residual artifacts.

This concept has been implemented in the current implementation of **calcVol**. Separate noise sliders are provided for setting independent noise thresholds for lost material and gained material. In addition, geomorphic functions such as erode and dilate are implemented separately for lost and gained material. Finally, the tuning parameters (noise slider positions, number of erodes executed, number of dilates executed) are saved using values established separately for both the lost and gained material. This has resulted in a more general solution – one that covers a wider variety of slope situations.

User Interaction with Calcvol

The following sliders, mouse navigation functions, and hot-key functions are provided:

Sliders (on right display):

Loss noise:

Blue cells in the difference surface that have a thickness less than the value of the slider position will be eliminated. Small negative-valued residual artifacts can be eliminated by adjusting the value of this slider.

Gain noise:

Red cells in the difference surface that have a thickness less than the value of the slider position will be eliminated. Small positive-valued residual artifacts can be eliminated by adjusting the value of this slider.

Veg adjust:

Future research-oriented capability not currently active.

Mouse-based navigation functions :

Left button down while moving mouse: Panning (up, down, left, right). Applies to both screens.

Right button down while moving mouse down: Zoom in. Applies to both screens.

Right button down while moving mouse up: Zoom out. Applies to both screens.

Middle button (or wheel) click: toggles between three displays on the right screen:

Lost rock only (shown in blue)

Gained rock only (shown in red)

Both lost and gained rock (blue for lost, red for gained)

Ctrl + mouse move: Draw a crop mask (can be used to create bounding ring and inside masks)

Uses the crop mask dot size previously set with up/down arrows.

Shift + mouse move: Erases a crop mask. Uses the crop mask dot size previously set with up/down arrows.

Hot-key functions:

r: Reset - cancels the effects of all previous erodes and dilates for both lost and gained material, and redraws the right display to reflect only the effect of the current noise-elimination slider values.

s: Saves the crop mask to a binary file in the site directory

g: Gets the previously saved crop mask stored in the site directory

d: Dilate operation for lost material. Adds a single layer of blue on each blue blob.

e: Erode operation for lost material. Subtracts a single layer of blue on each blue blob.

D: Dilate operation for gained material. Adds a single layer of red on each red blob.

E: Erode operation for gained material. Subtracts a single layer of red on each red blob.

i: Runs the 'internal' filter, which fills in single interior holes in large blobs. This function operates on lost and gained material independently.

v: Computes and displays the volume of lost and gained material, using the filters applied.

1: Sets the left display mode to 1 – the original color histogram-equalized difference surface

2: Sets the left display mode to 2 – base date RGB

3: Sets the left display mode to 3 – later date RGB

4: Sets the left display mode to 4 – base-date Intensity

5: Sets the left display mode to 5 – later-date Intensity

up triangle: Increases the crop dot radius

down triangle: Decreases the crop dot radius

left triangle: Clears all cropping

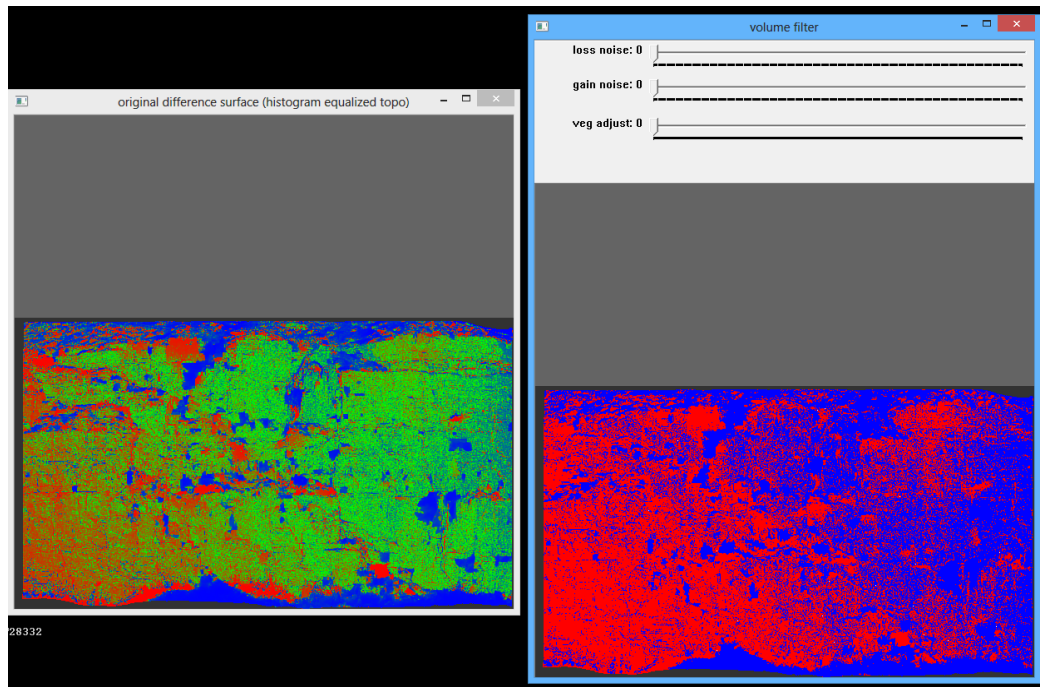
right triangle: Completes the cropping – fills in the area outside the manually-drawn bounding ring

(Note: The above four hot-keys are also called 'arrow' keys, but they are **not** the arrows coincident with the numeric keypad)

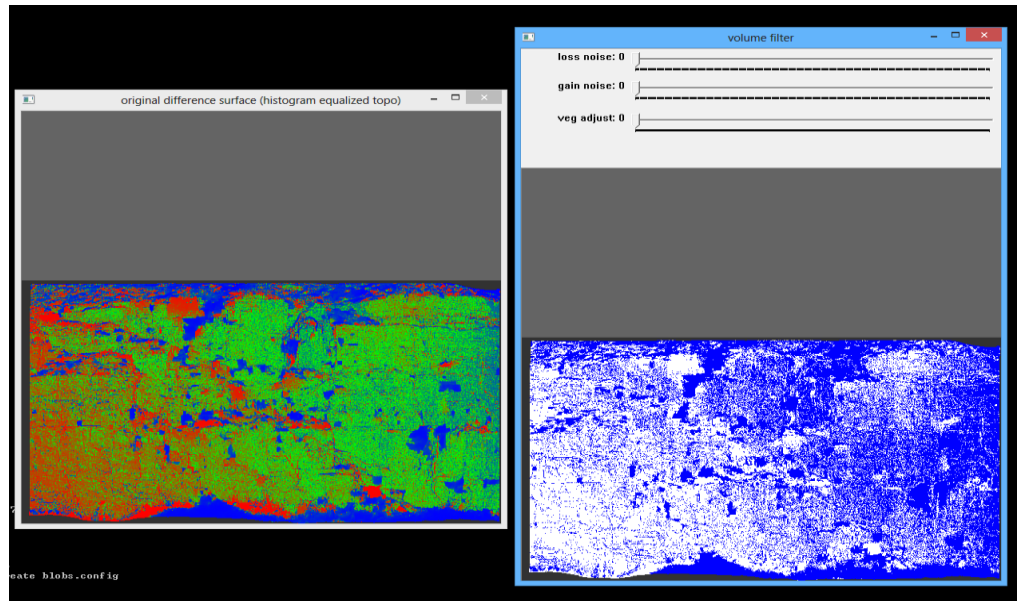
escape: Triggers the generation of the pictures in pixMask and pixRocks directories, saves the tuning parameters in a file called volume.config, and terminates the **calcvol** program.

Strategy for a typical calcvol session

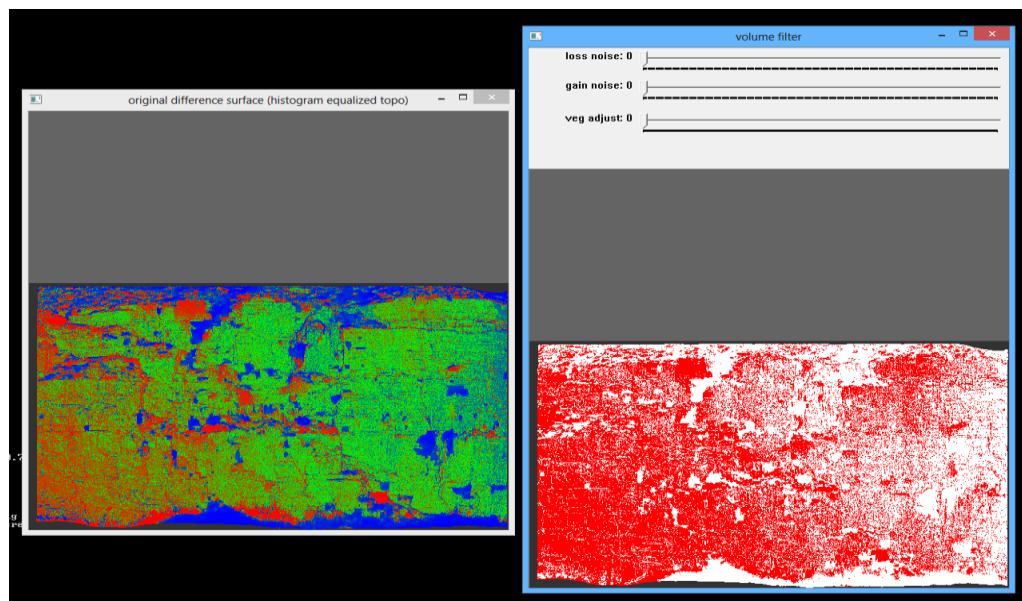
The difference surface contains many artificial artifacts which must be identified and removed. The initial screen displays two windows – the left window initially displays the histogram-equalized difference surface, and the right window displays the result of filtering actions:



The left window displays the difference surface - green indicates no change, blue indicates lost material, red indicates gained material. The left window can also display the base date RGB image, the later date RGB image, the base date intensity image, or the later-date intensity image by using the hot keys 1-5. The right window displays the result of filtering operations – primarily the result of successive erodes and dilates on both the lost material and gained material overlays. The initial mode for the right window displays both lost (blue) and gained (red) material.



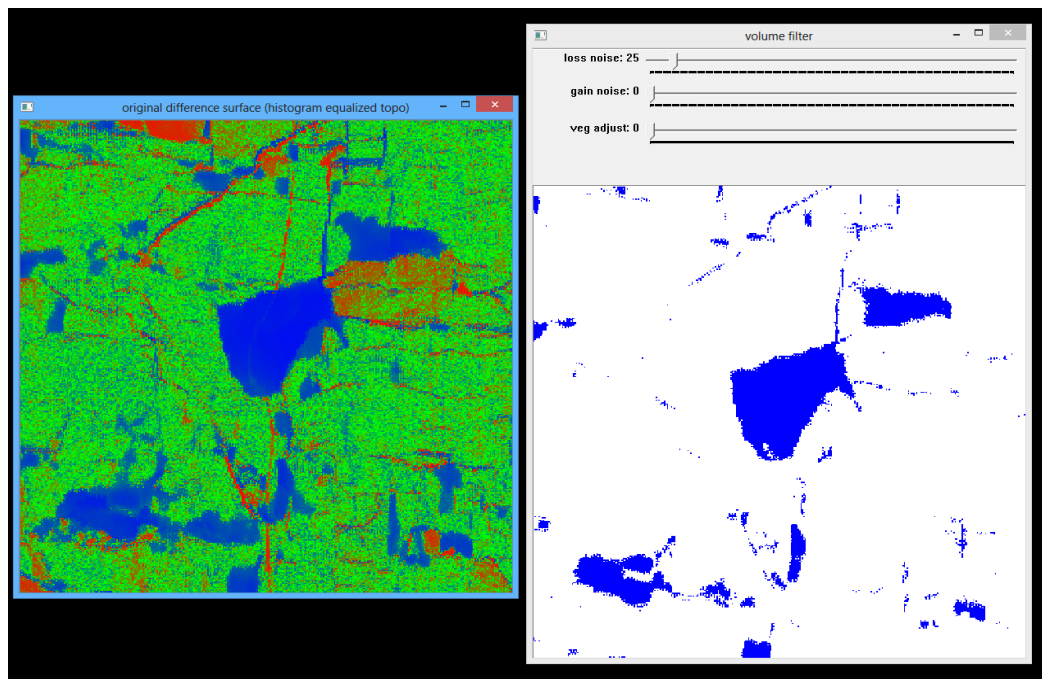
The right window can be toggled between three views using the middle wheel-button on the mouse. The three views are: lost material only (blue), gained material only (red), or both lost and gained material (blue and red). Each cell represents either lost (negative) or gained (positive) volume. The right display initially displays both lost and gained material, but can be changed to lost-only by toggling the middle mouse button, as shown above.



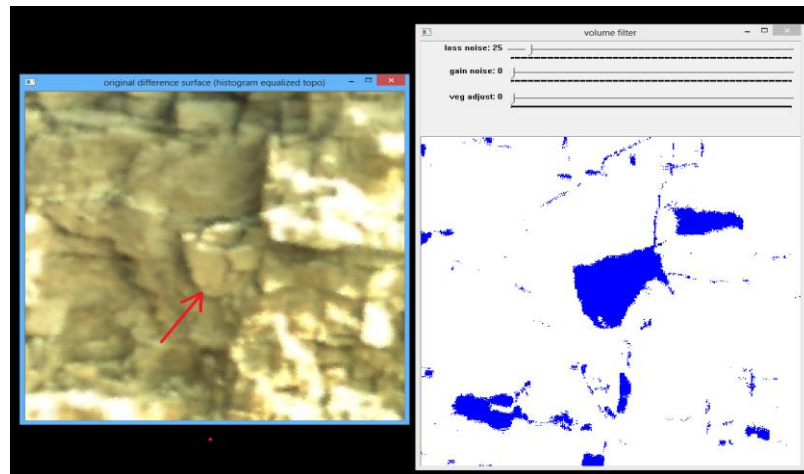
Toggling the middle mouse button again changes the right display to gained material only (red), as seen above.

The first step is to set the noise sliders for both the lost and gained material. These sliders define the minimum thickness of the difference surface that is considered 'real'. The slider values are in mm of depth, but in setting these 'noise' levels, it is best to do this visually, rather than be overly concerned about the value of the numbers. In many cases, the threshold for noise seems rather high (40 mm, for example). One might question why apparent rocks 40mm in depth are being regarded as 'noise'. The analyst should remember that there are many opportunities for various errors to creep into the processing model. Inherent Lidar accuracy, registration residuals, vegetation not fully removed, and parallax errors all contribute different types of errors. Therefore, it is better to make the noise-level adjustments by visually examining a few representative areas to decide what is real and what is merely an artifact.

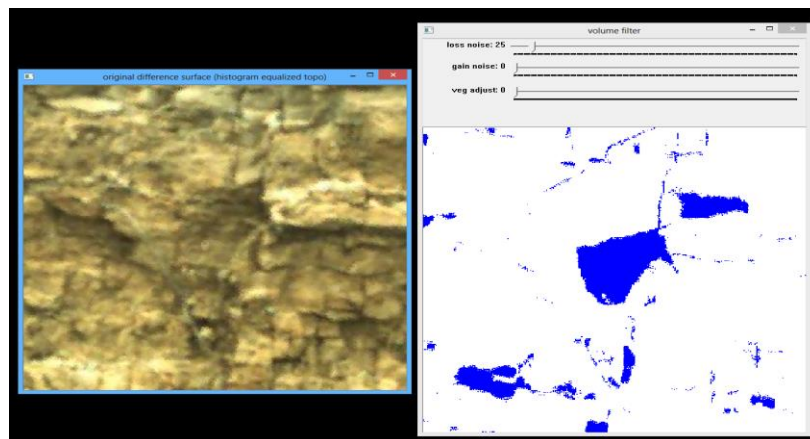
To assist in this type of assessment, the user can zoom into an area of interest and quickly flip the left display to show (alternatively) the base date RGB and the later date RGB images (using the '2' and '3' hot-keys). For example, in the image below, the user is trying to ascertain if the big blue area is a real missing rock, or a data anomaly. First, zoom to the area under study:



Next, rapidly alternate the '2' and '3' keys to show the 'before' and 'after' views of this same area as represented by the RGB images:

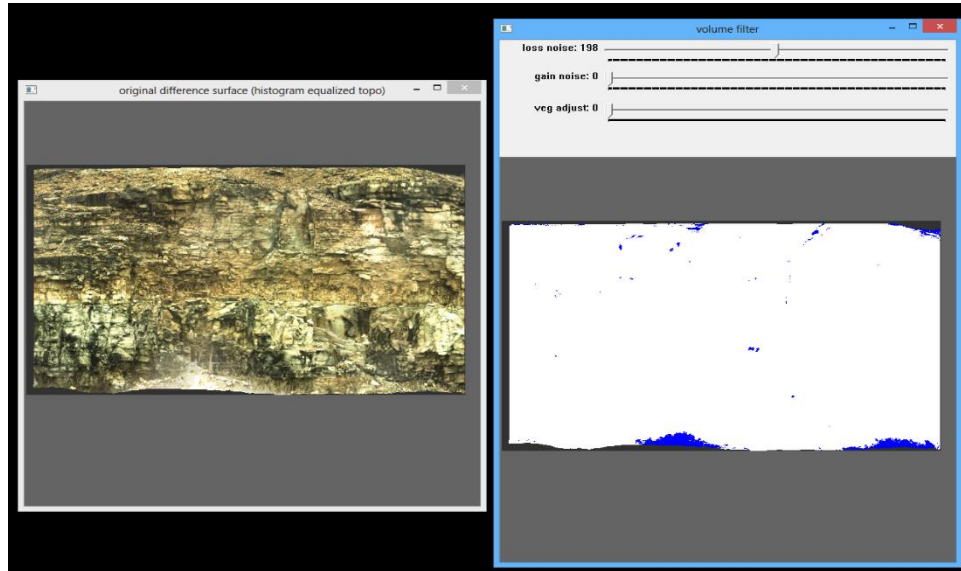


In the 'before' image above, a rock can be seen that equates to the large blue area in the middle of the right window.

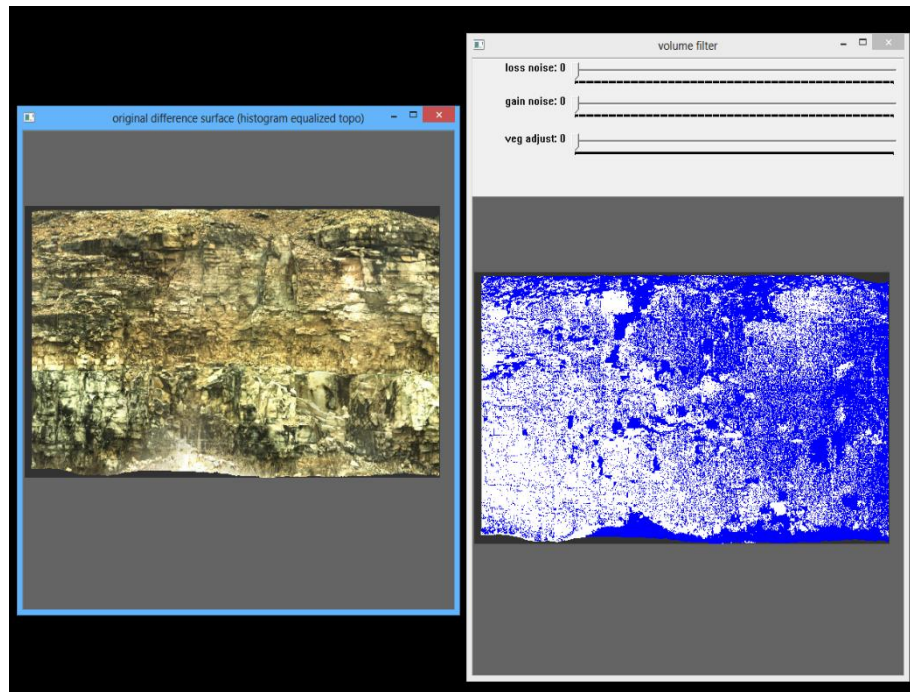


When the left display is changed to the 'later' date by hitting the '3' key, it is clear that the rock has fallen away. Therefore, in this case, the blue area represents a real rock loss, and not an anomaly. The sliders are adjusted to show all the features which appear to be 'real' – while at the same time, eliminating many of the smaller features that are mere artifacts in the data.

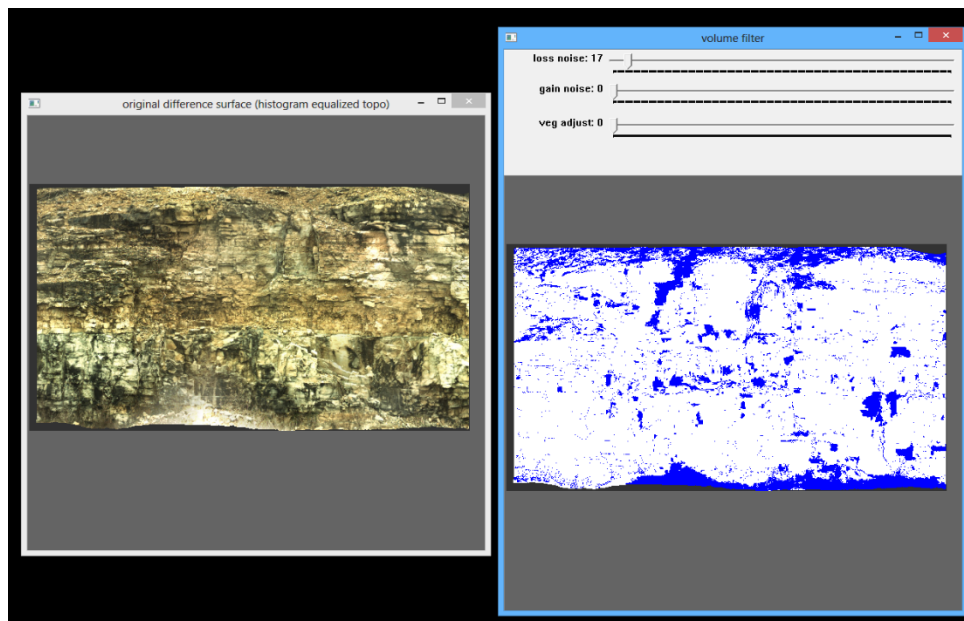
Care must be taken to set the noise slider at a reasonable setting. If the slider is moved too far to the right, the rejection criteria will be set too high. All the noise will disappear, but so will the real rocks:



On the other hand, if the slider is moved too far to the left, then all the rocks are retained, but so are all the data artifacts:

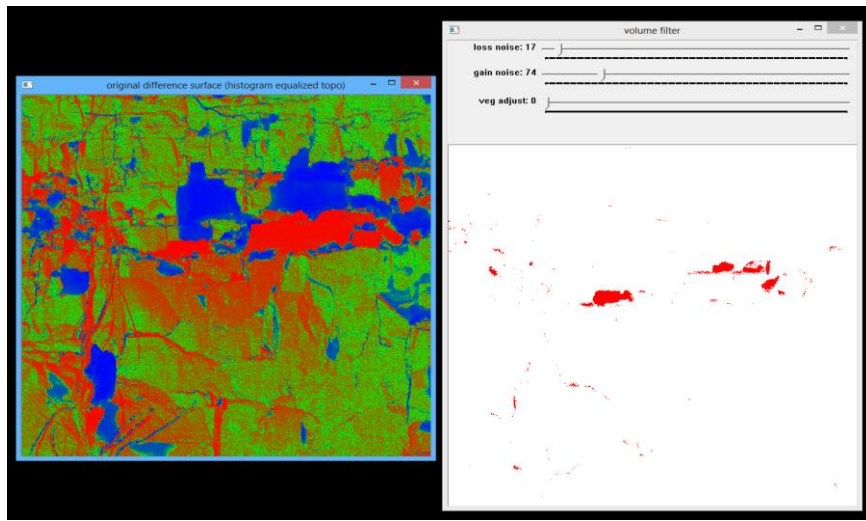


In this case, a reasonable setting of '17', as shown below, shows all the probable rocks, and eliminates much of the noise. There are further tools to use to eliminate the remaining noise, so at this early stage, the best strategy is to ensure that all the rocks are shown and the noise is kept to a minimum. If a real rock disappears because too high of a noise threshold was used, further filtering tools can never bring it back – so it is better to use the noise sliders to eliminate as much noise as possible without affecting the size or shape of the features which appear to be real rocks.

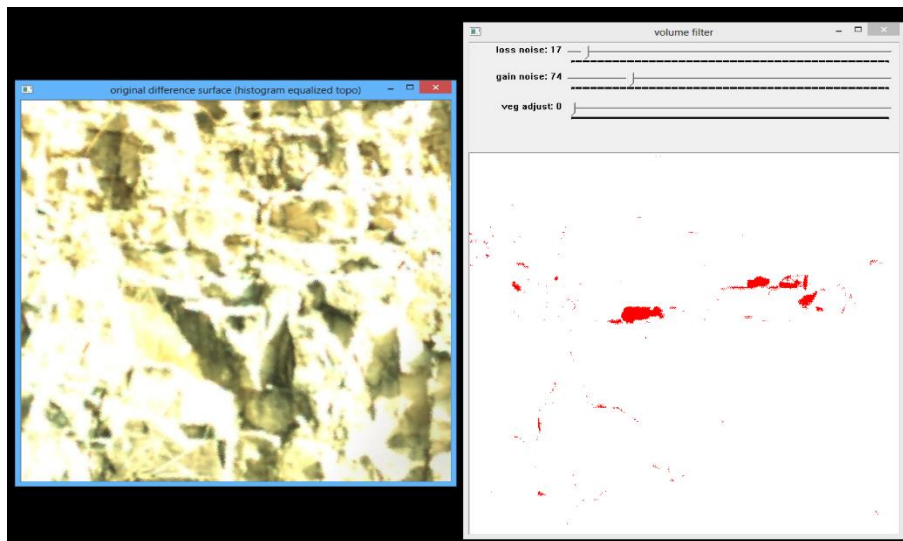


Next, the same operation is conducted for the gained material. Again, it is advisable to zoom into any suspect areas and use the before-after flip keys to show either the before and after RGB images ('2' and '3' keys) or the before and after Intensity images ('4' and '5' keys):

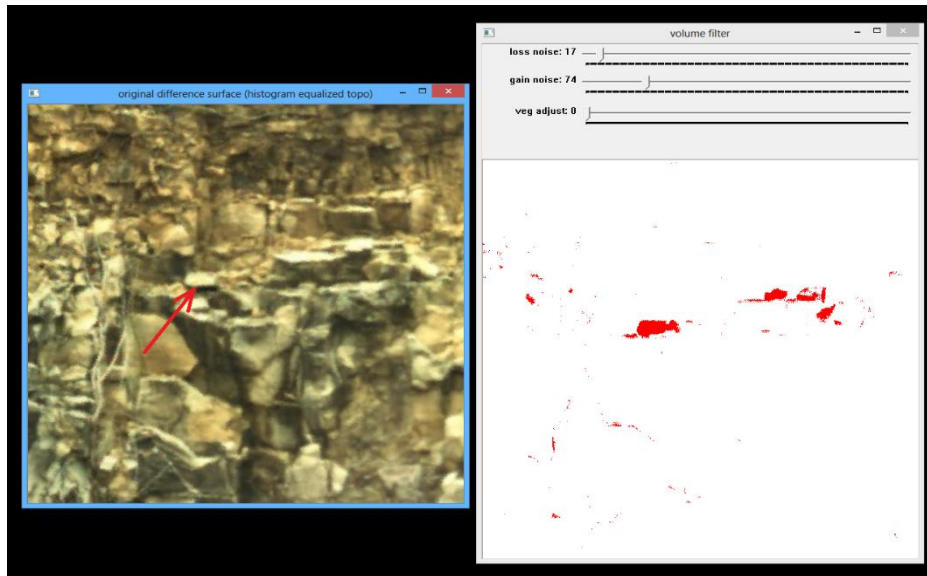
To determine if the red area is a real rock gain, or just an artifact, zoom into the area of interest:



Next, toggle the left window to determine if this feature is a real gained rock, or just a data artifact:



In the 'before' image above, it is clear that no rock is resting on the ledge (yet).



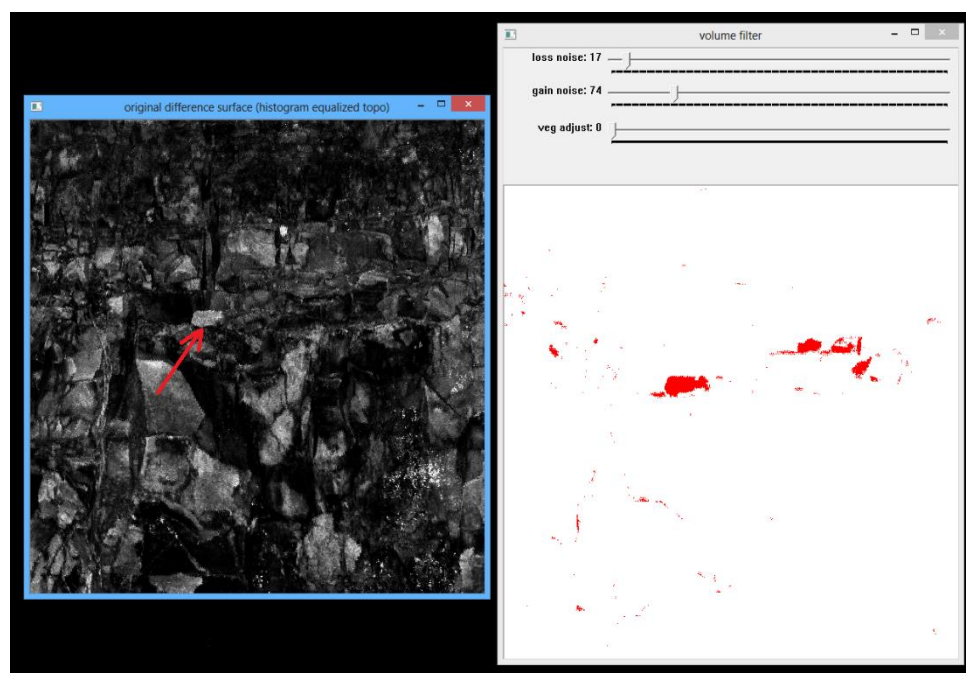
In the 'after' picture above, the newly gained rock is clearly visible.

In some cases, the changes are hard to see in the RGB images – this can be caused by improper camera exposure settings during the scan (too light or too dark), or simply from the fact that the RGB images are acquired from a separate lower-resolution camera that is not precisely registered to the rest of the Lidar data. In this case, the Intensity images can be viewed in the same rapid 'before' and 'after' mode (using hot keys '4' and '5') to determine if the feature is real.

The following sequence of screen-shots illustrates the intensity images of the 'before' date:

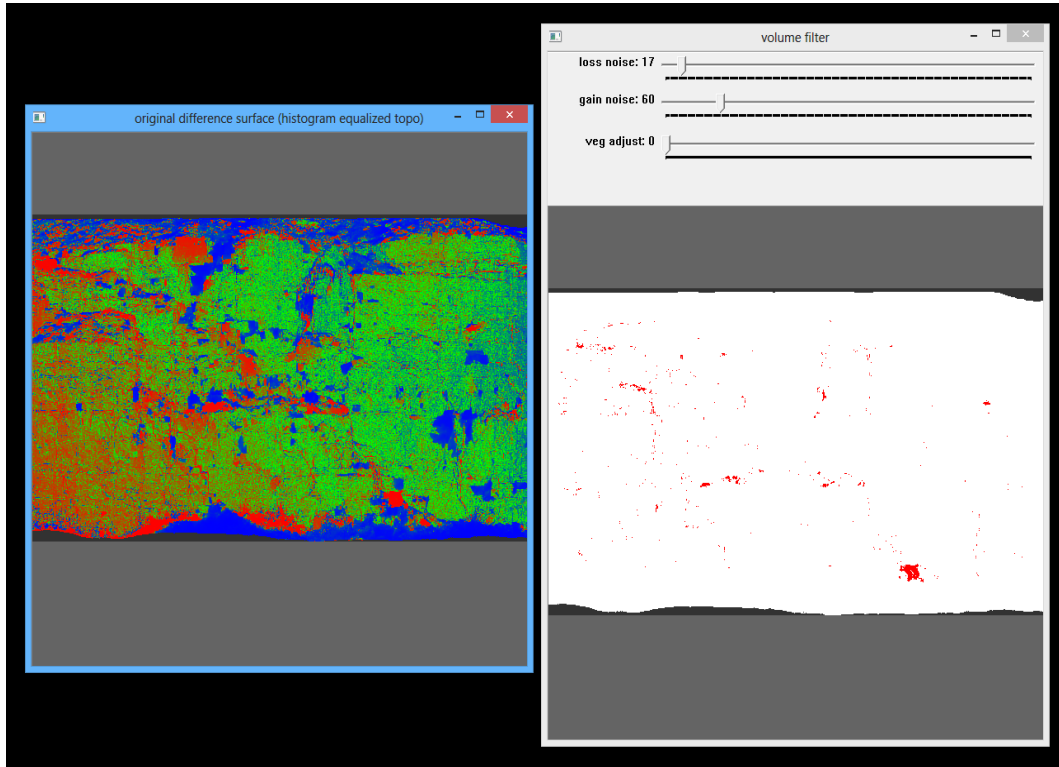


.....and the 'after' date:



By alternating these images quickly, the 'gained' rock is clearly identifiable. These display keys are useful in determining the appropriate noise level to set with the noise slider.

At this point, the gain noise setting of 60 appears reasonable – this setting eliminates most of



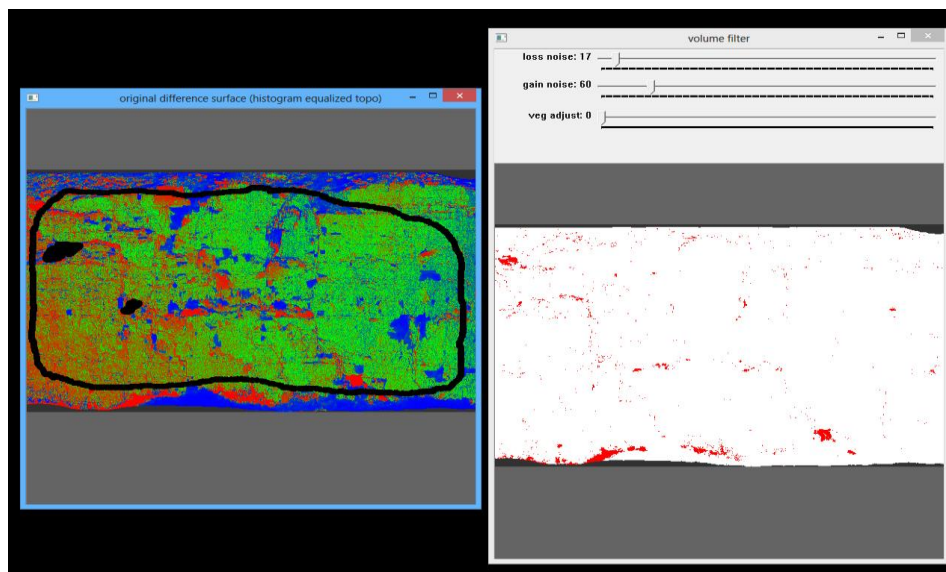
the noise, yet preserves the real gained rocks:

The next step is to define a common cropping boundary for all the dates (base and all later dates) in the site. Changes in volume can only be computed if the same domain is used to define the area under study. Because individual scans may have slightly varying domains, a single domain representing the intersection of all scans (picture this as a logical 'AND' for the areal extents of each scan). In other words, a domain must be defined such that every scan completely covers this domain. The cropping domain should be an area completely covered by each and every scan in the site.

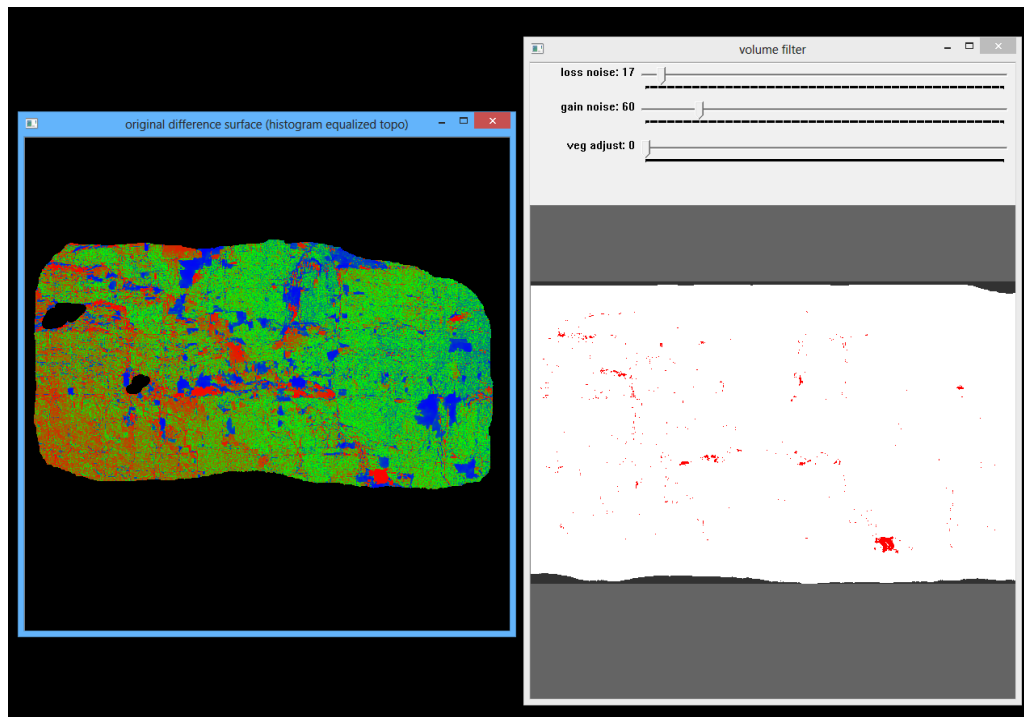
To define a clipping domain, the user draws a single polygon around an area covered by all scans by holding down the 'ctrl' key while drawing with the mouse (no buttons pressed on the mouse while drawing). The thickness of the boundary line may be adjusted by using the up and down arrows. Mistakes can be corrected by holding down the 'shift' key while using the mouse as an eraser. If the user wants to eliminate the cropping boundary and start over, the left arrow key can be used.

In addition to the single outside polygon, interior areas representing artifacts (residual vegetation, for example) can also be masked out. The user should take care that the masked area not include very short-range areas, or areas near the horizon, as these areas may not be represented in all the scans. Finally, it is important that the single exterior polygon be complete with no gaps in the bounding polygon line.

A typical masking domain definition might look like the following:



The final step in domain definition is to 'complete' the mask by hitting the right arrow key. This defines a cropping mask to the edge of the data:



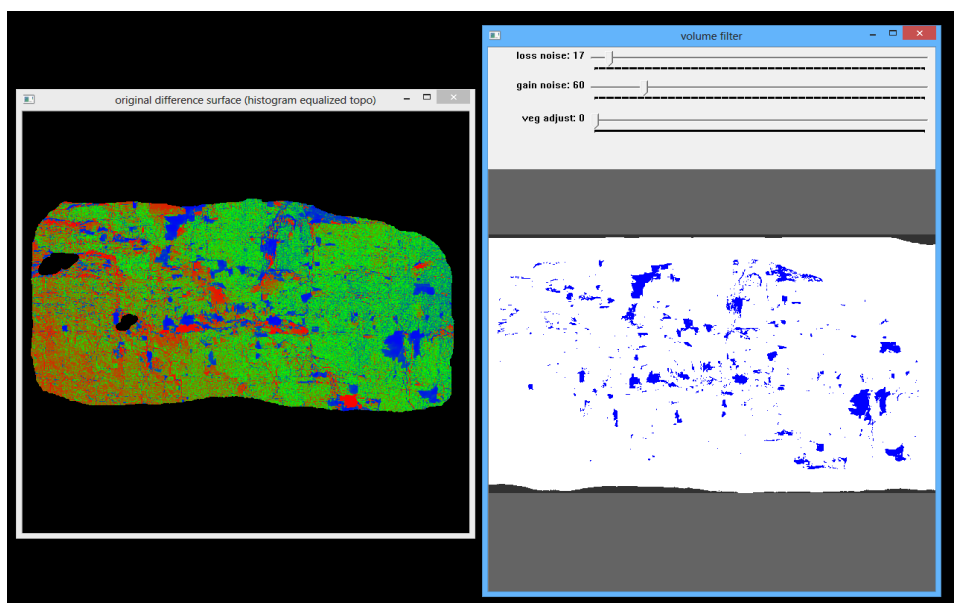
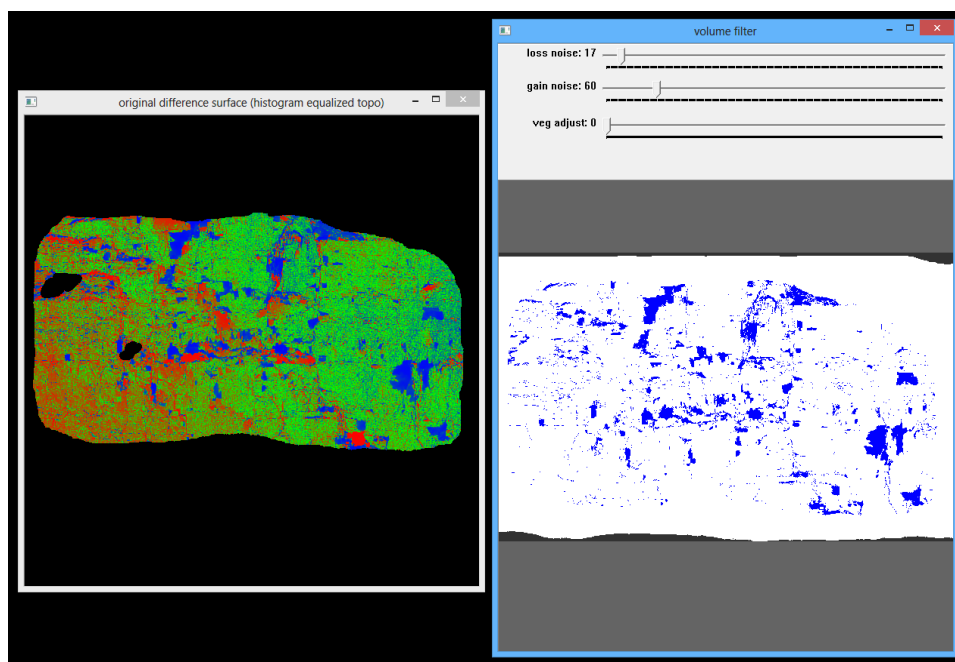
The volume computations will only use data inside the cropping boundary and not masked off with any interior masks.

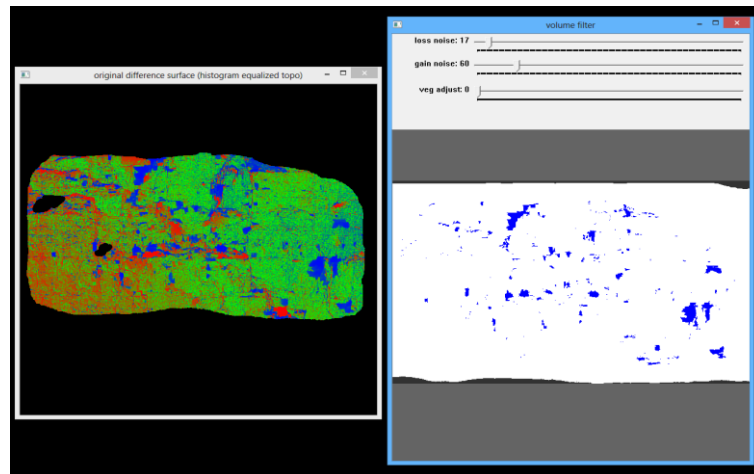
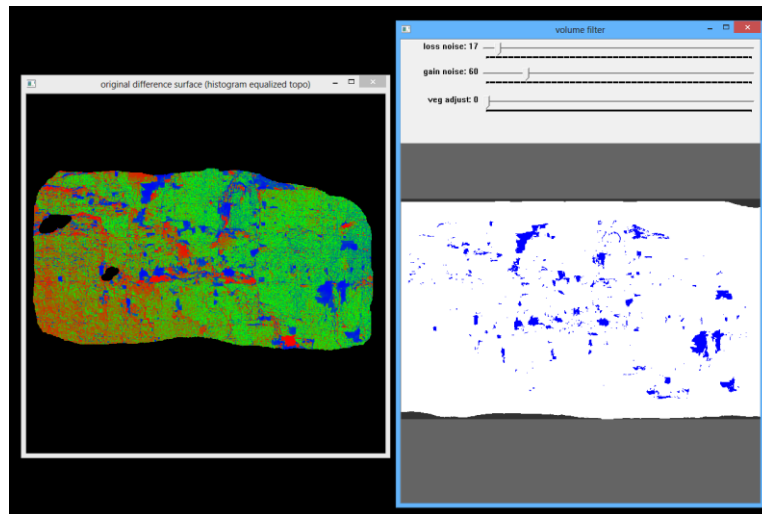
The next step in artifact removal is to apply geomorphic operators such as erode and dilate to further eliminate small noise cells. Erode is a function which peels away cells from the periphery of a blob of either red or blue cells. Dilate performs just the opposite operation – it adds cells to the periphery of either a blue or red blob of cells.

On each erode cycle, one layer of cells is peeled away. Once a blob becomes 1 cell wide, an additional erode cycle will eliminate it. Once eliminated, cells cannot be reconstituted by using the dilate function. Dilate only expands existing blobs.

The Erode function is run first by hitting either the 'e' key (for lost material) or the 'E' key (for gained material). After so many erode cycles, the Dilate function is run next by hitting either the 'd' key (for lost material) or the 'D' key (for gained material). Usually, the number of dilates should equal the number of erodes, but again, the number of erodes and dilates should be determined by visually examining the effect on the right window. The user may use the reset key ('r') to eliminate all the filtering performed by the erode and dilate functions. After hitting the reset key, the right display is based only on the noise-slider values.

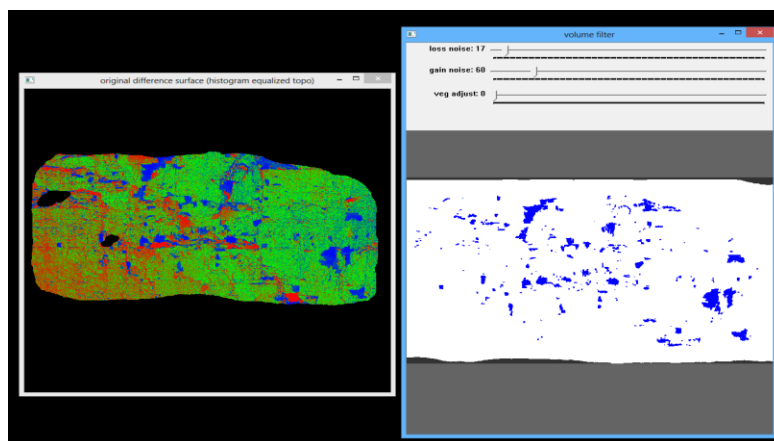
On the following set of screen-shots, the erode key is hit a number of times. Notice how the blue blobs react by getting smaller. The single-cell blobs (noise) disappear after a few erode cycles:



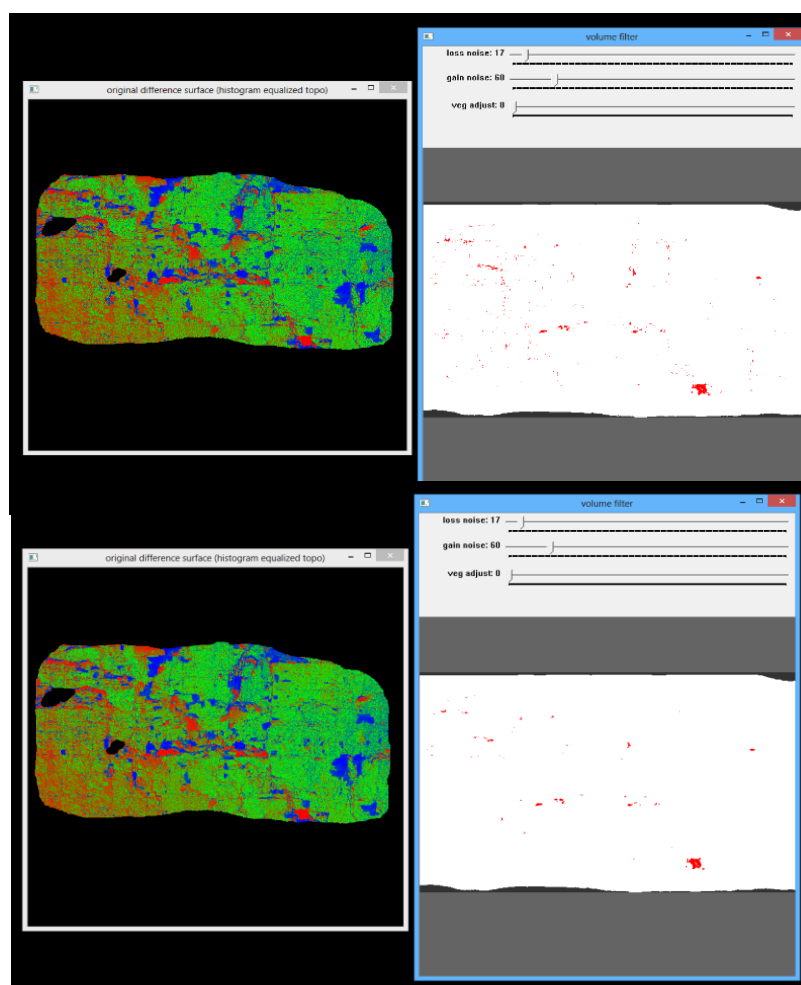


The above sequence shows the result of using the erode function four times. Notice how the rocks got smaller and the noise was largely eliminated.

Next, the dilate function is run on the lost material by using the 'd' key. In this case, the best results were obtained by running dilate four times. Notice how the rocks regained their original size, but the noise that was eliminated did not re-appear:



Finally, the same erode and dilate functions are run on the gained material using the 'E' and 'D' keys. In this case, the optimal results were obtained by running two cycles of erode, followed by two cycles of dilate:



At this point, all residual artifacts have been removed and the volume statistics can be generated by running the volume ('v' key) function. The results are shown on the console window:

```

lost rock volume: -223.57 liters
gained rock volume: 21.8937 liters
net change in rock volume: -201.676 liters

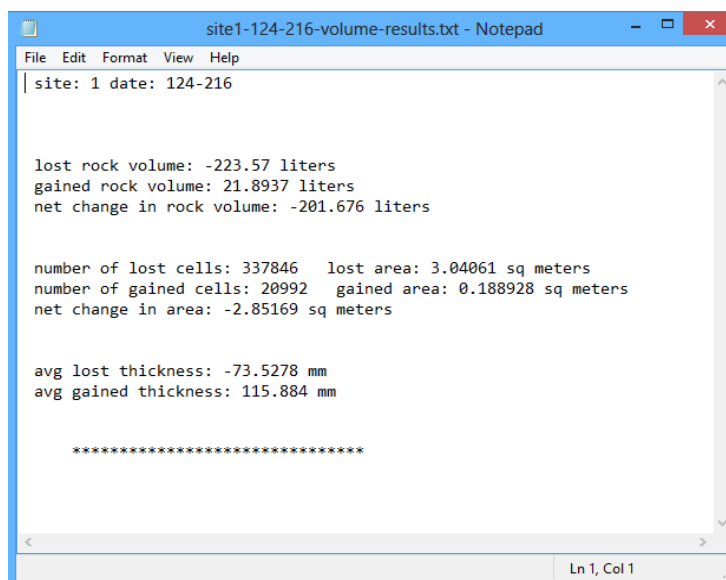
number of lost cells: 337846    lost area: 3.04061 sq meters
number of gained cells: 20992   gained area: 0.188928 sq meters
net change in area: -2.85169 sq meters

avg lost thickness: -73.5278 mm
avg gained thickness: 115.884 mm

writing results to file: F:/OutcropData/Site1/site1-124-216-volume-results.txt

```

As indicated, the same results are also written to a file named with the diff-date:



```

site: 1 date: 124-216

lost rock volume: -223.57 liters
gained rock volume: 21.8937 liters
net change in rock volume: -201.676 liters

number of lost cells: 337846    lost area: 3.04061 sq meters
number of gained cells: 20992   gained area: 0.188928 sq meters
net change in area: -2.85169 sq meters

avg lost thickness: -73.5278 mm
avg gained thickness: 115.884 mm

*****

```

To terminate the calcvol program, hit the 'escape' key. This will trigger the generation of diagnostic pictures and will also save the tuning parameters in a file named 'volume.config' located in the site directory. Always check for the 'orderly end of program' message to indicate the program came to a normal successful completion:

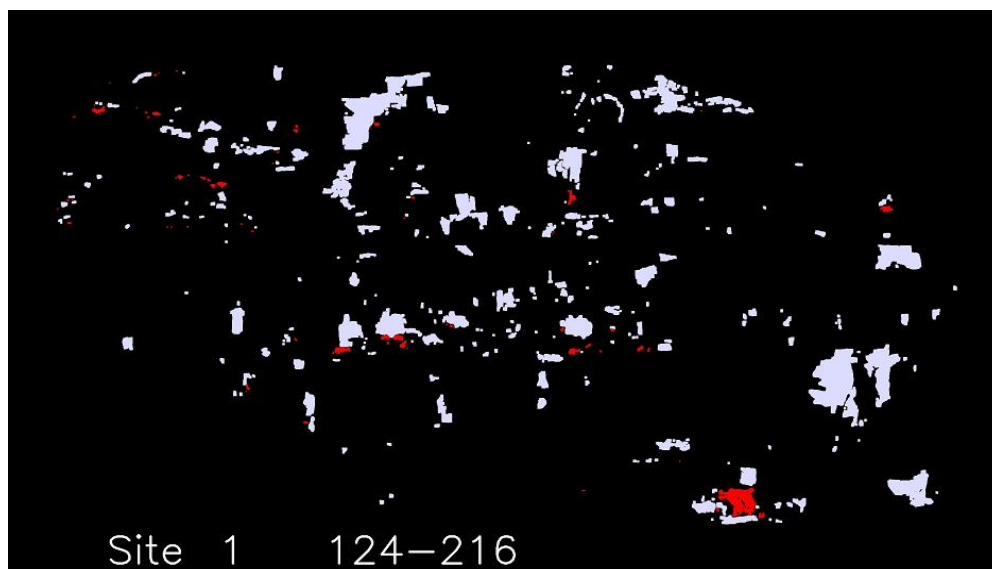
```

saving volume parameters to : F:/OutcropData/Site1/volume.config
making image : F:/OutcropData/Site1/pixMask/124-216-1-mask.jpg
just before creating images
in makeImg h: 0
in makeImg h: 1000
in makeImg h: 2000
in makeImg h: 3000
making image : F:/OutcropData/Site1/pixRocks/124-216-1-rock.jpg
just before creating images
in makeImg h: 0
in makeImg h: 1000
in makeImg h: 2000
in makeImg h: 3000
deleting dynamic classes

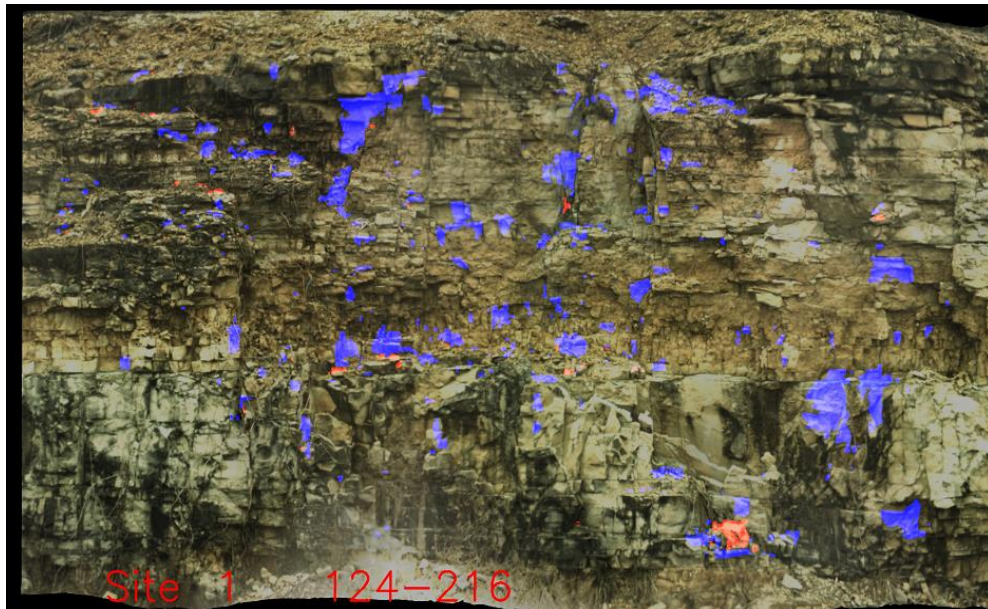
orderly end of program

```

Two diagnostic images are created. The first is a binary image showing the lost material (in light blue) and the gained material (in red). This image is located in the PixMask directory within the site:

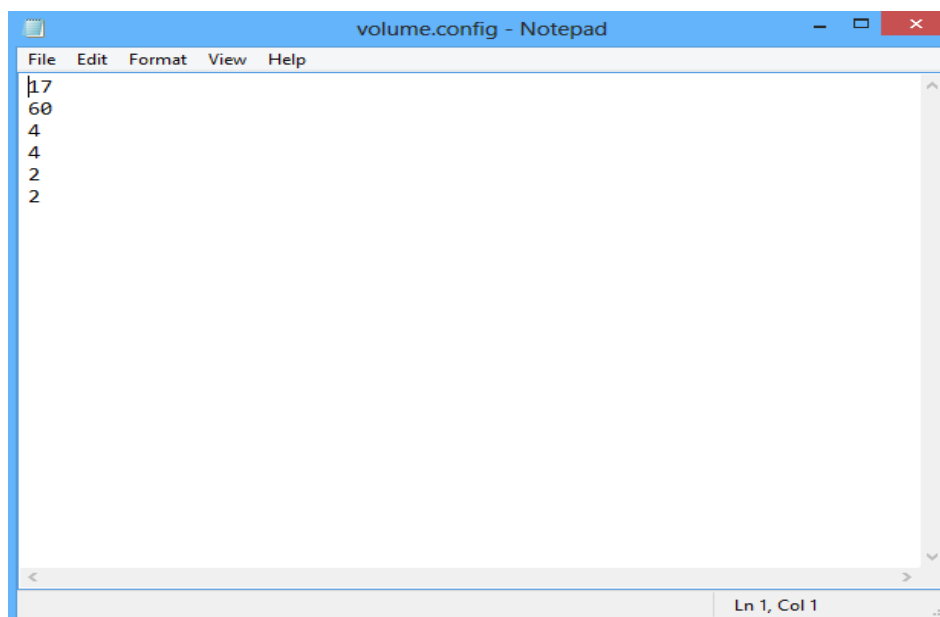


A second diagnostic image shows the same information, but with the lost and gained rocks overlaid on the RGB image for the site. The lost material is shown as a transparent blue tint, with the gained material showing as a red transparent tint:



The final output is the volume.config file which stores the tuning parameters used during the interactive calcvol session. This is a simple text file which may be viewed in any simple editor such as Notepad.

In this case, the file shows that the lost material noise slider was set at 17 mm while the gained material noise slider was set to 60 mm. Next, the erode and dilate functions were run four times each on the lost material (e,e,e,d,d,d,d). Finally, the erode and dilate functions were run two times each on the gained material (E,E,D,D).



Because the resultant volume statistics are highly dependent on the tuning parameters, it is recommended that a single set of tuning parameters be used on all dates of a site. Once tuning is accomplished, the file 'volume.config' will be produced. The next time any other date for that site is run thru the calcvol program, calcvol sees that the volume.config file exists, and proceeds in a batch mode – running the process using the pre-set tuning parameters. If the user desires to restart with a new set of tuning parameters, the file 'volume.config' must either be renamed to something else (saved-volume.conf), or deleted. This way, when calcvol is run, it doesn't find the file 'volume.config', so it operates in the interactive mode – ready for the user to select a new set of tuning parameters.

view2surf – Views two surfaces side-by-side

Purpose

This utility program is used to examine two surfaces to see the results of some prior operation, such as registration or vegetation elimination. It is most commonly used to examine the result of vegetation elimination for the purpose of determining if the operation was successful, or if re-running the operation is required. The program displays two windows and uses the same navigation functions provided in the program **register**. This program is for viewing only – no edit or saving functions are provided.

This utility program is also used to tag spherical targets with roles and Ids, and to examine a surface to determine the distances at various spot locations.

How to run program and Run-time Parameters

view2surf site first-directory first-date second-directory second-date <enter>

site: site number

first-directory: source directory for Lidar data displayed on left window

first-date: date of Lidar data (yyyy-mm-dd format) to be displayed on left window

second-directory: source directory for Lidar data displayed on right window

second-date: date of Lidar data (yyyy-mm-dd format) to be displayed on right window

Example to examine the results of vegetation removal for the July 17, 2013 scan in site 25:

```
view2surf 25 registered 2013-07-17 noVeg 2013-07-17 <enter>
```

Example to examine the results of registration for the August 3, 2012 scan in site 234:

```
view2surf 234 meshed 2012-08-03 registered 2012-08-03 <enter>
```

The following mouse-based navigation functions (similar to those provided in the program **register**) are provided:

Left button down while moving mouse: Panning

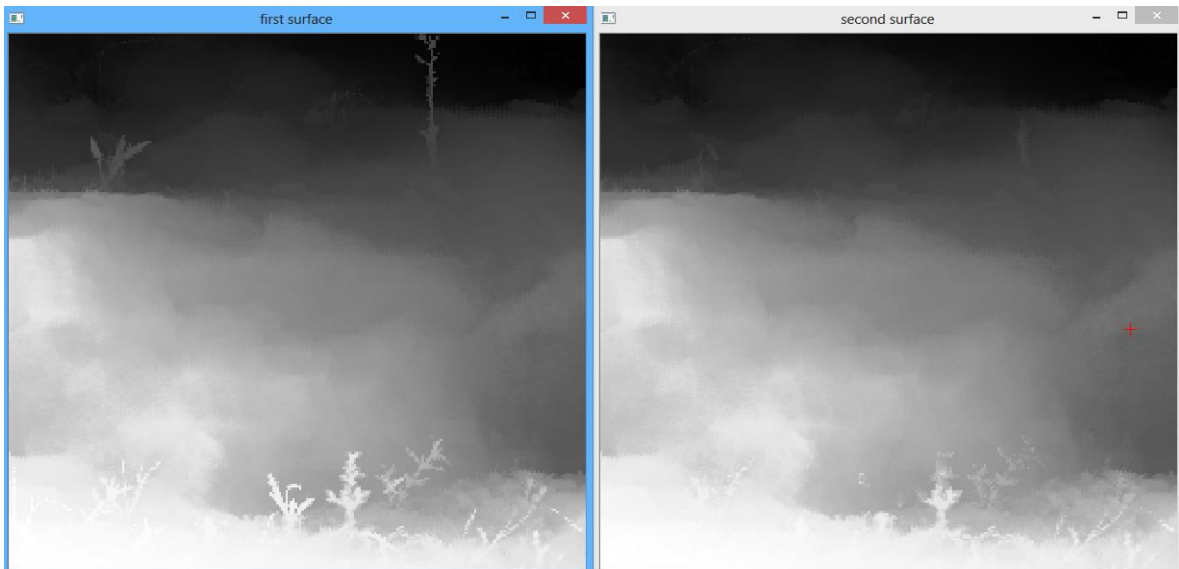
Right button down while moving mouse down: Zoom in

Right button down while moving mouse up: Zoom out

Middle button (or wheel) click: Circular toggle of display image (color image, linear depth-image, histogram- equalized depth image, intensity image)

Left click while mouse is motionless: displays H and V values of cell (used for debugging)

The following screen-shots provide an example of the typical output displayed by this program. In this example, the results of vegetation removal are being examined:



Input Directory for Lidar Data: Defined in the run-time parameters

Other input sources: None – other than mouse clicks during the interactive session.

Output Directory for Lidar Data: None – this program is for viewing only

Other output destinations: None – other than left and right window displays.

Configuration file setup: None.

Explanation of Console Output

A left click while the mouse is motionless will display the H and V values of the cell the cursor is pointing to. This information is mainly used for debugging.

Operational Strategy

When examining the results of vegetation removal, the surfaces to be examined should be the same date, the first directory should be set to 'registered', and the second directory should be set to 'noVeg'.

When reviewing vegetation removal results, the user should navigate around the study area and examine the remaining vegetation artifacts. Thick vegetation cannot be removed, so remnants are commonly visible. These remnants will not usually affect volume determination because they will be present in both the 'before' and 'after' surfaces – thus they will tend to cancel each other out. The vegetation elimination is designed to detect and eliminate thin vegetation which may move in position between the 'before' and 'after' scans. The study area should be examined to ensure that most of the thin vegetation was properly removed. If too much thin vegetation remains, this is an indication that the parameters used during vegetation elimination must be adjusted.

When examining the results of registration, the first directory should be set to 'meshed' and the first date should be set to the base-date (earliest date) for that site. The second directory should be set to 'registered' and the second date should be some 'later date' for that site.

When reviewing registration results, the user should navigate around the study area, and examine how well the 'before' and 'after' images match each other in terms of relative position. The depth or intensity images should be used for this comparison, as they do not contain the inherent 'offset' common with the color images.

BIBLIOGRAPHY

Andrew, R., Arndt, B., Turner, K. A., (2012). Instrumentation and Monitoring Technology, Rockfall characterization and control. Transportation Research Board of the National Academies Press: Washington, D.C, pp. 212-276.

Béland, M., Widlowski, J.-L., & Fournier, R. A. (2014). A model for deriving voxel-level tree leaf area density estimates from ground-based LiDAR. *Environmental Modelling & Software*, 51, 184-189.

Brawner, C. (1994). Rockfall hazard mitigation methods. NHI course, 13219.

Bray, J. W., & Hoek, E. (1981). *Rock slope engineering*: Taylor & Francis.

Brodu, N., & Lague, D. (2012). 3D terrestrial lidar data classification of complex natural scenes using a multi-scale dimensionality criterion: Applications in geomorphology. *ISPRS Journal of Photogrammetry and Remote Sensing*, 68, 121-134.

Clark, C. T., & Liu, J. A Case Study of Integrating 3D High Definition Laser Scanning Technology and BIM into Drywall Installation.

DeMann, A. (2010). LiDAR/3D High Density Scanning Bridge Scan/Model Project-Taggart Bridge.

Goodman, R. E., & Kieffer, D. S. (2000). Behavior of rock in slopes. *Journal of Geotechnical and Geoenvironmental Engineering*, 126(8), 675-684.

hoek. (2007). *Practical Rock Engineering* (2007 edition) <http://www.rocscience.com>.

Jon Rooper. (2013). Methods Used to Obtain Measurements of a Large Truss Bridge with No Plans. T-19: AASHTO Technical Subcommittee for Software and Technology.

Kassebaum, T. (2013). Using LIDAR as a Monitoring Device to calculate Volume of Rockfall over Time (Master), Missouri University of Science and Technology.

Kuhn, D., & Prüfer, S. (2014). Coastal cliff monitoring and analysis of mass wasting processes with the application of terrestrial laser scanning: A case study of Rügen, Germany. *Geomorphology*, 213, 153-165.

Lan, H., Martin, C. D., Zhou, C., & Lim, C. H. (2010). Rockfall hazard analysis using LiDAR and spatial modeling. *Geomorphology*, 118(1), 213-223.

Lato, M., Diederichs, M. S., Hutchinson, D. J., & Harrap, R. (2009). Optimization of LiDAR scanning and processing for automated structural evaluation of discontinuities in rockmasses. *International Journal of Rock Mechanics and Mining Sciences*, 46(1), 194-199.

- Lato, M. J., & Diederichs, M. S. (2014). Mapping shotcrete thickness using LiDAR and photogrammetry data: Correcting for over-calculation due to rockmass convergence. *Tunnelling and Underground Space Technology*, 41, 234-240.
- Lato, M. J., & Vöge, M. (2012). Automated mapping of rock discontinuities in 3D lidar and photogrammetry models. *International Journal of Rock Mechanics and Mining Sciences*, 54, 150-158.
- Maerz, N. H. (2000). Highway rock cut stability assessment in rock masses not conducive to stability calculations. Paper presented at the Proceedings of the 51st Annual Highway Geology Symposium, Aug.
- Maerz, N. H., Otoo, J., Kassebaum, T., & Boyko, K. (2012). Using LIDAR in highway rock cuts. Paper presented at the Proceedings of the 63rd annual highway geology symposium, Redding, CA.
- Majid, Z., Setan, H., Hashim, M. G., & Goh, J. (2008). 3D Campus Modeling using Terrestrial Laser Scanning Technology—First Experience in Malaysia. *3D Geoinfo*.
- Markland, J. T. (1972). A Useful Technique For Estimating the Stability of Rock Slopes when the Rigid Wedge Slide Type of Failure is Expected: Imperial College of Science & Technology.
- Mizoguchi, T., Koda, Y., Iwaki, I., Wakabayashi, H., Kobayashi, Y., Shirai, K., Lee, H.-S. (2013). Quantitative scaling evaluation of concrete structures based on terrestrial laser scanning. *Automation in Construction*, 35, 263-274.
- Mongus, D., Lukač, N., & Žalik, B. (2014). Ground and building extraction from LiDAR data based on differential morphological profiles and locally fitted surfaces. *ISPRS Journal of Photogrammetry and Remote Sensing*.
- Otoo, J., Maerz, N., Xiaoling, L., & Duan, Y. (2011). 3-D discontinuity orientations using combined optical imaging and LiDAR techniques. Paper presented at the Proceedings of the 45th US rock mechanics symposium, Chicago.
- Pantelidis, L. (2009). Rock slope stability assessment through rock mass classification systems. *International Journal of Rock Mechanics and Mining Sciences*, 46(2), 315-325.
- Piteau, D. (1972). Engineering geology considerations and approach in assessing the stability of rock slopes.
- Piteau, D. (1979). Engineering geology considerations and basic approach to rock slope stability analysis for highways Part A., *Rock Slope Engineering Reference Manual: FHWA Report—FHWA-TS-79-208*.

Piteau, D. (1979). Methods of obtaining geological, structural, strength and related engineering geology data Part B, Rock Slope Engineering Reference Manual: FHWA Report–FHWA-TS-79-208.

Piteau, D. R. (1979). Approach and techniques in geological structural analysis Part C, Rock Slope Engineering Reference Manual: FHWA Report. FHWA-TS-79-208 (Part C ed.).

PITEAU, D. R. (1979). Rock slope stabilization, protection and warning-instrumentation measures and related construction considerations Part E, Rock Slope Engineering Reference Manual: FHWA Report. FHWA-TS-79-208.

PITEAU, D. R. (1979). Slope stability analysis methods Part D, Rock Slope Engineering Reference Manual: FHWA Report. FHWA-TS-79-208.

Piteau, D. R., & Martin, D. C. (1982). Mechanics of rock slope failure. Paper presented at the Proc. 3rd International Conference on Stability in Surface Mining (Vancouver, June 1-3, 1981).

Selby, M. Hillslope Materials and Processes, 1993.

Umili, G., Ferrero, A., & Einstein, H. (2013). A new method for automatic discontinuity traces sampling on rock mass 3D model. *Computers & Geosciences*, 51, 182-192.

Vöge, M., Lato, M. J., & Diederichs, M. S. (2013). Automated rockmass discontinuity mapping from 3-dimensional surface data. *Engineering Geology*, 164, 155-162.

Wyllie, D. C., & Norrish, N. I. (1996). LANDSLIDES: INVESTIGATION AND MITIGATION. CHAPTER 14-ROCK STRENGTH PROPERTIES AND THEIR MEASUREMENT' Transportation Research Board Special Report (pp. 391-423).

Youssef, A. M., Maerz, N. H., & Al-Otaibi, A. A. (2012). Stability of rock slopes along Raidah escarpment road, Asir Area, Kingdom of Saudi Arabia. *Journal of Geography and Geology*, 4(2), p48.

VITA

Abdullah Ayed Al-otaibi, was born in Makkah Al-Mukaramh, Saudi Arabia. He received his bachelor degree in geological engineering from King Abdulaziz University, Jeddah, Saudi Arabia, in spring 2003.

He was employed as an engineering geologist by the Saudi Geological Survey in May 2005. He joined a master's degree program in geological engineering at Missouri University of Science and Technology, Rolla, Missouri, with a scholarship from the Saudi Geological Survey in spring 2013.